



fiducial reference
temperature
measurements



esa

Fiducial Reference Measurements for validation of Surface Temperature from Satellites (FRM4STS)

ESA Contract No. 4000113848_15I-LG

D100 - Technical Report 2: Results from the 4th CEOS TIR FRM Field Radiometer Laboratory Inter-comparison Exercise

Part 2 of 4: Laboratory comparison of radiation thermometers

JUNE 2017


Reference OFE-D100(Part 2)-V1-Iss-1-Ver-1-Draft
Issue 1
Revision 1
Date of Issue 23 June 2017
Document Type TR-2

Approval/Acceptance

ESA
Craig Donlon
Technical Officer

Signature

NPL
Andrew Brown
Project Manager


Andrew Brown, NPL

Signature

2016 comparison of IR brightness temperature measurements in support of satellite validation. Part 2: Laboratory comparison of radiation thermometers.

I. Barker-Snook, E. Theocharous and N. P. Fox

June 2017

2016 comparison of IR brightness temperature measurements in support of satellite validation. Part 2: Laboratory comparison of radiation thermometers.

I. Barker Snook, E. Theocharous and N. P. Fox
Environmental Division

Abstract

Under the auspices of CEOS a comparison of terrestrial based infrared (IR) radiometric instrumentation used to support calibration and validation of satellite borne sensors with emphasis on sea/water/land surface temperature was completed at NPL during June and July 2016. The objectives of the 2016 comparison were to establish the “degree of equivalence” between terrestrially based IR Cal/Val measurements made in support of satellite observations of the Earth’s surface temperature and to establish their traceability to SI units through the participation of National Metrology Institutes (NMIs). During the 2016 comparison, NPL acted as the pilot laboratory and provided traceability to SI units during laboratory comparisons. Stage 1 consisted of Lab comparisons, and took place at NPL during the week starting on 20th June 2016. This Stage involved laboratory measurements of participants’ blackbodies calibrated using the NPL reference transfer radiometer (AMBER) and the PTB infrared radiometer, while participants’ radiometers were calibrated using the NPL ammonia heat-pipe reference blackbody. Stage 2 took place at Wraysbury reservoir during the week starting on 27th June 2016 and involved field measurements of the temperature of the surface of the water. Stage 2 also included the testing of the same radiometers alongside each other, completing direct daytime and night-time measurements of the surface temperature of the water. Stage 3 took place in the gardens of NPL during the week starting on 4th July 2016 and involved field measurements of the temperature of the surface of a number of solid targets. Stage 3 included the testing of the same radiometers alongside each other, completing direct daytime and night-time measurements of the surface temperature of targets, including short grass, clover, soil, sand, gravel and tarmac/asphalt. This report provides the results of Stage 1, together with uncertainties as provided by the participants, for the comparison of the participants’ radiometers. During the 2016 comparison, all participants were encouraged to develop uncertainty budgets for all measurements they reported. All measurements reported by the participants, along with their associated uncertainties, were analysed by the pilot laboratory and are presented in this report.

© NPL Management Ltd, 2017

ISSN: 2059-6030

National Physical Laboratory
Hampton Road, Teddington, Middlesex, TW11 0LW

Extracts from this report may be reproduced provided the source is acknowledged
and the extract is not taken out of context.

Approved on behalf of NPLML by Teresa Goodman, Earth Observation, Climate and
Optical Group

Contents

1	INTRODUCTION.....	1
2	ORGANISATION OF THE COMPARISON	1
	2.1THE AMMONIA HEAT-PIPE BLACKBODY.....	2
	2.2MEASUREMENT PROCEDURE	3
3	PARTICIPANTS’ RADIOMETERS AND MEASUREMENTS	4
	3.1 MEASUREMENTS MADE BY VALENCIA UNIVERSITY	4
	3.1.1 Description of the Radiometer and Route of Traceability	4
	3.1.2 Uncertainty Contributions Associated with UoV’s measurements at NPL.....	6
	3.1.3 Comparison of UoV radiometers to the NPL reference blackbody	8
	3.2 MEASUREMENTS MADE BY BALL AEROSPACE.....	23
	3.2.1 Description of radiometer and route of traceability.....	23
	3.2.2 Uncertainty contributions associated with Ball Aerospace’s radiometer	24
	3.2.3 Comparison of BESST radiometer to NPL reference blackbody	25
	3.3 MEASUREMENTS MADE BY KIT	27
	3.3.1 Description of radiometer and route of traceability	27
	3.3.2 Uncertainty Contributions associated KIT’s measurements at NPL.....	28
	3.3.3 Comparison of KIT Heitronics KT15.85 IIP to the NPL reference blackbody	29
	3.4 MEASUREMENTS MADE BY ONERA	33
	3.4.1 Description of radiometer and route of tracibility	33
	3.4.2 Uncertainty contributions associated with ONERA’s measurements at NPL	33
	3.4.3 Comparison of radiometer to the NPL reference blackbody	35
	3.5 MEASUREMENTS MADE BY CSIRO.....	52
	3.5.1 Description of Radiometer and route of traceability Make and type of Radiometer:.....	52
	3.5.2 Uncertainty contributions associated with CSIRO’s measurements at NPL	53
	3.5.3 Comparison of CSIRO ISAR 5D to the NPL reference blackbody.....	53
	3.6 MEASUREMENTS MADE BY STFC RAL.....	57
	3.6.1 Description of the radiometer and route of tracibility	57
	3.6.2 Uncertainty contributions associated with STFC RAL’s measurements at NPL	59
	3.6.3 Comparison of RAL’s SISTeR to the NPL reference blackbody	59
	3.7 MEASUREMENTS MADE BY SOUTHAMPTON UNIVERSITY.....	64
	3.7.1 Description of radiometer and route of traceability.....	64
	3.7.2 Uncertainty contributions associated with UoS’ measurements at NPL	64
	3.7.3 Comparison of UoS’ ISAR to NPL reference blackbody.....	65
	3.8 MEASUREMENTS MADE BY DMI	69
	3.8.1 Description of radiometers and route of traceability	69
	3.8.2 Uncertainty contributions associated with DMI’s measurements at NPL	70
	3.8.3 Comparison of DMI’s radiometers to the NPL reference blackbody.....	71
	3.8.4 Additional comments from DMI regarding the radiometer lab comparison	77
	3.9 MEASUREMENTS MADE BY OUC, QINGDAO	77
	3.9.1 Description of radiometers and route of traceability	77
	3.9.2 Uncertainty contributions associated with OUC’s measurements at NPL	79
	3.9.3 Comparison of OUC’s radiometers to the NPL reference blackbody	80

	3.10 MEASUREMENTS MADE BY GOTA.....	89
	3.10.1 Description of radiometer and route of traceability.....	89
	3.10.2 Uncertainty contributions associated with GOTA’s measurements at NPL.....	91
	3.10.3 Comparison of CE312-2 to NPL reference blackbody.....	92
	3.11 MEASUREMENTS MADE BY RSMAS, UNIVERSITY OF MIAMI	99
	3.11.1 Description of radiometer and route of traceability.....	99
	3.11.2 Uncertainty contributions associated with RSMAS’ measurements at NPL.....	100
	3.11.3 Comparison of the RSMAS radiometer to NPL reference blackbody.....	102
4	SUMMARY OF THE RESULTS	ERROR! BOOKMARK NOT DEFINED.
5	DISCUSSION	ERROR! BOOKMARK NOT DEFINED.
	5.1 FIELD-OF-VIEW (FOV) ISSUES	115
	5.2 WATER CONDENSATION AND ICING OF CAVITY.....	116
	5.3 CALIBRATION RANGE OF RADIOMETERS.....	116
	5.4 LESSONS LEARNT.....	116
6	REFERENCES.....	117

1 INTRODUCTION

The measurement of the Earth's surface temperature and, more fundamentally, its temporal and spatial variation, is a critical operational product for meteorology and an essential parameter for climate monitoring. Satellites have been monitoring global surface temperature for some time. However, it is essential for long-term records that such measurements are fully anchored to SI units.

Field-deployed infrared radiometers¹ currently provide the most accurate surface-based measurements which are used for calibration and validation of Earth observation radiometers. These radiometers are in principle calibrated traceably to SI units, generally through a blackbody radiator. However, they are of varying design and are operated by different teams in different parts of the globe. It is essential for the integrity of their use, that any differences in their measurements are understood, so that any potential biases are removed and are not transferred to satellite sensors.

A comparison (under the auspices of CEOS) of terrestrial based infrared (IR) radiometric instrumentation used to support calibration and validation of satellite borne sensors with emphasis on sea/water surface temperature was completed in Miami in 2001 (Barton et al., 2004) (Rice et al., 2004) and at NPL and Miami in 2009 (Theocharous and Fox, 2010) (Theocharous et al., 2010). However, seven years had passed, and as many of the satellite sensors originally supported were nearing the end of their life, a similar comparison was repeated in 2016. The objectives of the 2016 comparison were to establish the "degree of equivalence" between terrestrially based IR Cal/Val measurements made in support of satellite observations of the Earth's surface temperature and to establish their traceability to SI units through the participation of NMIs.

2 ORGANISATION OF THE COMPARISON

During the 2016 comparison, NPL acted as the pilot laboratory and, with the aid of PTB, provided traceability to SI units during the laboratory comparisons at NPL. NPL was supported with specialist application advice from University of Southampton, RAL and KIT. The 2016 comparison consisted of three stages. Stage 1 took place at NPL in June 2016 and involved laboratory measurements of participants' blackbodies calibrated using the NPL reference transfer radiometer (AMBER) (Theocharous et al., 1998) and the PTB infrared radiometer, while the performance of the participants' radiometers was compared using the NPL ammonia heat-pipe reference blackbody. The performance of 8 blackbodies and 19 radiometers operating on 24 measurement channels was compared during Stage 1. Stage 2 took place on the platform which is located in the middle of Wraysbury reservoir in June/July 2016. The performance of 9 radiometers operating on 14 measurement channels was compared during Stage 2. Stage 2 included the testing of the participating radiometers alongside each other, completing direct daytime and night-time measurements of the skin temperature of the reservoir water. Stage 3 took place in the gardens of NPL during the week starting on 4th July 2016 and involved field measurements of the temperature of the surface of a number of solid targets. Stage 3 included the testing of the same radiometers alongside each other, completing direct daytime and night-time measurements of the surface temperature of targets, including short grass, clover, soil,

¹ This report describes the comparison of instruments which are referred to by participants as "radiometers". However, radiometers generally measure and report radiometric parameters in radiometric units (W, Wm⁻², etc.). The instruments dealt with here measure temperature (in units of degrees C units or K) so they are thermometers or "radiation thermometers". However, in view of the common usage of the terminology for this application, this report will continue to use the term "radiometer".

sand, gravel and tarmac/asphalt.

This report provides the results, together with uncertainties as provided by the participants, of the radiometer measurements of seven fixed temperatures as performed in one of NPL's temperature-controlled laboratories during the week beginning 20th June 2016. The laboratory comparison of the participants' blackbodies, as measured by the NPL AMBER radiometer and the PTB infrared radiometer, as well as the WST comparison at Wraysbury reservoir and the LST comparison that took place on the NPL gardens are being presented in other reports (Theocharous et al. 2017, Theocharous et al. 2017a, Barker Snook et al. 2017).

During the 2016 comparison, all participants were encouraged to develop uncertainty budgets for all measurements they reported. In order to achieve optimum comparability, lists containing the principal influence parameters for the measurements were provided to all participants. All measurements reported by the participants, along with their associated uncertainties, were analysed by the pilot laboratory and are presented in this report.

2.1 THE AMMONIA HEAT-PIPE BLACKBODY

The NPL ammonia heat-pipe reference blackbody (Chu and Machin, 1999) uses a heat-pipe to control the blackbody cavity temperature. This resulted in negligible temperature gradients along the length of the cavity. The length of the ammonia heat-pipe blackbody cavity was 300 mm, and it had a 75 mm internal diameter with a 120° cone angle at the end wall. The blackbody cavity was coated with a high-emissivity Nextel black paint. The emissivity of the blackbody cavity was calculated using the series integral method (Berry, 1981). The effective emissivity of the cavity was estimated to be 0.9993 assuming an emissivity of 0.96 for the Nextel black coating (Betts, *et al.*, 1985).

The temperature of the blackbody cavity was obtained from an ITS-90 calibrated platinum resistance thermometer (PRT) which was inserted into a well of 150 mm depth in the rear of the blackbody cavity. The front of the reference source contained a circular support which allowed aperture plates with different diameters to be positioned in front of the blackbody cavity.

The ammonia heat-pipe blackbody could be operated with a 70 mm diameter aperture in the front of the blackbody. However, during the 2016 comparison, a 50 mm diameter aperture was used in front of the blackbody cavity to improve its emissivity characteristics. Furthermore, there was a length of foam insulation located between the front aperture and the front of the heat pipe. The foam insulation had an aperture of approximately the same diameter as the ammonia heat-pipe aperture (75 mm diameter). The depth of the foam insulation was approximately 40 mm. There was also a 35 mm spacing between the aperture and the foam which meant that there was a total distance of approximately 75 mm from the front of the aperture to the actual blackbody cavity. This, in turn, meant that if radiometers with a large field of view were measuring the reference blackbody, then there was a possibility that they could be seeing the foam rather than the inside of the blackbody cavity, even when they are placed right up against the front of the blackbody casing. While participants were free to position and align their blackbodies in front of the reference blackbody, most of the participants placed their radiometers right up against the reference blackbody, in order to ensure that blackbody cavity overfilled the entire FoV of their radiometers.

The temperature of the blackbody cavity was controlled by a cylindrical heat exchanger which fitted closely around the blackbody cavity. Heat transfer fluid was circulated through a continuous 6 mm wide helical groove which was machined in the surface of the internal cylinder. Full information on the ammonia heat-pipe blackbody can be found elsewhere (Chu and Machin, 1999).

At sub-ambient temperatures i.e. at temperatures below the Dew point, the blackbody cavity was purged with dry nitrogen, in order to prevent water from condensing on the internal surfaces of the cavity which could damage the internal black coating and change the effective emissivity of the cavity. The dry nitrogen gas was fed into the blackbody cavity from the rear. Its temperature was iso-thermalised within the feed tube which was embedded within the wall of the heat pipe. The gas was introduced into the front of the blackbody cavity via a gas distribution ring consisting of 12 holes of 1.5 mm diameter. In order to reduce the effect of convection currents from the surroundings, the aperture of the blackbody cavity was open whilst measurements were being made but was blocked at all other times with an insulation plug.

2.2 MEASUREMENT PROCEDURE

The reference blackbody was set at a certain temperature and enough time was allowed for its cavity temperature to stabilise to the new setting. Once the operating temperature had been selected, the system required 30 minutes to reach temperatures greater than 0 °C but required 3 hours to reach temperatures on the region of -30 °C. Once the set-point had been reached, the blackbody required another 0.5 to 1 hour to stabilize at the new temperature.

Each participant was allowed a maximum period of 30 minutes to position his radiometer in front of the reference blackbody, align it to the aperture of the blackbody and take measurements at that particular temperature setting. The order with which radiometers completed the measurements at the beginning of the comparison depended on the readiness of the radiometers of the different participants to do measurements at that particular time. Towards the end of the comparison, participants were allocated 30 minute periods, according to tables which were circulated to all participants. Participants with more than one radiometer were asked to arrange for the 30 minute measurement period to be shared between all their measuring radiometers.

The temperature of the reference blackbody was continuously logged using UTC and the participants were asked to use the same time reference. This allowed the comparison of the measurements of each participant with the corresponding measurements of the reference blackbody.

Participants were asked to provide their measurements in spreadsheets. The top of each spreadsheet indicated the date on which the measurements shown in the spreadsheet were performed. Each spreadsheet consisted of a minimum of three columns. The first column indicated time of the measurement, in a UTC format. The second column gave the brightness temperature of the reference blackbody, as measured by the participant, at the time indicated in the first column. The third column provided the combined (total) uncertainty of the measurement of the brightness temperature measured by the participant corresponding to the measurement indicated in the second column.

Participants were also encouraged to develop and provide full uncertainty budgets for their measurements. In order to help participants to do this, tables were provided listing the

parameters which were likely to contribute to the uncertainty of the measurement. Some participants provided completed tables, providing extensive information on each uncertainty contribution. Other participants provided considerably less information on their uncertainty budgets.

3 PARTICIPANTS' RADIOMETERS AND MEASUREMENTS

Section 3 gives brief descriptions of the radiometers participating in the 2016 laboratory radiometer comparison at NPL and presents the results of the measurements which were completed by the radiometers during these comparisons, along with the corresponding combined uncertainty values which were provided by the participants. Section 3 also provides the uncertainty budgets of the measurements using the participating radiometers, as provided by the participants. In some cases the level of detail provided by participants in the uncertainty budgets of their measurements is fairly limited and not ideal. However, whatever was provided by the participants is included in this report, along with a summary of the results for each participant for each stage of the comparison.

3.1 MEASUREMENTS MADE BY VALENCIA UNIVERSITY

Dept. of Earth Physics and Thermodynamics, University of Valencia.
50, Dr. Moliner. ES-46100, Burjassot (Valencia), Spain
Contact Names: César Coll and Raquel Niclòs
Email: cesar.coll@uv.es , raquel.niclos@uv.es

3.1.1 Description of the Radiometer and Route of Traceability

Make and type of the Radiometer. CIMEL Electronique CE312-2, six spectral bands (two units)

Outline Technical description of the instrument. Type of detector used by the radiometer: thermopile, operating at ambient temperature. Six spectral bands: B1 8.0-13.3 μm , B2 10.9-11.7 μm , B3 10.2-11.0 μm , B4 9.0-9.3 μm , B5 8.5-8.9 μm , and B6 8.3-8.6 μm . Broad band: Germanium window and zinc sulphide filters. Narrow bands: interference filters. Field of view: 10°. The instrument has a built-in radiance reference made of a concealable gold-coated mirror which enables comparison between the target radiance and the reference radiation from inside the detector cavity. The temperature of the detector is measured with a calibrated PRT, thus allowing compensation for the cavity radiation. The relevant outputs of the radiometer are the detector temperature and the difference in digital counts between the signals from the target and the detector cavity.

References for further information on the radiometers:

1. Sicard, M., Spyak, P. R., Brogniez, G., Legrand, M., Abuhassan, N. K., Pietras, C., and Buis, J. P. (1999). Thermal infrared field radiometer for vicarious cross-calibration: characterization and comparisons with other field instruments. *Optical Engineering*, 38 (2), 345-356.
2. M. Legrand, C. Pietras, G. Brogniez, M. Haeffelin, N. K. Abuhassan and M. Sicard (2000). A high-accuracy multiwavelength radiometer for in situ measurements in the thermal infrared. Part I: characterization of the instrument, *J. Atmos. Ocean Techn.*, 17, 1203-1214.

Establishment or traceability route for primary calibration including date of last realisation and breakdown of uncertainty. The following error analysis is based on laboratory measurements with the Landcal blackbody P80P (blackbody combined uncertainty was 0.34 K; Appendixes B and E) on May 13-18, 2016, and estimates from the above references. Blackbody measurements were taken at six fixed temperatures (0-50 °C) in two different runs with instrument realigning. The values reported below are typical values for all blackbody temperatures considered for each band of each radiometer (units 1 and 2). The mean values considering all bands of each radiometer are also given.

Type A

- Repeatability: Typical value of the standard deviation of 15 measurements at fixed blackbody temperature without re-alignment of radiometer.

Unit 1	B1	B2	B3	B4	B5	B6	mean
K	0.01	0.04	0.04	0.06	0.06	0.08	0.05
% (at 300 K)	0.002	0.012	0.012	0.019	0.019	0.025	0.015

Unit 2	B1	B2	B3	B4	B5	B6	mean
K	0.01	0.03	0.03	0.04	0.05	0.05	0.03
% (at 300 K)	0.002	0.009	0.009	0.015	0.017	0.018	0.012

- Reproducibility: Typical value of difference between two runs of radiometer measurements at the same black body temperature including re-alignment.

Unit 1	B1	B2	B3	B4	B5	B6	mean
K	0.08	0.10	0.08	0.06	0.09	0.05	0.08
% (at 300 K)	0.027	0.033	0.025	0.021	0.029	0.018	0.026

Unit 2	B1	B2	B3	B4	B5	B6	mean
K	0.06	0.06	0.06	0.05	0.05	0.04	0.06
% (at 300 K)	0.021	0.021	0.019	0.017	0.017	0.015	0.018

Total Type A uncertainty (RSS):

Unit 1	B1	B2	B3	B4	B5	B6	mean
K	0.08	0.11	0.08	0.09	0.10	0.09	0.09
% (at 300 K)	0.028	0.035	0.028	0.029	0.035	0.031	0.031

Unit 2	B1	B2	B3	B4	B5	B6	mean
K	0.06	0.07	0.06	0.07	0.07	0.07	0.07
% (at 300 K)	0.022	0.023	0.021	0.023	0.024	0.023	0.022

Type B

- **Primary calibration:** 0.34 K (estimation of the total uncertainty of the Landcal blackbody P80P).

- **Linearity of radiometer:** 0.06 K (Typical value for all bands in the temperature range 0-40 °C according to reference 2).

- **Drift since last calibration:** It has been corrected using the calibration measurements performed with the Landcal blackbody P80P mentioned above. A linear correcting equation has been derived for each band and radiometer, with the radiometer measured temperature and the detector temperature as inputs. The uncertainty for this correction is the RSS of the typical estimation uncertainty of the linear regression (0.05 K for unit 1 and 0.04 K for unit 2) and the uncertainties resulting from the propagation of input temperature errors (standard deviations for 15 measurement at a fixed temperature) in the linear correcting equation. The resulting uncertainty in the correction of calibration drift is 0.07 K for unit 1 and 0.05 K for unit 2.

- **Ambient temperature fluctuations:** The effect of ambient temperature fluctuations is compensated in the CE312 radiometers by measuring the detector cavity temperature by means of a calibrated PRT. The uncertainty in this process is the uncertainty of the internal PRT, which is 0.04 K according to reference 2.

- **Atmospheric absorption/emission:** Negligible due to very short path length and radiometers working in the atmospheric window.

Total Type B uncertainty (RSS): 0.35 K for both units 1 and 2.

Type A + Type B uncertainty (RSS): 0.37 K for unit 1 and 0.36 K for unit 2.

Operational methodology during measurement campaign. The Landcal Blackbody Source P80P was set at six fixed temperatures (0-50 °C) in two different runs. Enough time was allowed for the blackbody to reach equilibrium at each temperature. Radiometers were aligned with the blackbody cavity, and placed at a distance so that the field of view was smaller than the cavity diameter. Standard processing (see references above) was applied to the radiometer readouts to calculate the equivalent brightness temperature. Due to the radiometer responsivity drift with time, a correction is applied depending on the difference between the measured brightness temperature (T_m) and the detector temperature (T_d):

$$T_c = T_m + a(T_m - T_d) + b$$

where T_c is the corrected brightness temperature, and a and b are band-dependent coefficients derived from linear regression from the calibration measurements at the six temperatures in the two runs.

Blackbody usage (deployment), previous use of instrument and planned applications. Field measurements of land surface temperature and emissivity for validation of thermal infrared products from satellite sensors.

3.1.2 Uncertainty Contributions Associated with UoV's measurements at NPL

The tables below show the uncertainty breakdown for the measurement of the laboratory radiometer comparison at NPL. The RMS total refers to the square root of the sum of the squares of all the individual uncertainty terms.

CE312-2 Unit 1

Uncertainty Contribution	Type A	Type B	
	Uncertainty in Value / %	Uncertainty in Value / (appropriate units)	Uncertainty in Brightness temperature/K
Repeatability of measurement	0.015		0.05
Reproducibility of measurement	0.026		0.08
Primary calibration			0.34
Linearity of radiometer			0.06
Drift since calibration			0.07
Ambient temperature fluctuations			0.04
Atmospheric absorption/emission			
RMS total	0.09 K/0.031 %		0.37

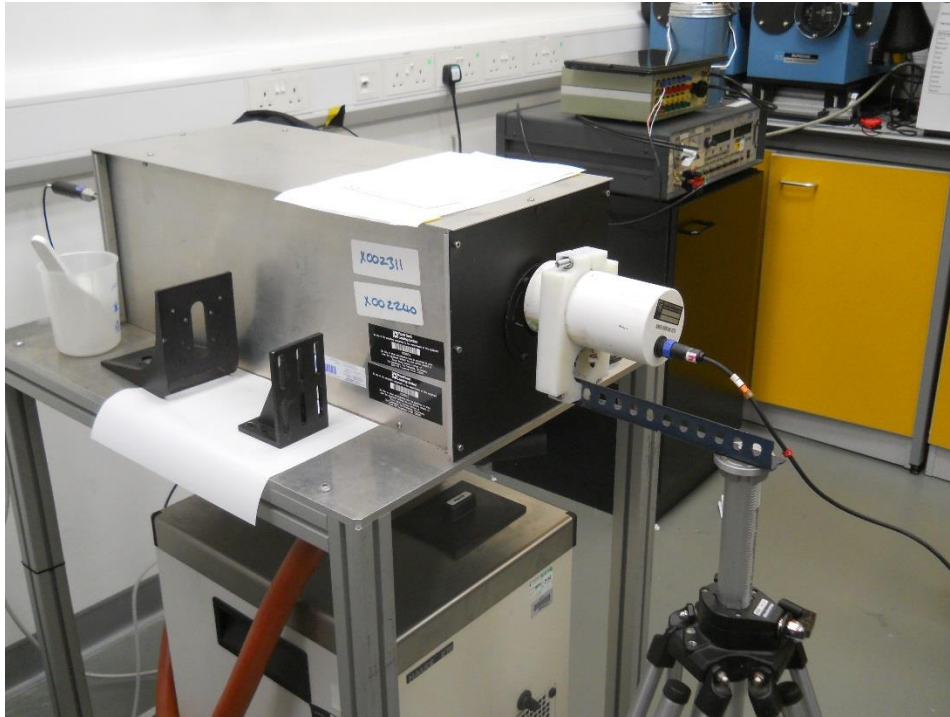
CE312-2 Unit 2

Uncertainty Contribution	Type A	Type B	
	Uncertainty in Value / %	Uncertainty in Value / (appropriate units)	Uncertainty in Brightness temperature/K
Repeatability of measurement	0.012		0.03
Reproducibility of measurement	0.018		0.06
Primary calibration			0.34
Linearity of radiometer			0.06
Drift since calibration			0.05
Ambient temperature fluctuations			0.04
Atmospheric absorption/emission			
RMS total	0.07 K/0.022 %		0.36

3.1.3 Comparison of UoV radiometers to the NPL reference blackbody

3.1.3.1 Comparison of CE312-2 Unit 1 to the NPL reference blackbody

The photo below shows the UoV radiometer viewing the NPL reference blackbody.



The UoV radiometer viewing the NPL reference blackbody

Figures 3.1.1 to 3.1.7 show the output of the six channels of the CIMEL CE312-2 unit 1 radiometer when it was viewing the NPL reference blackbody maintained at different temperatures. The same figures also show the brightness temperature of the NPL reference blackbody as a function of time. The uncertainty bars in the figures represent the uncertainty values provided by Valencia University which correspond to the measurements shown in the Figures, as well as the uncertainty of the NPL reference blackbody. Tables 3.1.1 to 3.1.7 which are shown below each Figure, list the difference between the average temperature displayed by each radiometer channel during the monitoring period and the corresponding average brightness temperature of the NPL reference blackbody.

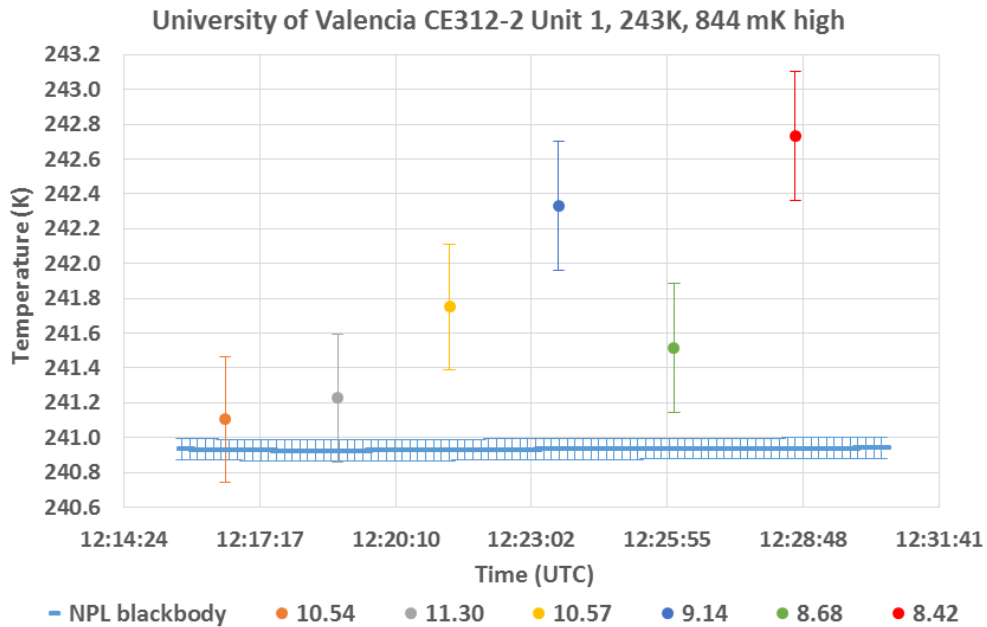


Figure 3.1.1: Plot of the measurements of the different channels of the CIMEL CE312-2 Unit 1 radiometer when it was viewing the NPL reference blackbody while it was maintained at about $-30\text{ }^{\circ}\text{C}$.

Table 3.1.1: The deviation of the different radiometer channels δT of the CIMEL CE312-2 Unit 1 radiometer from the average blackbody temperature, over the measurement interval for a nominal blackbody temperature of $-30\text{ }^{\circ}\text{C}$.

Channel (μm)	δT (mK)
10.54	171
11.30	293
10.57	819
9.14	1398
8.68	583
8.42	1798

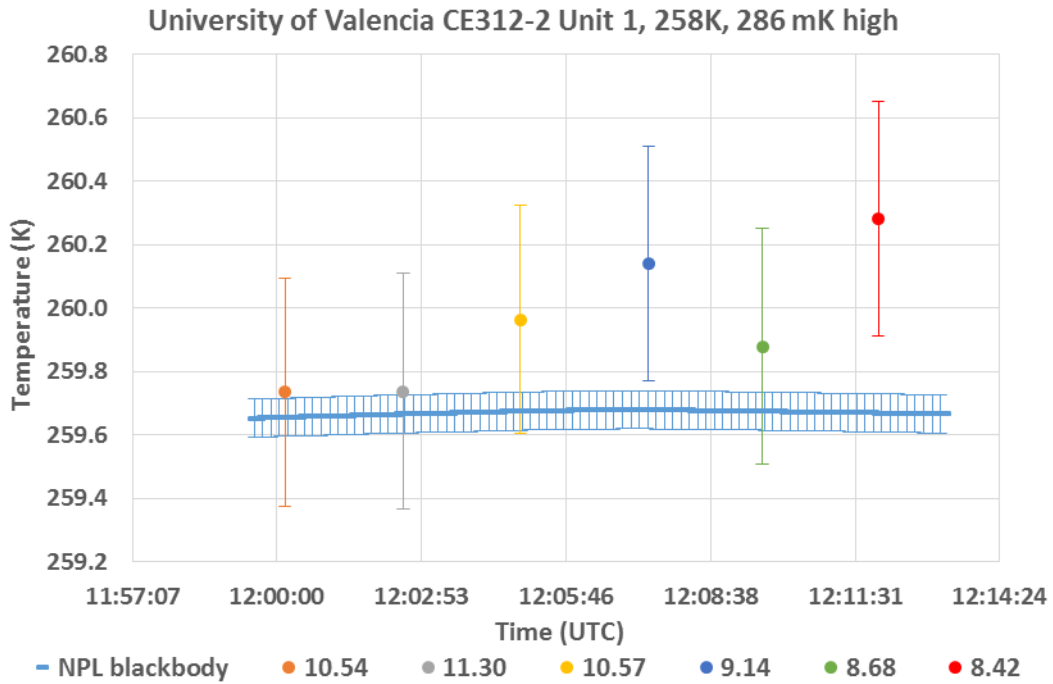


Figure 3.1.2: Plot of the measurements of the different channels of the CIMEL CE312-2 Unit 1 radiometer when it was viewing the NPL reference blackbody while it was maintained at about -15 °C.

Table 3.1.2: The deviation of the different radiometer channels δT of the CIMEL CE312-2 Unit 1 radiometer from the average blackbody temperature, over the measurement interval for a nominal blackbody temperature of -15 °C.

Channel (μm)	δT (mK)
10.54	65
11.30	68
10.57	293
9.14	469
8.68	209
8.42	611

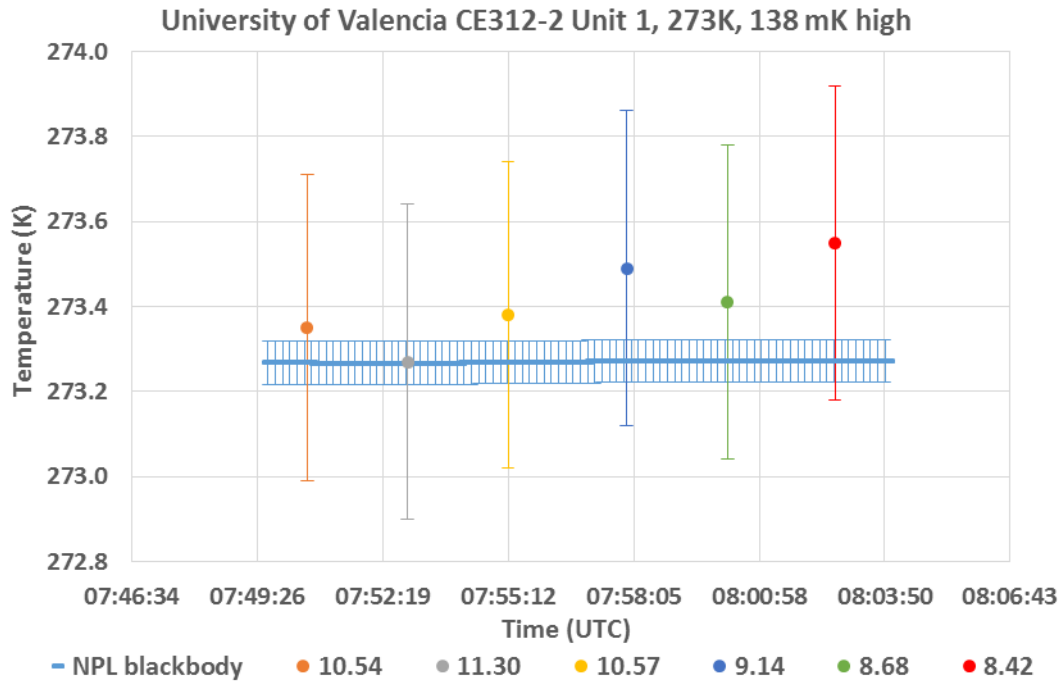


Figure 3.1.3: Plot of the measurements of the different channels of the CIMEL CE312-2 Unit 1 radiometer when it was viewing the NPL reference blackbody while it was maintained at about at 0 °C.

Table 3.1.3: The deviation of the different radiometer channels δT of the CIMEL CE312-2 Unit 1 radiometer from the average blackbody temperature, over the measurement interval for a nominal blackbody temperature of about 0 °C.

Channel (μm)	δT (mK)
10.54	80
11.30	0
10.57	110
9.14	220
8.68	140
8.42	280

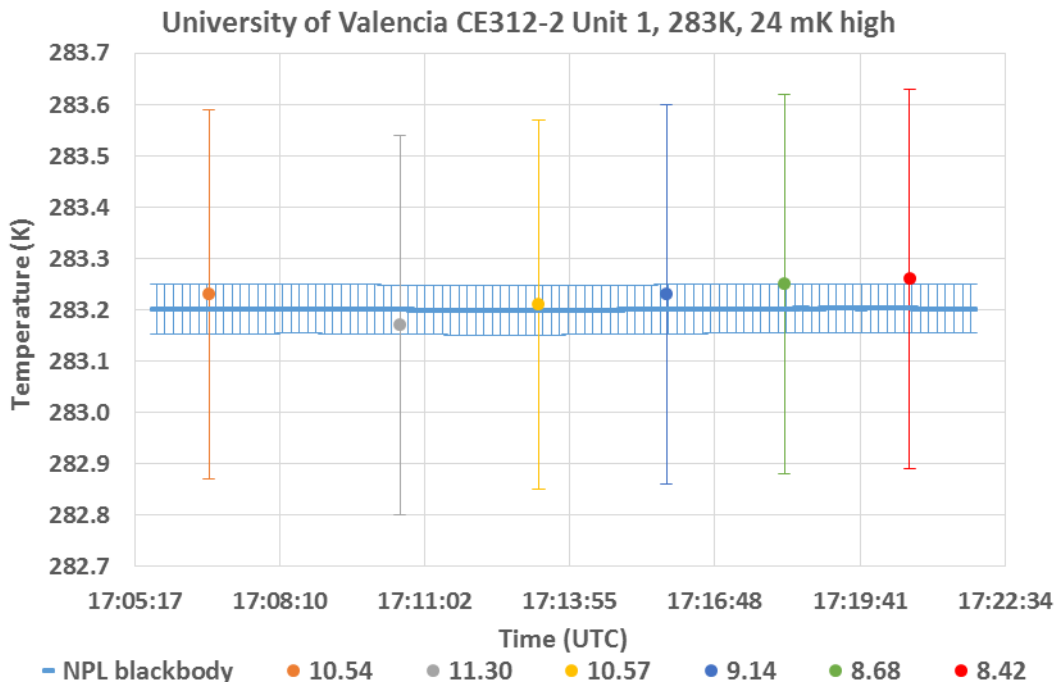


Figure 3.1.4: Plot of the measurements of the different channels of the CIMEL CE312-2 Unit 1 radiometer when it was viewing the NPL reference blackbody while it was maintained at about 10 °C.

Table 3.1.4: The deviation of the different radiometer channels δT of the CIMEL CE312-2 Unit 1 radiometer from the average blackbody temperature, over the measurement interval for a nominal blackbody temperature of about 10 °C.

Channel (μm)	δT (mK)
10.54	29
11.30	-31
10.57	9
9.14	29
8.68	49
8.42	59

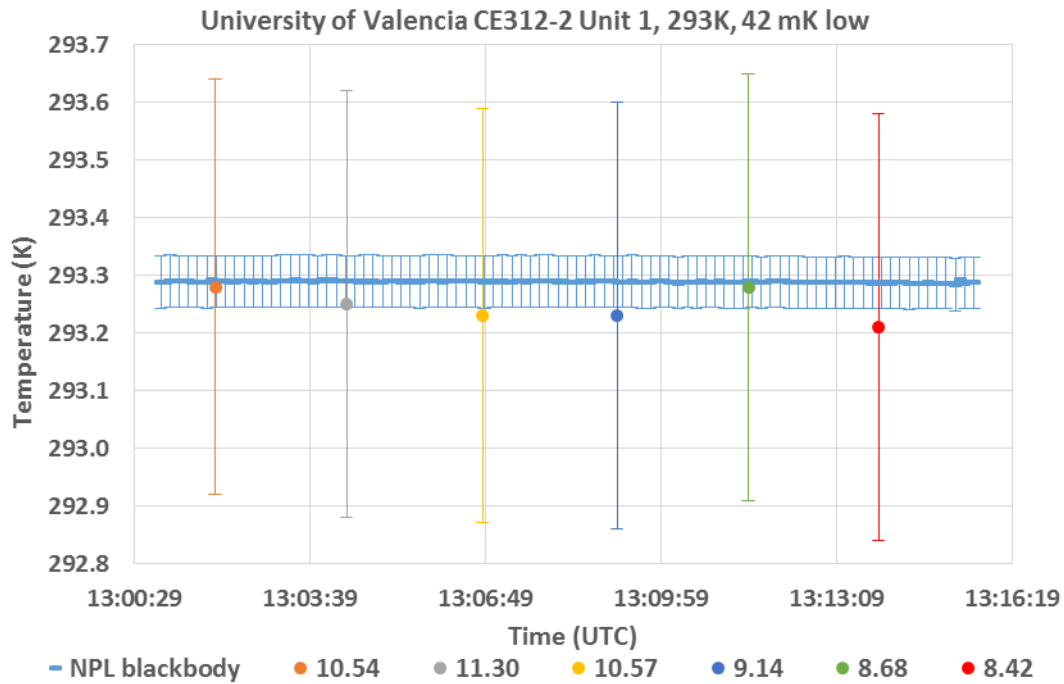


Figure 3.1.5: Plot of the measurements of the different channels of the CIMEL CE312-2 Unit 1 radiometer when it was viewing the NPL reference blackbody while it was maintained at about 20 °C.

Table 3.1.5: The deviation of the different radiometer channels δT of the CIMEL CE312-2 Unit 1 radiometer from the average blackbody temperature, over the measurement interval for a nominal blackbody temperature of about 20 °C.

Channel (μm)	δT (mK)
10.54	-9
11.30	-39
10.57	-59
9.14	-59
8.68	-9
8.42	-79

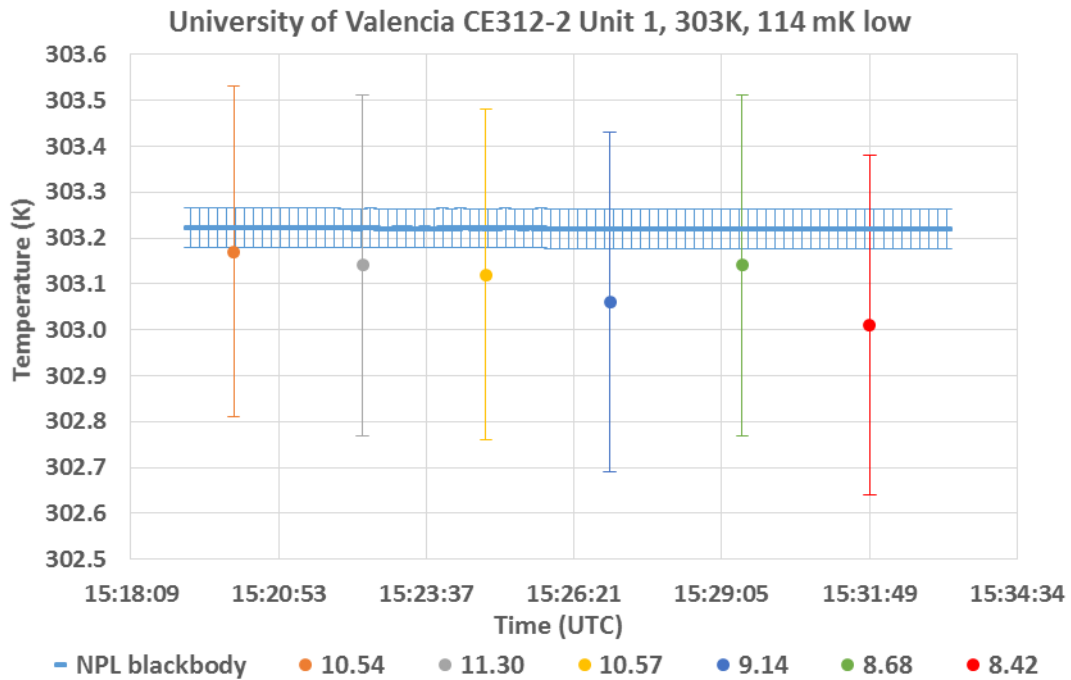


Figure 3.1.6: Plot of the measurements of the different channels of the CIMEL CE312-2 Unit 1 radiometer when it was viewing the NPL reference blackbody while it was maintained at about 30 °C.

Table 3.1.6: The deviation of the different radiometer channels δT of the CIMEL CE312-2 Unit 1 radiometer from the average blackbody temperature, over the measurement interval for a nominal blackbody temperature of about 30 °C.

Channel (μm)	δT (mK)
10.54	-51
11.30	-81
10.57	-101
9.14	-161
8.68	-81
8.42	-211

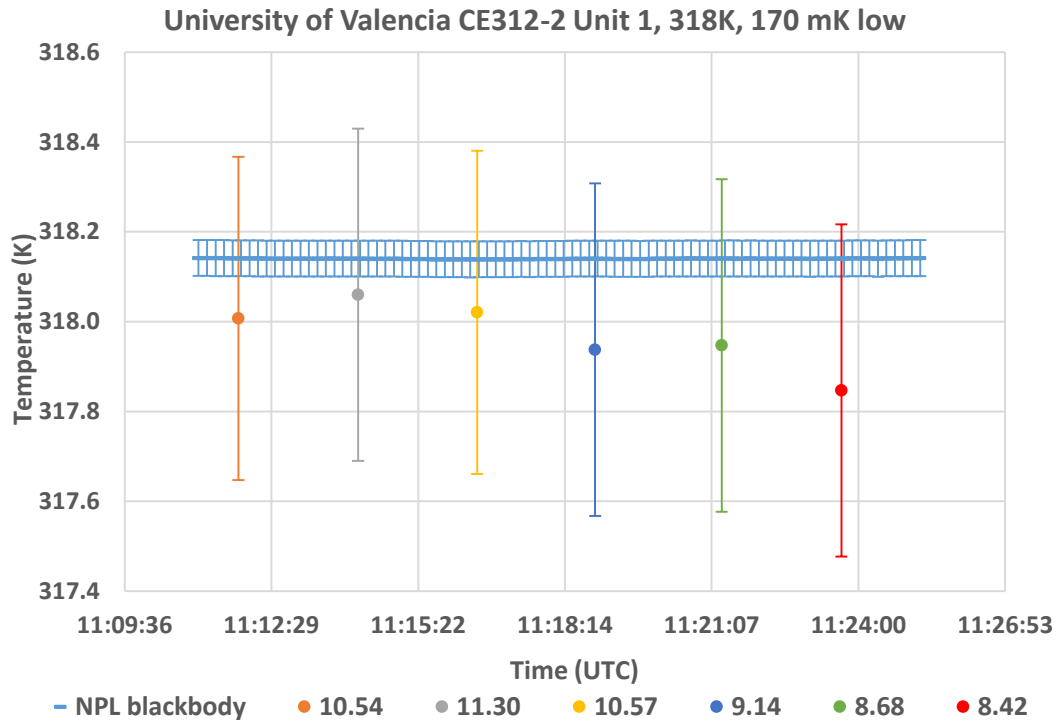


Figure 3.1.7: Plot of the measurements of the different channels of the CIMEL CE312-2 Unit 1 radiometer when it was viewing the NPL reference blackbody while it was maintained at about 45 °C.

Table 3.1.7: The deviation of the different radiometer channels δT of the CIMEL CE312-2 Unit 1 radiometer from the average blackbody temperature, over the measurement interval for a nominal blackbody temperature of about 45 °C.

Channel (μm)	δT (mK)
10.54	-133
11.30	-81
10.57	-120
9.14	-203
8.68	-193
8.42	-293

3.1.3.2 Comparison of CE312-2 Unit 2 to the NPL reference blackbody

Figures 3.1.8 to 3.1.14 show the output of the six channels of the CIMEL CE312-2 radiometer unit 2 when it was viewing the NPL blackbody maintained at different temperatures. The same Figures also show the brightness temperature of the NPL blackbody as a function of time. The uncertainty bars in the figures represent the uncertainty values provided by Valencia University which correspond to the measurements shown in the Figures, as well as the uncertainty of the NPL reference blackbody. Tables 3.1.8 to 3.1.14 shown below each Figure list the difference between the average temperature displayed by each radiometer channel during the monitoring period and the corresponding average brightness temperature of the NPL reference blackbody.

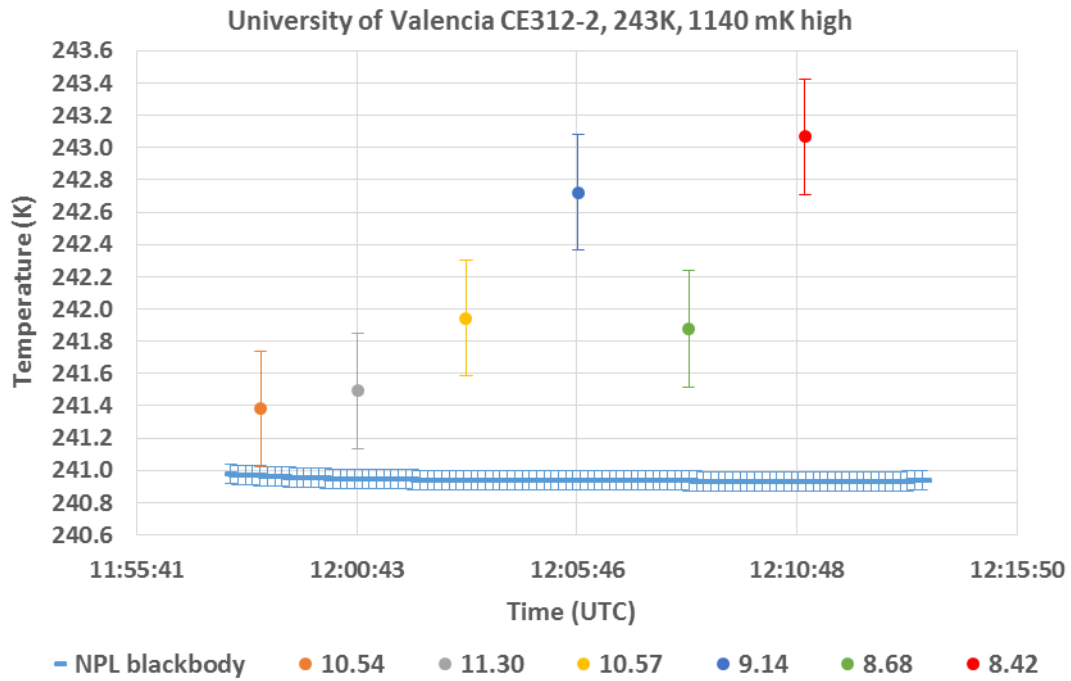


Figure 3.1.8: Plot of the measurements of the different channels of the CIMEL CE312-2 Unit 2 radiometer when it was viewing the NPL reference blackbody while it was maintained at about -30 °C.

Table 3.1.8: The deviation of the different radiometer channels δT of the CIMEL CE312-2 Unit 2 radiometer from the average blackbody temperature, over the measurement interval for a nominal blackbody temperature of -30 °C.

Channel (μm)	δT (mK)
10.54	441
11.30	552
10.57	1004
9.14	1782
8.68	935
8.42	2126

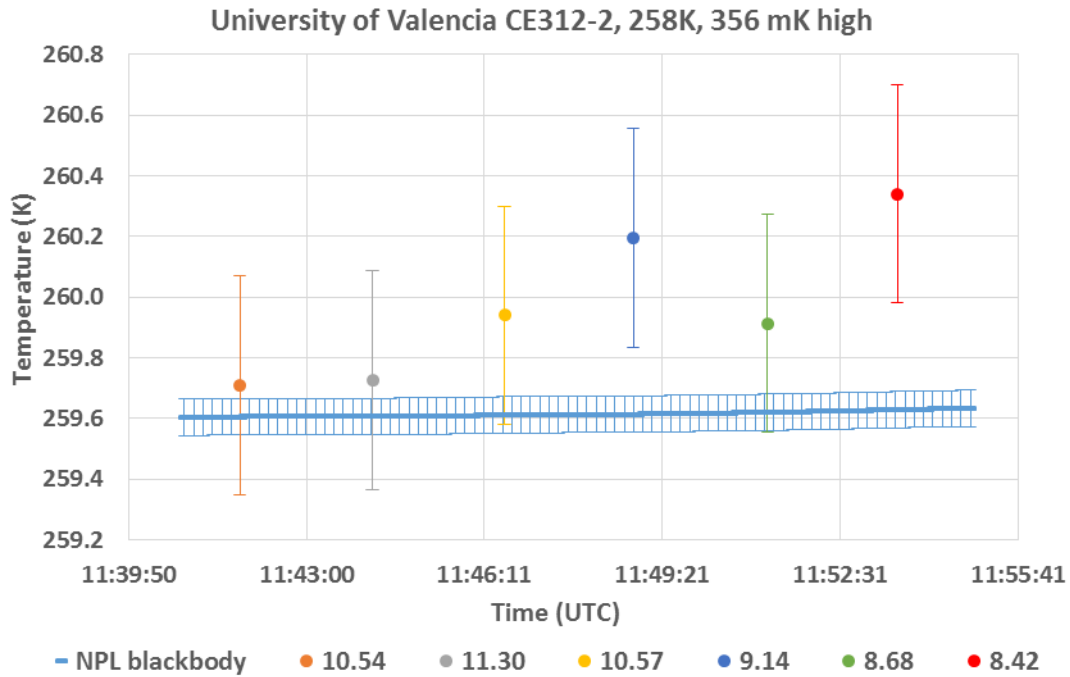


Figure 3.1.9: Plot of the measurements of the different channels of the CIMEL CE312-2 Unit 2 radiometer when it was viewing the NPL reference blackbody while it was maintained at about $-15\text{ }^{\circ}\text{C}$.

Table 3.1.9: The deviation of the different radiometer channels δT of the CIMEL CE312-2 Unit 2 radiometer from the average blackbody temperature, over the measurement interval for a nominal blackbody temperature of about $-15\text{ }^{\circ}\text{C}$.

Channel (μm)	δT (mK)
10.54	94
11.30	111
10.57	326
9.14	581
8.68	299
8.42	726

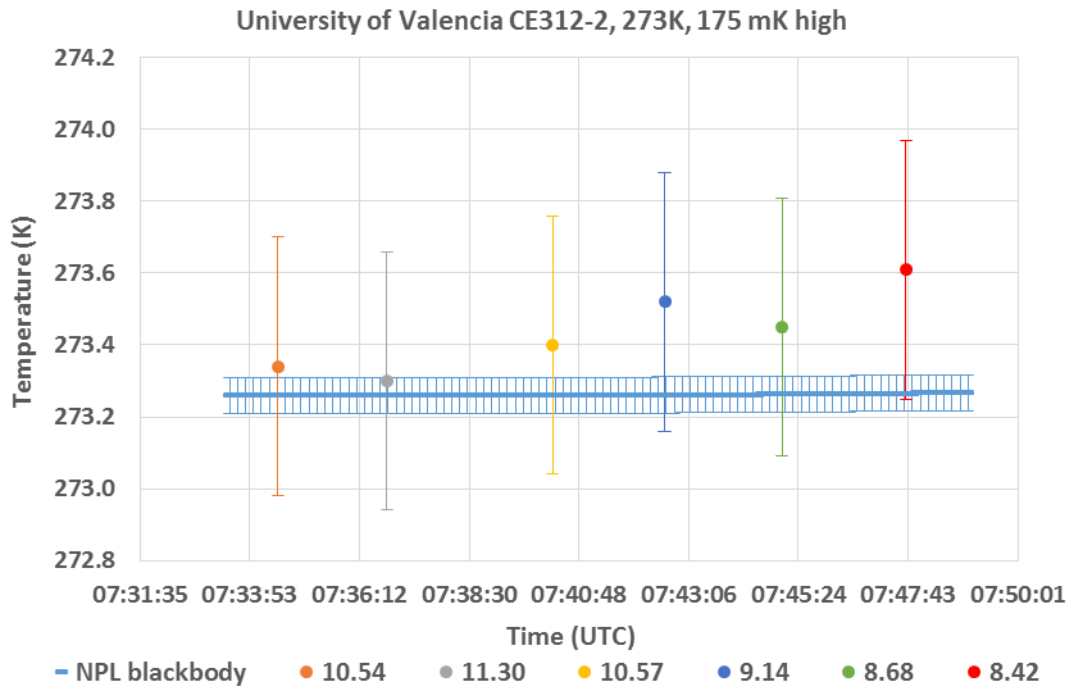


Figure 3.1.10: Plot of the measurements of the different channels of the CIMEL CE312-2 Unit 2 radiometer when it was viewing the NPL reference blackbody while it was maintained at about 0 °C.

Table 3.1.10: The deviation of the different radiometer channels δT of the CIMEL CE312-2 Unit 2 radiometer from the average blackbody temperature, over the measurement interval for a nominal blackbody temperature of about 0 °C.

Channel (μm)	δT (mK)
10.54	79
11.30	39
10.57	139
9.14	259
8.68	189
8.42	349

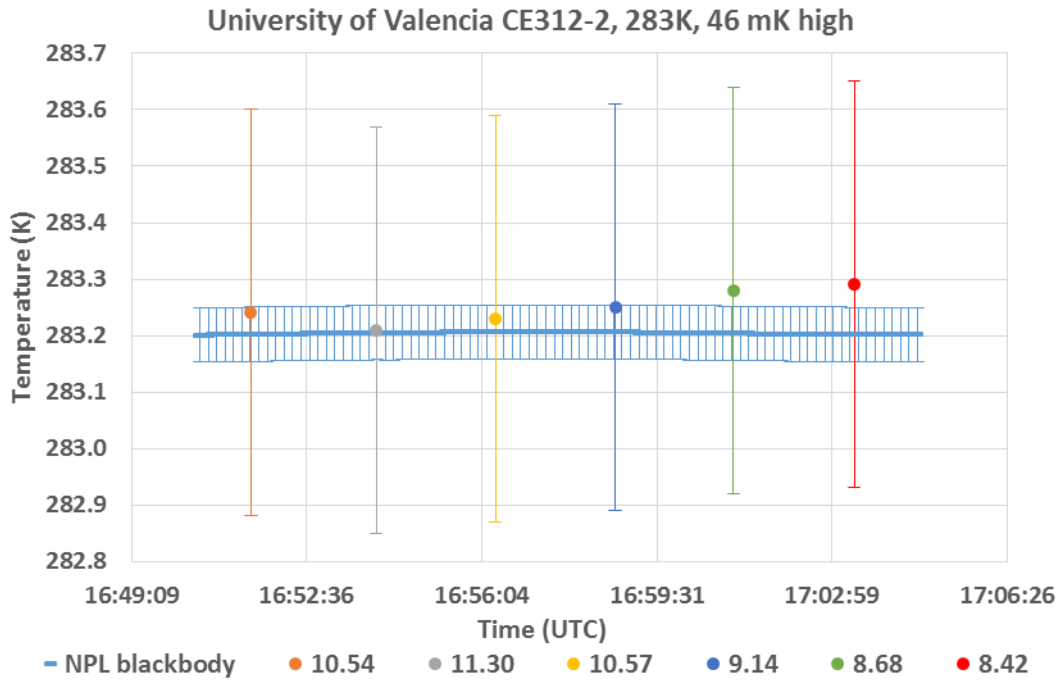


Figure 3.1.11: Plot of the measurements of the different channels of the CIMEL CE312-2 Unit 2 radiometer when it was viewing the NPL reference blackbody while it was maintained at about 10 °C.

Table 3.1.11: The deviation of the different radiometer channels δT of the CIMEL CE312-2 Unit 2 radiometer from the average blackbody temperature, over the measurement interval for a nominal blackbody temperature of about 10 °C.

Channel (μm)	δT (mK)
10.54	36
11.30	6
10.57	26
9.14	46
8.68	76
8.42	86

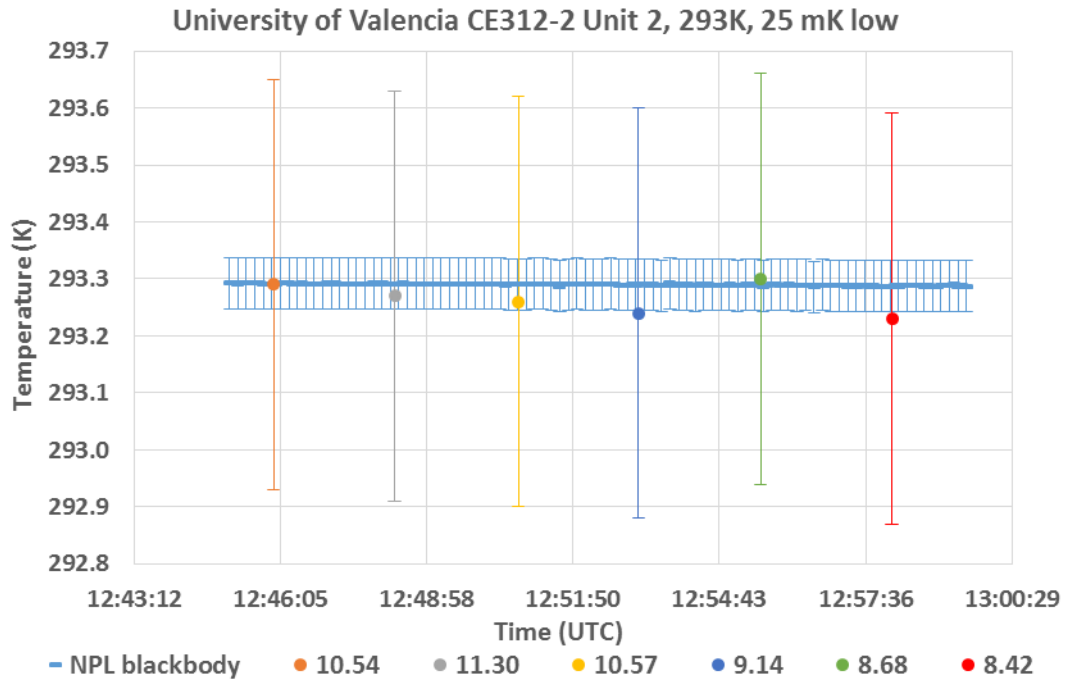


Figure 3.1.12: Plot of the measurements of the different channels of the CIMEL CE312-2 Unit 2 radiometer when it was viewing the NPL reference blackbody while it was maintained at about 20 °C.

Table 3.1.12: The deviation of the different radiometer channels δT of the CIMEL CE312-2 Unit 2 radiometer from the average blackbody temperature, over the measurement interval for a nominal blackbody temperature of about 20 °C.

Channel (μm)	δT (mK)
10.54	0
11.30	-20
10.57	-30
9.14	-50
8.68	10
8.42	-60

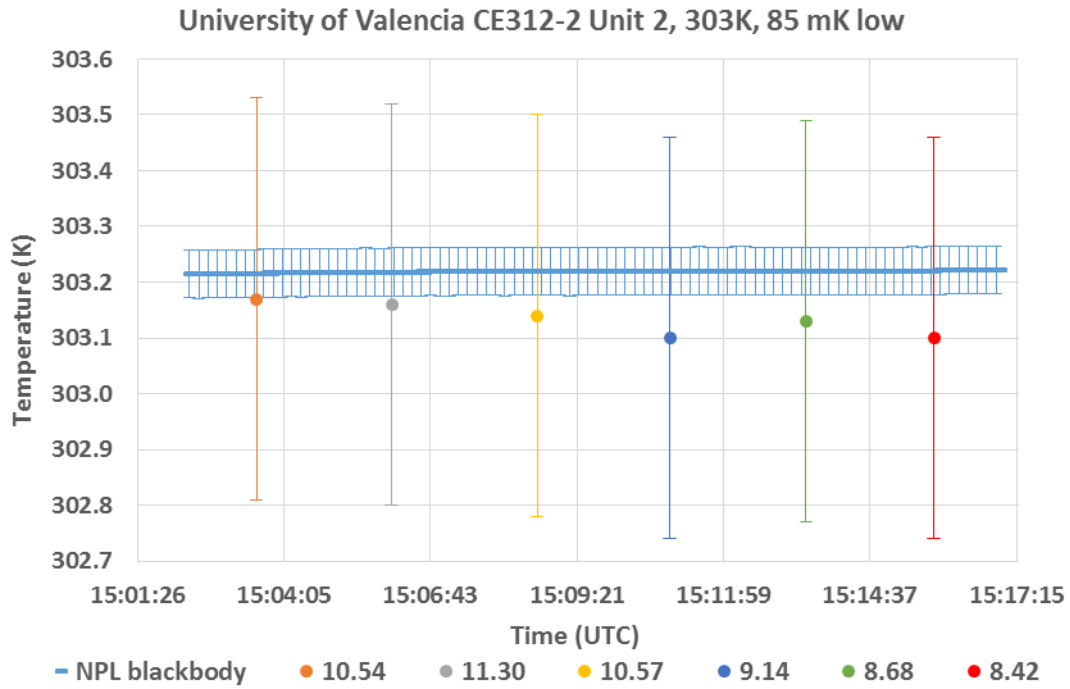


Figure 3.1.13: Plot of the measurements of the different channels of the CIMEL CE312-2 Unit 2 radiometer when it was viewing the NPL reference blackbody while it was maintained at about 30 °C.

Table 3.1.13: The deviation of the different radiometer channels δT of the CIMEL CE312-2 Unit 2 radiometer from the average blackbody temperature, over the measurement interval for a nominal blackbody temperature of about 30 °C.

Channel (μm)	δT (mK)
10.54	-49
11.30	-59
10.57	-79
9.14	-119
8.68	-89
8.42	-119

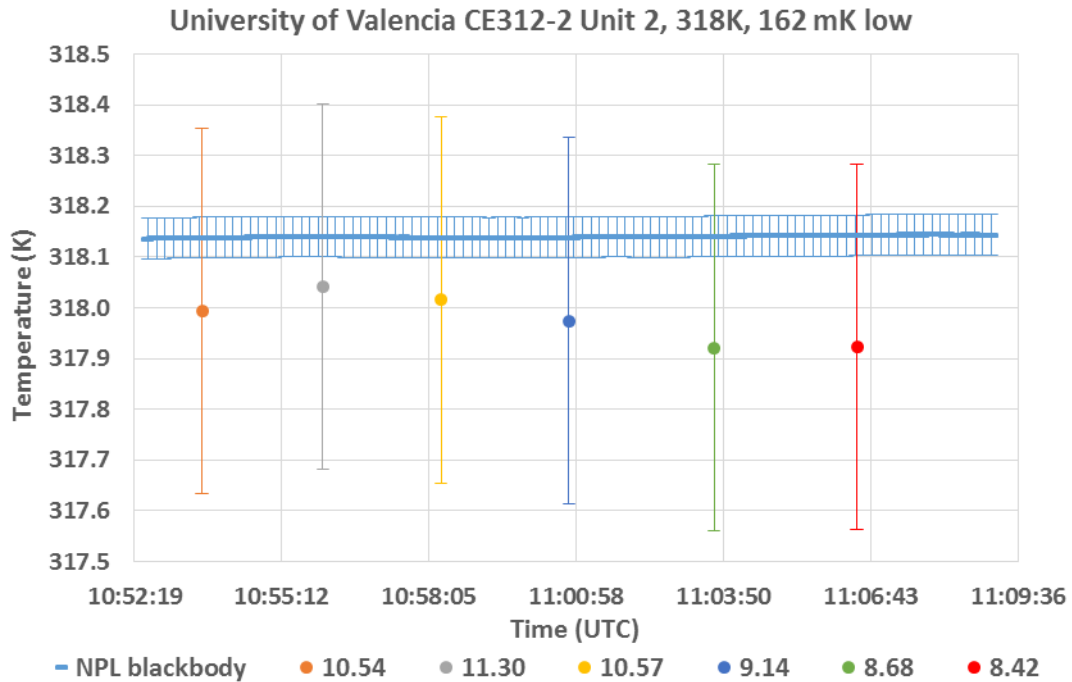


Figure 3.1.14: Plot of the measurements of the different channels of the CIMEL CE312-2 Unit 2 radiometer when it was viewing the NPL reference blackbody while it was maintained at about 45 °C.

Table 3.1.14: The deviation of the different radiometer channels δT of the CIMEL CE312-2 Unit 2 radiometer from the average blackbody temperature, over the measurement interval for a nominal blackbody temperature of about 45 °C.

Channel (μm)	δT (mK)
10.54	-147
11.30	-97
10.57	-125
9.14	-165
8.68	-219
8.42	-217

3.2 MEASUREMENTS MADE BY BALL AEROSPACE

Institute/organisation: Ball Aerospace
10 Longs Peak Drive Broomfield, CO 80021 United States
Contact Name: David Osterman
Email: dosterma@ball.com

3.2.1 Description of radiometer and route of traceability

Make and type of Radiometer

The Ball Experimental Sea Surface Radiometer (BESST) is an imaging radiometer for the 8 μm to 12 μm wavelength range, designed and built by Ball Aerospace & Technologies Corporation.

Outline Technical description of instrument

BESST is an imaging radiometer operated from an aircraft in the nadir pointing orientation. The instrument scans the sea surface in an 18 degree cross track field of view with a 200 pixel wide region of a 2-D format uncooled microbolometer focal plane array. Two sources integrated into the instrument provide calibration to blackbodies, one at the instrument ambient temperature and one at a temperature approximately 12 $^{\circ}\text{C}$ above ambient. BESST measures radiance in three spectral bands simultaneously: 8 to 13 μm , 10.2 to 10.9 μm and 11.3 to 12.1 μm . Further details can be found in: “Absolute Thermal Radiometry from a UAS”, W. S. Good et al, AIAA Infotech@Aerospace, Conference, St. Louis, MO, USA, 2011.

Establishment or traceability route for primary calibration including date of last realisation and breakdown of uncertainty:

BESST was calibrated against a NIST traceable water bath blackbody operated by the University of Miami. Further details of traceability are presented in: W. Emery et al., A Microbolometer Airborne Calibrated Radiometer: The Ball Airborne Calibrated Sea Surface Radiometer, IEEE Transactions On Geosci and Remote Sensing, Vol. 52, No. 12, Dec 2014.

Operational methodology during measurement campaign:

During flight campaigns the focal plane array frame rate is slightly less than 3 frames per sec. A typical measurement cycle comprises 7 seconds of calibration alternating with 53 seconds of radiometric imaging.

Radiometer usage (deployment), previous use of instrument and planned applications.

Recent BESST flight campaigns have radiometrically imaged an oil spill in the Gulf of Mexico and ice flows off the northern coast of Alaska, the latter for the NOAA “Operation Icebridge”.

3.2.2 Uncertainty contributions associated with Ball Aerospace's radiometer

Uncertainty Contribution	Type A Uncertainty in Value / %	Type B Uncertainty in Value / (appropriate units)	Uncertainty in Brightness temperature K	Comment (D. Osterman, 090916)
Repeatability of measurement	U_{Repeat}		0.095	Lab calibration 08/10/16
Repeatability of measurement	U_{Repro}		0.19	Lab calibrations 07/27/16 and 08/10/16
Primary calibration temperature		U_{prim}	0.086 (10 °C) 0.064 (20 °C) 0.086 (30 °C) 0.160 (45 °C)	Electro-Optical Industries CES 200-04-MG; combines temperature accuracy, stability, uniformity
Primary calibration emissivity		+/-0.004 (emissivity)	0.44 (10 °C) 0.46 (20 °C) 0.50 (30 °C) 0.54 (45 °C)	Electro-Optical Industries CES 200-04-MG
Linearity of radiometer		U_{Lin}	0.29 (10 °C) 0.14 (20 °C) 0.15 (30 °C) 0.03 (45 °C)	Deviation from best fit line to 08/10/16 lab measurements, 12 °C to 45 °C
Drift since calibration		0	0	Accounted for in reproducibility
Ambient temperature fluctuations		1.67 (°C room temp pk-pk)	0.08	Assume max ambient temperature pk-pk fluctuation 3 F = 1.67 °C
Atmospheric absorption/emission		0	0	Negligible absorption in 38 mm path length
RMS Total			0.59 (10 °C) 0.54 (20 °C) 0.58 (30 °C) 0.63 (45 °C)	

3.2.3 Comparison of BESST radiometer to NPL reference blackbody

Figures 3.2.1 to 3.2.4 show the measurements completed by the Ball Aerospace radiometer BESST when it was viewing the NPL blackbody maintained at different temperatures. Due to the calibration range of the instrument, only blackbody temperatures in the range 10 °C to 45 °C were measured. The uncertainty bars shown in orange in the figures represent the uncertainties provided by Ball Aerospace associated with the measurements shown in the Figures. Also shown in blue in these Figures are the values of the brightness temperature of the NPL reference blackbody along with their combined uncertainty values.

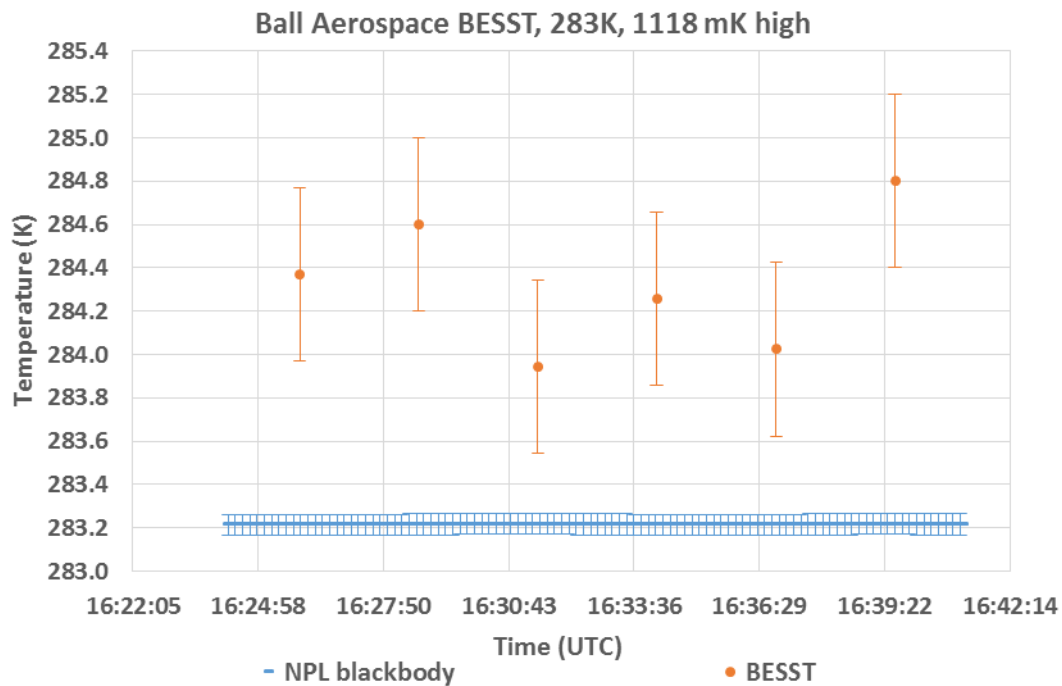


Figure 3.2.1: The Ball Aerospace radiometer BESST viewing the NPL blackbody maintained at about 10 °C. The deviation of the BESST radiometer from the average blackbody temperature over the measurement interval was 1118 mK.

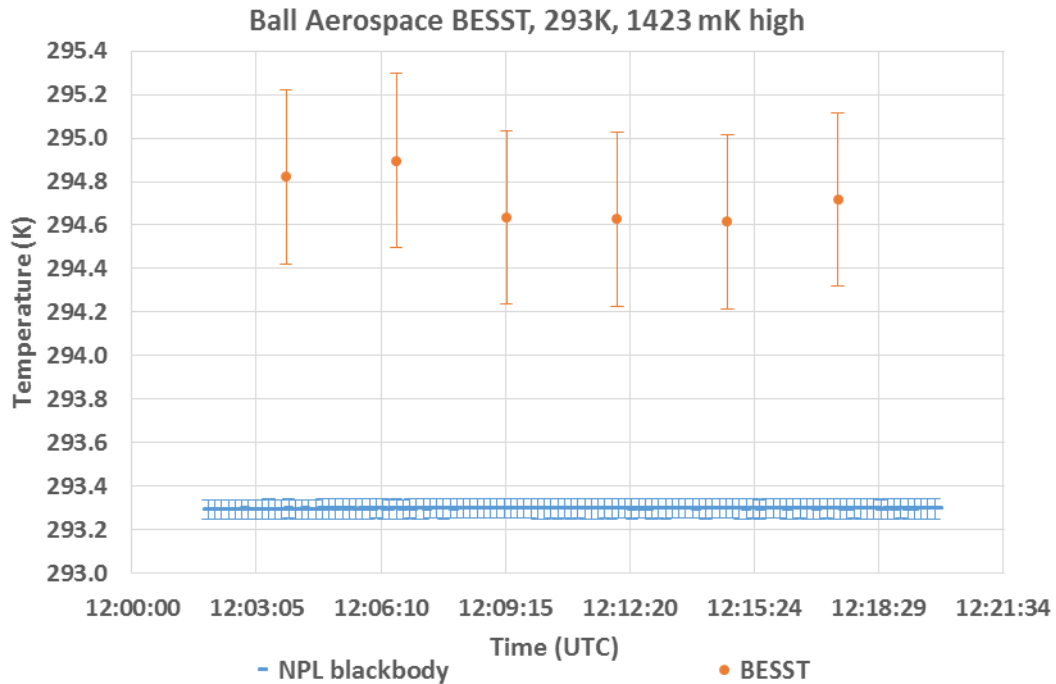


Figure 3.2.2: The Ball Aerospace radiometer BESST viewing the NPL blackbody maintained at about 20 °C. The deviation of the BESST radiometer from the average blackbody temperature over the measurement interval was 1423 mK.

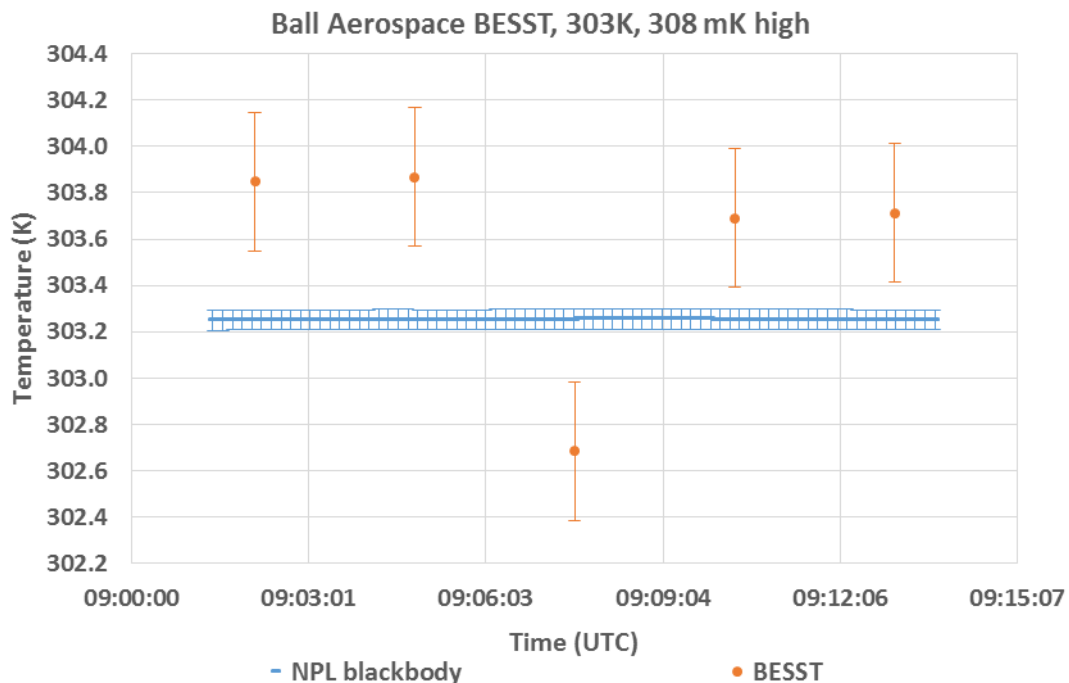


Figure 3.2.3: The Ball Aerospace radiometer BESST viewing the NPL blackbody maintained at about 30 °C. The deviation of the BESST radiometer from the average blackbody temperature over the measurement interval was 308 mK.

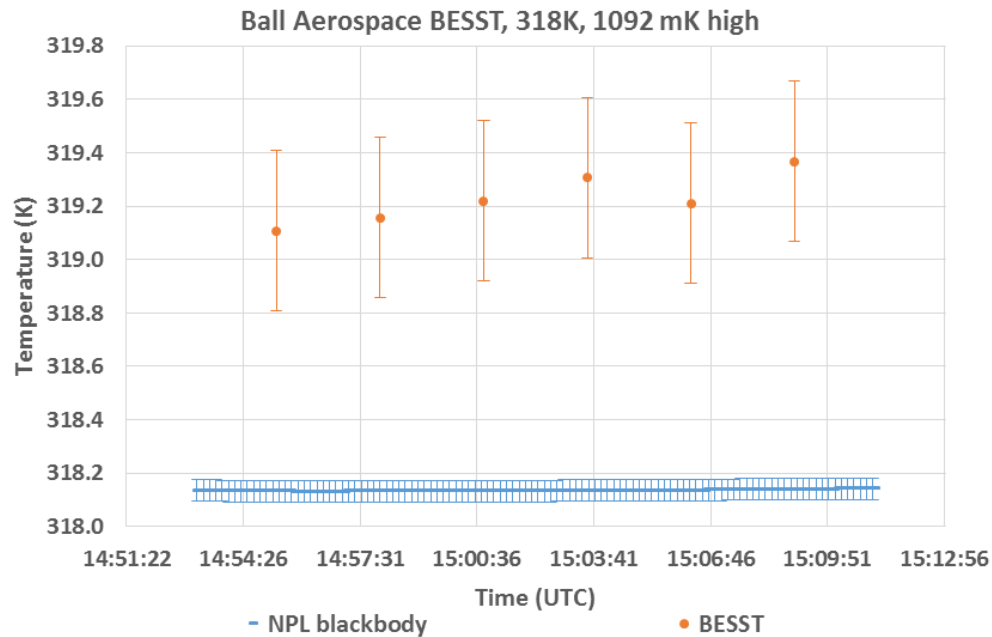


Figure 3.2.4: The Ball Aerospace radiometer BESST viewing the NPL blackbody maintained at about 45 °C. The deviation of the BESST radiometer from the average blackbody temperature over the measurement interval was 1092 mK.

3.3 MEASUREMENTS MADE BY KIT

IMK-ASF, Karlsruhe Institute of Technology (KIT)
 Hermann-von-Helmholtz-Platz 1, 76344 Eggenstein-Leopoldshafen, Germany
 Contact Name: Dr. Frank-M. Goettsche
 e-mail: frank.Goettsche@kit.edu

3.3.1 Description of radiometer and route of traceability

Make and type of Radiometer: Heitronics KT15.85 IIP with L6 lens

Outline Technical description of instrument: The KT15.85 IIP is a single channel radiometer based on a pyroelectric infrared detector. This type of sensor links radiance measurements via beam-chopping to internal reference temperature measurements and thermal drift can practically be eliminated. The KT15.85 IIP covers the spectral range from 9.6 μm to 11.5 μm , has an uncertainty of about 0.3K over the temperature range relevant to land surfaces and offers excellent long-term stability. The response time of the surface observing radiometer (serial #11650) was set to 10 sec and its temperature range to -25 °C to +100 °C. The type L6 lens used has a full-view angle of 8.3° and is well-suited for directional measurements.
www.heitronics.com

Establishment or traceability route for primary calibration including date of last realisation and breakdown of uncertainty:

Primary calibrations to within specifications were performed on the 03.07.2015 (serial #11650) and 05.05.2015 (serial #11615) by Heitronics GmbH, Wiesbaden, Germany. Breakdowns of uncertainties are not available.

Operational methodology during measurement campaign:

KIT's standard operational methodology for the KT15.85 IIP radiometer is to take measurements every 10 sec with a Campbell Scientific CR1000 data logger, average these over 1 minute and store the result together with standard deviation. Unfortunately, at the first day of the LICE at NPL the data logger was electrically destroyed: it could only be replaced for the water part (2nd week) and land part (3rd week) of the LICE. The measurements performed in the laboratory (1st week) had to be read directly from the KT15.85 IIP's display, which limited temperature resolution to 0.1 K. The second radiometer (serial #11615, temperature range -100°C to +100°C) was used for blackbody temperatures below -25 °C. Each blackbody temperature was measured 10 times at 10-15 sec intervals and uncertainties were estimated based on manufacturer's specifications. The radiometers were mounted on a tripod, placed directly in front of the blackbody aperture and aligned manually.

Radiometer usage (deployment), previous use of instrument and planned applications.

The KT15.85 IIP's were used for inter-calibrations at KIT's validation stations Dahra, Senegal and Evora, Portugal. They will be deployed for several years in support of KIT's long-term satellite LST validation activities.

3.3.2 Uncertainty Contributions associated KIT's measurements at NPL

Uncertainty Contribution	Type A Uncertainty in Value / %	Type B Uncertainty in Value / (appropriate units)	Uncertainty in Brightness temperature K
Repeatability of measurement	0.12		0.024
Reproducibility of measurement	0.12		0.024
Primary calibration		0.250 K	0.250
Linearity of radiometer		0.070 K	0.070
Drift since calibration		0.176 K	0.176
Temperature resolution		0.050 K	0.050
Ambient temperature fluctuations		0.035 K	0.035
Atmospheric absorption/emission		0.035 K	0.035
RMS total	0.173		0.323

The reported uncertainty is based on a standard uncertainty (coverage factor $k=1$), providing a confidence level of approximately 68%.

Comments:

Uncertainty estimates assume 20 K temperature difference between blackbody and sensor housing. Relative uncertainties are given ‘at reading’ at 20 °C. Estimates are given for a representative emissivity of 0.970 and assume 20 K temperature difference between target and sensor housing. Relative uncertainties are ‘at reading’ at 25°C.

The reported uncertainty is based on a standard uncertainty (coverage factor $k=1$), providing a confidence level of approximately 68%.

3.3.3 Comparison of KIT Heitronics KT15.85 IIP to the NPL reference blackbody

Figures 3.3.1 to 3.3.7 show the measurements completed by the KIT radiometer Heitronics KT15.85 IIP when it was viewing the NPL reference blackbody maintained at different temperatures. The uncertainty bars (shown in orange) in the figures represent the uncertainties provided by KIT associated with the measurements shown in the Figures. Also shown (in blue) in these Figures are the values of the brightness temperature of the blackbody along with its combined uncertainty.

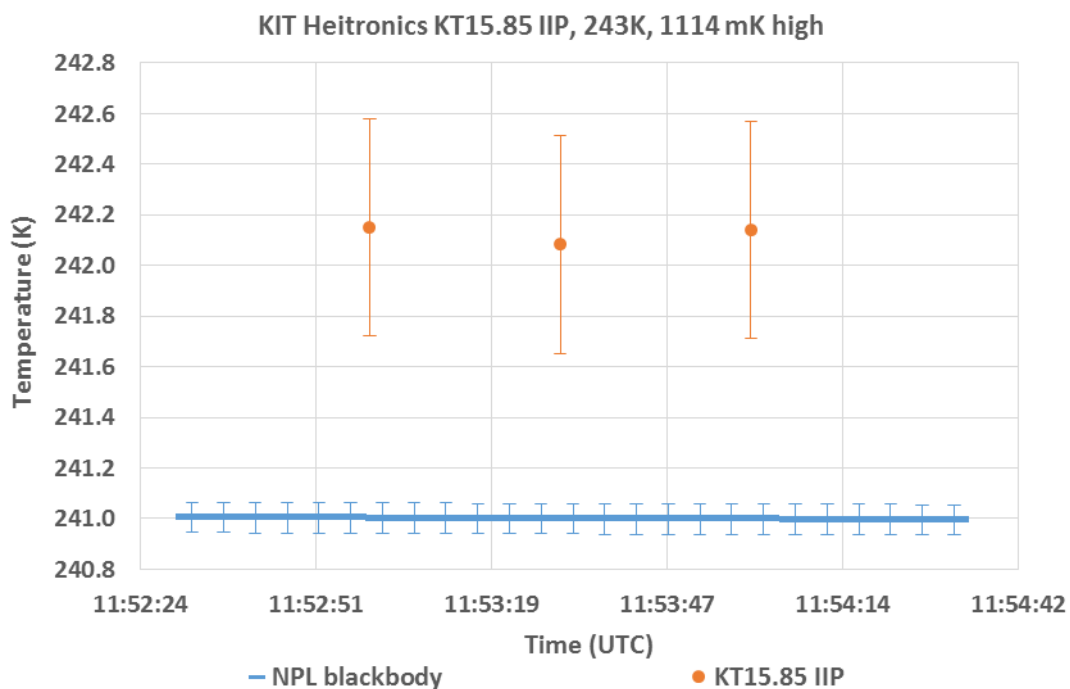


Figure 3.3.1: The KT15.85 IIP KIT radiometer viewing the NPL blackbody maintained at about -30 °C. The deviation of the KIT radiometer δT from the average blackbody temperature over the measurement interval was 1114 mK.

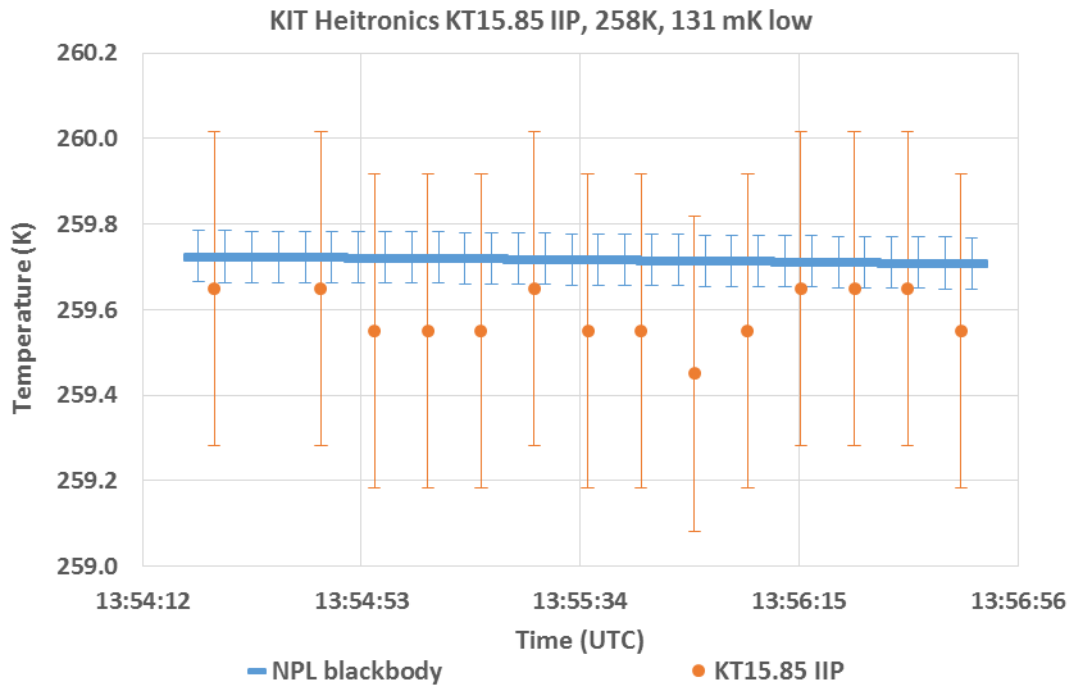


Figure 3.3.2: The KT15.85 IIP KIT radiometer viewing the NPL blackbody maintained at about -15 °C. The deviation of the KIT radiometer δT from the average blackbody temperature over the measurement interval was 131 mK.

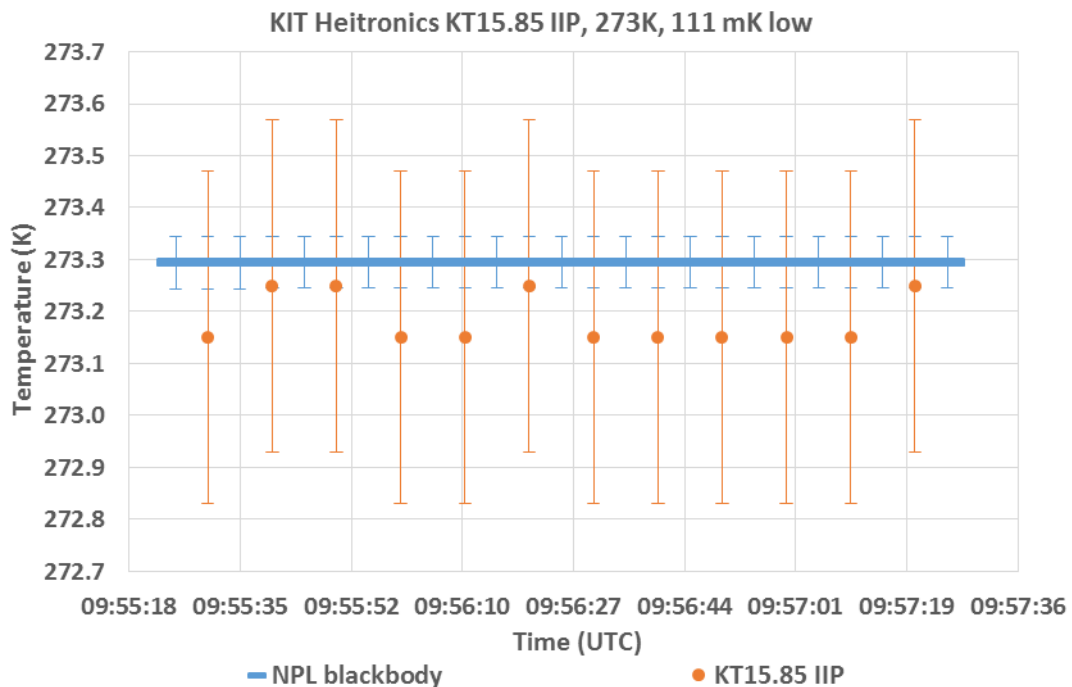


Figure 3.3.3: The KT15.85 IIP KIT radiometer viewing the NPL blackbody maintained at about 0 °C. The deviation of the KIT radiometer δT from the average blackbody temperature over the measurement interval was 111 mK.

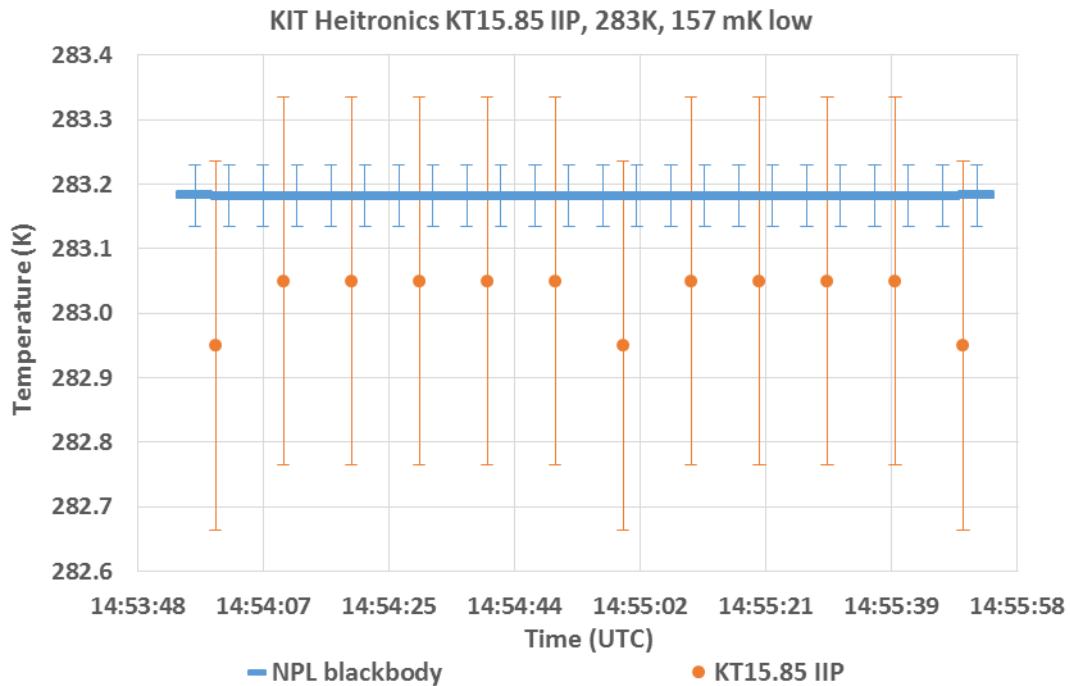


Figure 3.3.4: The KT15.85 IIP KIT radiometer viewing the NPL blackbody maintained at about 10 °C. The deviation of the KIT radiometer δT from the average blackbody temperature over the measurement interval was 157 mK.

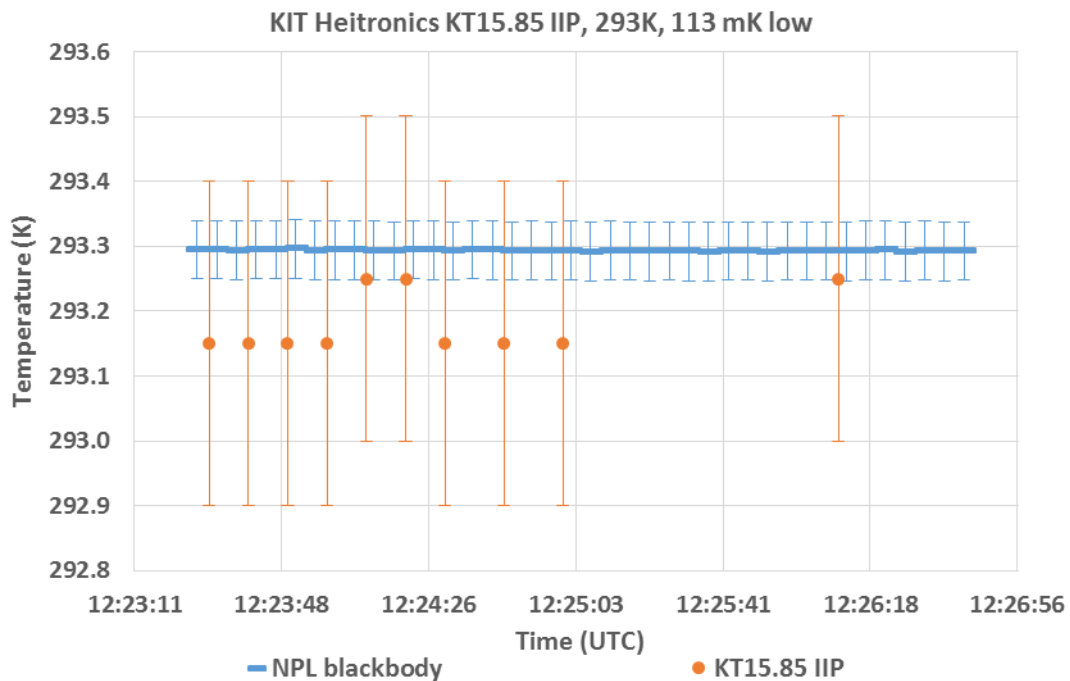


Figure 3.3.5: The KT15.85 IIP KIT radiometer viewing the NPL blackbody maintained at about 20 °C. The deviation of the KIT radiometer δT from the average blackbody temperature over the measurement interval was 113 mK.

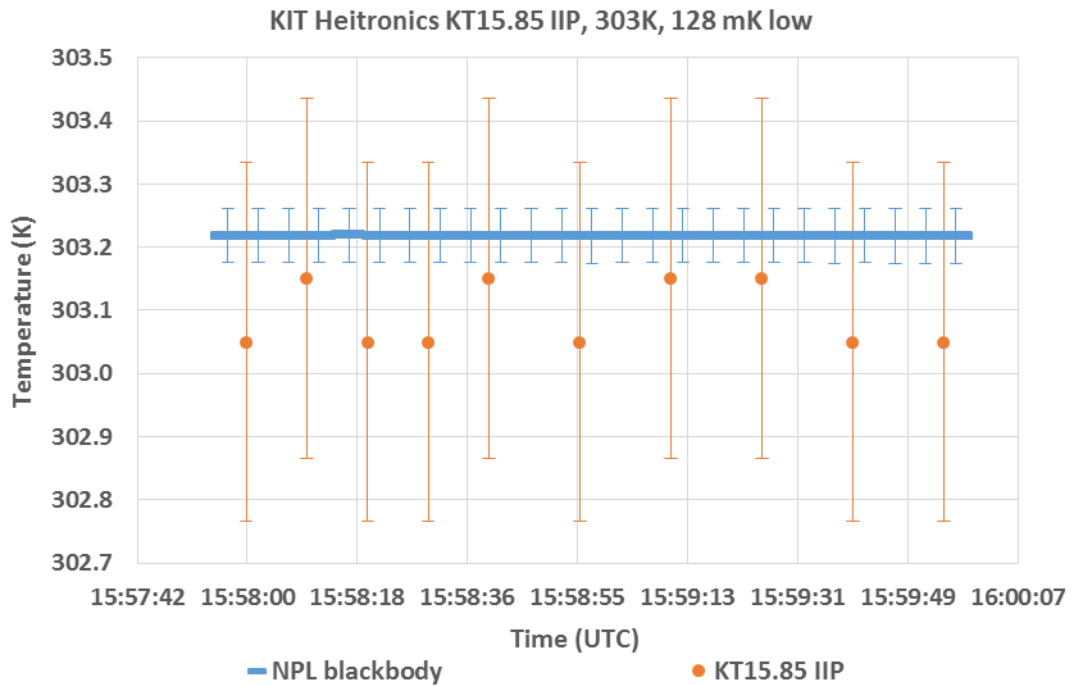


Figure 3.3.6: The KT15.85 IIP KIT radiometer viewing the NPL blackbody maintained at about 30 °C. The deviation of the KIT radiometer δT from the average blackbody temperature over the measurement interval was 128 mK.

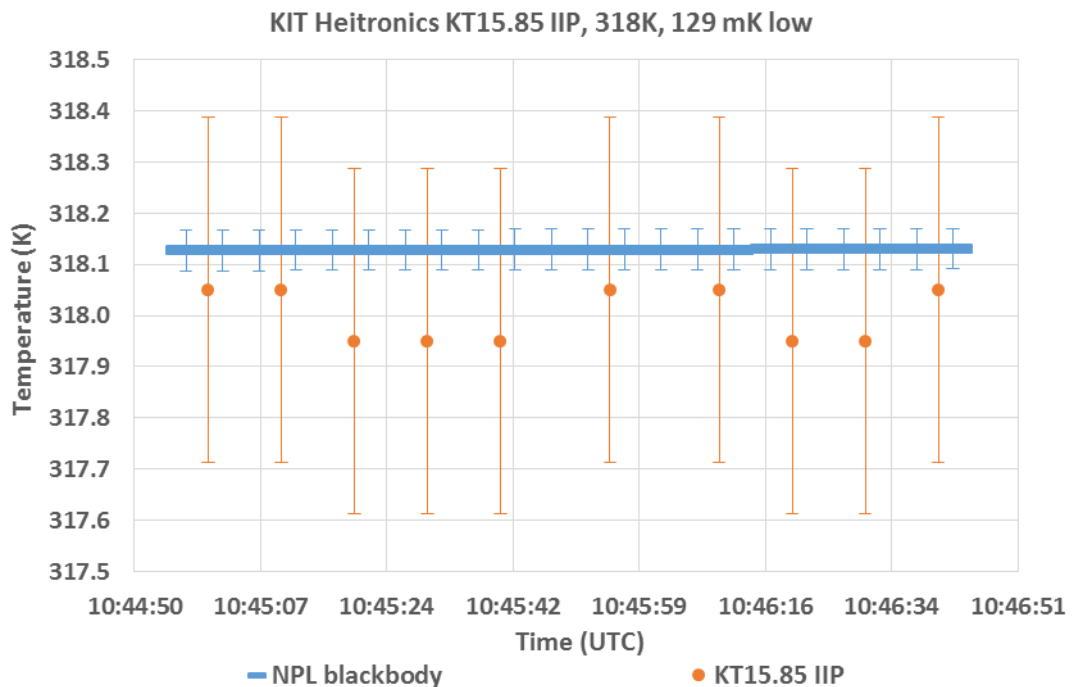


Figure 3.3.7: The KT15.85 IIP KIT radiometer viewing the NPL blackbody maintained at about 45 °C. The deviation of the KIT radiometer δT from the average blackbody temperature over the measurement interval was 129 mK.

3.4 MEASUREMENTS MADE BY ONERA

Institute/organisation: ONERA

2, avenue Edouard Belin – 31055 Toulouse Cedex4 - France.

Contact Name: Laurent Poutier

Email: laurent.poutier@onera.fr

3.4.1 Description of radiometer and route of tracibility

3.4.1.1 Radiometer ONERA-A:

Type:	Heitronics KT19.85 II
Field of View:	95mm target diameter at a 2m range.
Spectral band:	9.6 - 11.5 μ m
Temperature resolution:	± 0.06 °C
Uncertainty in measurement:	± 0.5 °C + 0.7% of the difference between target and housing temperature

3.4.1.2 Radiometer ONERA-B:

Type:	Mikron Spectroradiometer BOMEM MR354SC
Detector Type:	MCT Photoconductive
Spectral response:	3 to 13 μ m @ 4 cm ⁻¹
FOV:	20° full angle
Scan rate:	34 scan/s
Objective:	None

Outline Technical description of the ONERA-B instrument: The spectroradiometer is a Michelson FTIR instrument with two Stirling-cooled detectors in order to cover the 3-13 μ m spectral domain.

3.4.2 Uncertainty contributions associated with ONERA's measurements at NPL

3.4.2.1 Radiometric calibration and uncertainty contribution ONERA-A

The calibration of the radiometer was also checked using the Mikron M345 blackbody, at two specific set temperatures.

The primary calibration error is the one given by the manufacturer (± 0.5 °C plus 0.7% of the difference between target and housing temperature). The Root Mean Square (RMS) difference between the Mikron set temperature and the radiometer output calculated over the 14 datasets acquired in the temperature range of 12 to 55 °C leads to a typical difference below 0.1 K for the radiometer. Therefore, if we consider that this setup can be modelled as a blackbody surrounded by reflective coatings, so that the error in the Mikron source is limited to its temperature accuracy (equal to 0.1 K), then the primary calibration error could be decreased down to $\sqrt{2} \times 0.1 \cong 0.15$ K. This ideal modelling is probably optimistic and the final primary

calibration error is consequently higher. Meanwhile it could be less than the manufacturer’s estimation.

Finally, the uncertainty contributions following the NPL presentation is summed up in Table 3.4.1.

Table 3.4.1: Uncertainty contribution for the Heitronics KT19 radiometers.

Uncertainty Contribution	Type A Uncertainty in Value / %	Type B Uncertainty in Value / (appropriate units)	Uncertainty in Brightness temperature K
Repeatability of measurement	±0.05K		±0.05K
Reproducibility of measurement			<0.05K
Primary calibration		±0.5°C+0.7% ×ΔT _{target-inst}	±0.5°C+0.7% ×ΔT _{target-inst}
Linearity		0.02K	
RMS total			

3.4.2.2 Radiometric calibration and uncertainty contribution ONERA-B

The instrument output is a raw interferogram expressed in Volts as a function of the optical path difference. The spectroradiometer is very sensitive to its internal temperature, especially the beamsplitter temperature, which is maintained around 20 °C above ambient temperature. The calibration is done with the ONERA Mikron M345 4-inch by 4-inch blackbody. The radiance spectrum is processed using the two reference acquisitions corresponding to the two Mikron set temperatures and the interferogram of the NPL source. The uncertainty is estimated by combining the following uncertainty sources.

Sources of uncertainty considered for the error budget.

- Blackbody temperature short term stability ±0.04 K (dependent on the reference measurement)
- Blackbody temperature accuracy ±0.1 K (bias common to the 2 reference measurements)
- Blackbody emissivity accuracy ±0.01
- Skin Bomem temperature uncertainty ±4 K

The overall uncertainty is shown in the Table 3.4.2 below, for the different reference blackbody temperatures. Logically, when extrapolating regarding the calibration values, the uncertainty grows. The retrieved brightness temperature tends to exhibit a noticeable spectral signature when the measured temperature is outside the calibration interval. This extrapolation behaviour is probably due to the non-linearity of the detector and/or issues with the calibration source model.

Table 3.4.2: Calibration temperatures and estimated uncertainty for the brightness temperatures derived from the BOMEM spectroradiometer.

Set temperature of the experiment	Calibration first temperature (°C)	Calibration second temperature (°C)	RMS uncertainty for the brightness temperature (K)
-15	12	45	0.4
0	15	40	0.3
10	15	40	0.24
20	15	40	0.2
30	20	40	0.19
45	30	55	0.2

3.4.3 Comparison of radiometer to the NPL reference blackbody

3.4.3.1 Comparison of ONERA-A Unit 1 to the NPL reference blackbody

Figures 3.4.1 to 3.4.7 show the measurements completed by the ONERA-A Heitronics KT19.85 II radiometer Unit 1 when it was viewing the NPL reference blackbody maintained at different temperatures. The uncertainty bars (shown in orange) in the figures represent the uncertainty values provided by ONERA which correspond to the measurements shown in the Figures. Also shown in blue in these Figures are the values of the brightness temperature of the NPL reference blackbody along with their combined uncertainty values.

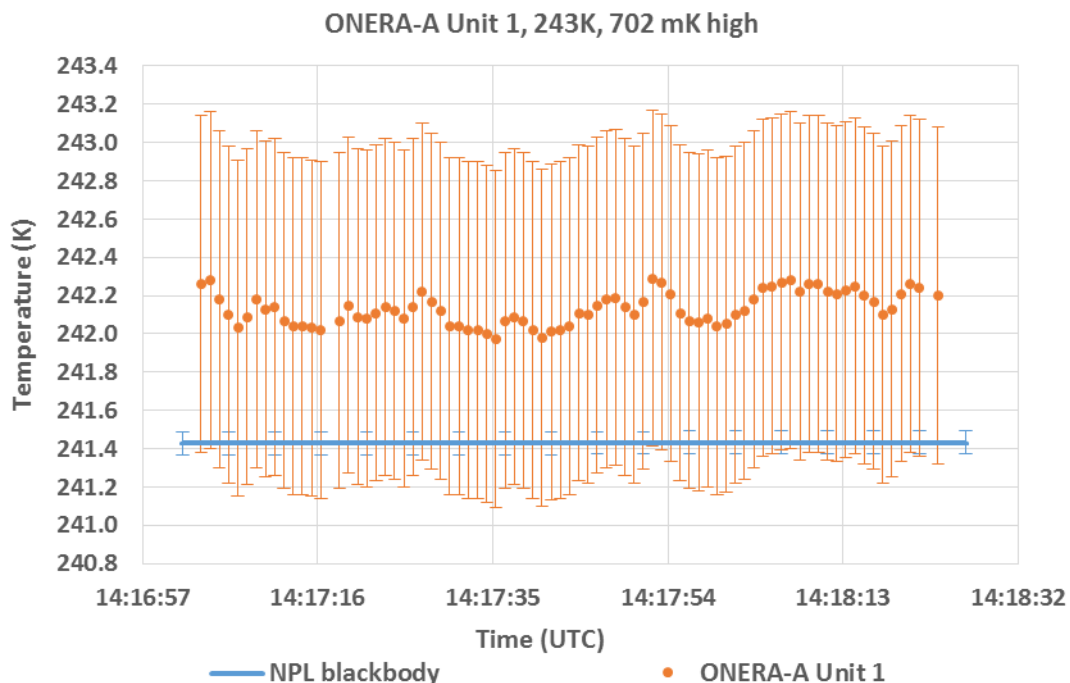


Figure 3.4.1: The KT19.85 II ONERA-A radiometer Unit 1 viewing the NPL blackbody maintained at about -30 °C. The deviation of the ONERA radiometer δT from the average blackbody temperature over the measurement interval was 702 mK

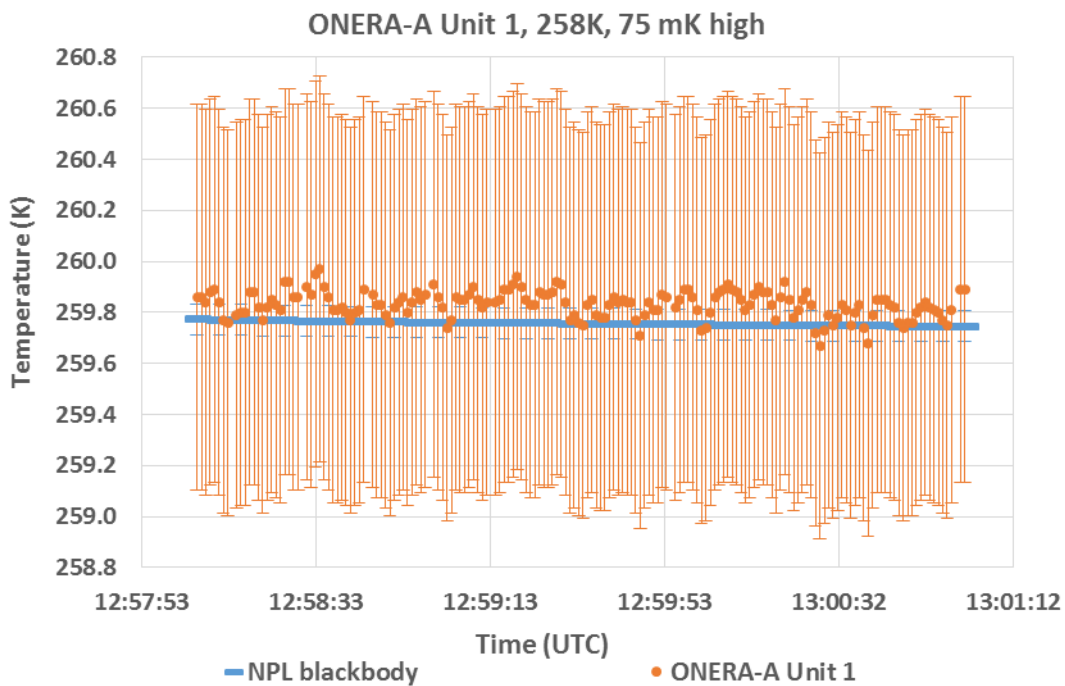


Figure 3.4.2: The KT19.85 II ONERA-A radiometer Unit 1 viewing the NPL blackbody maintained at about -15 °C. The deviation of the ONERA radiometer δT from the average blackbody temperature over the measurement interval was 75 mK.

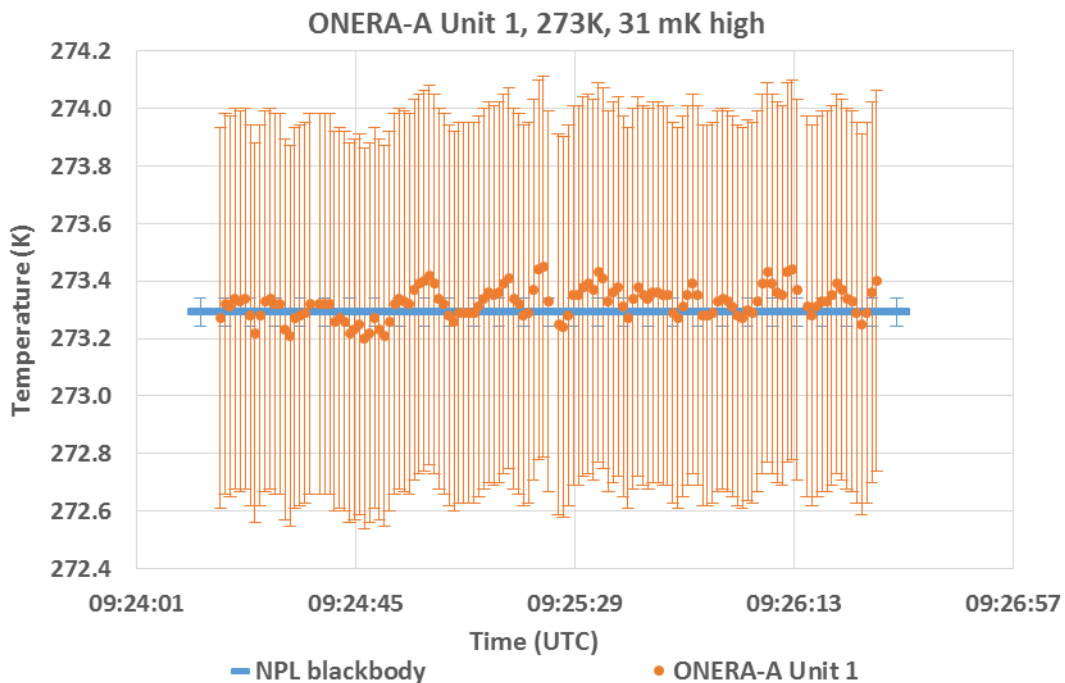


Figure 3.4.3: The KT19.85 II ONERA-A radiometer Unit 1 viewing the NPL blackbody maintained at about 0 °C. The deviation of the ONERA radiometer δT from the average blackbody temperature over the measurement interval was 31 mK.

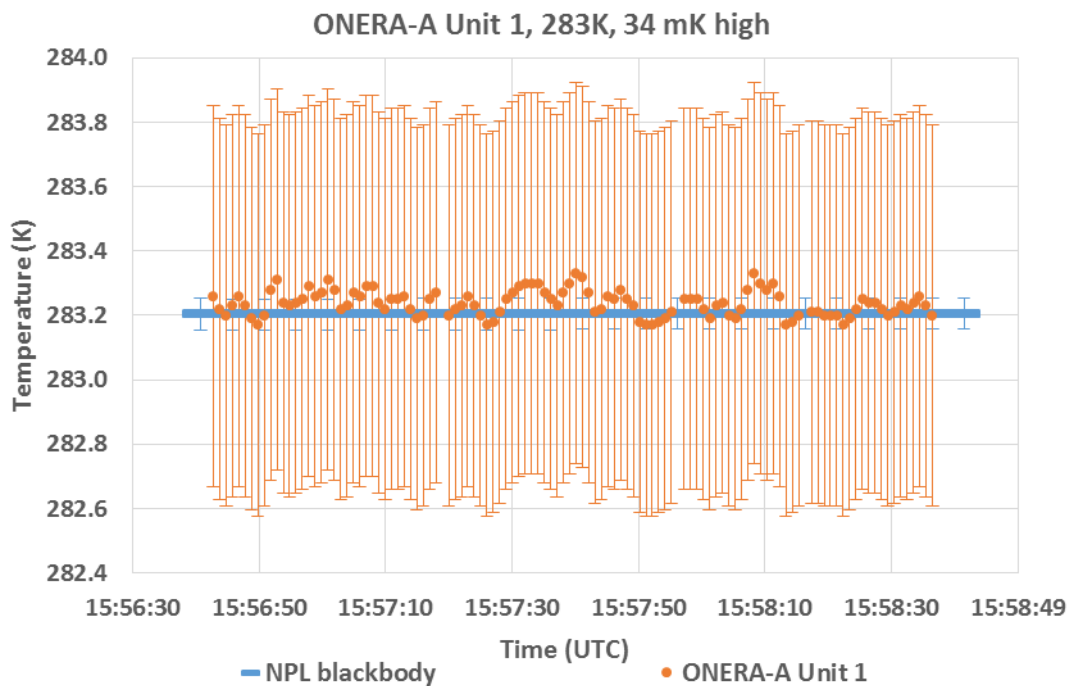


Figure 3.4.4: The KT19.85 II ONERA-A radiometer Unit 1 viewing the NPL blackbody maintained at about 10 °C. The deviation of the ONERA radiometer δT from the average blackbody temperature over the measurement interval was 34 mK.

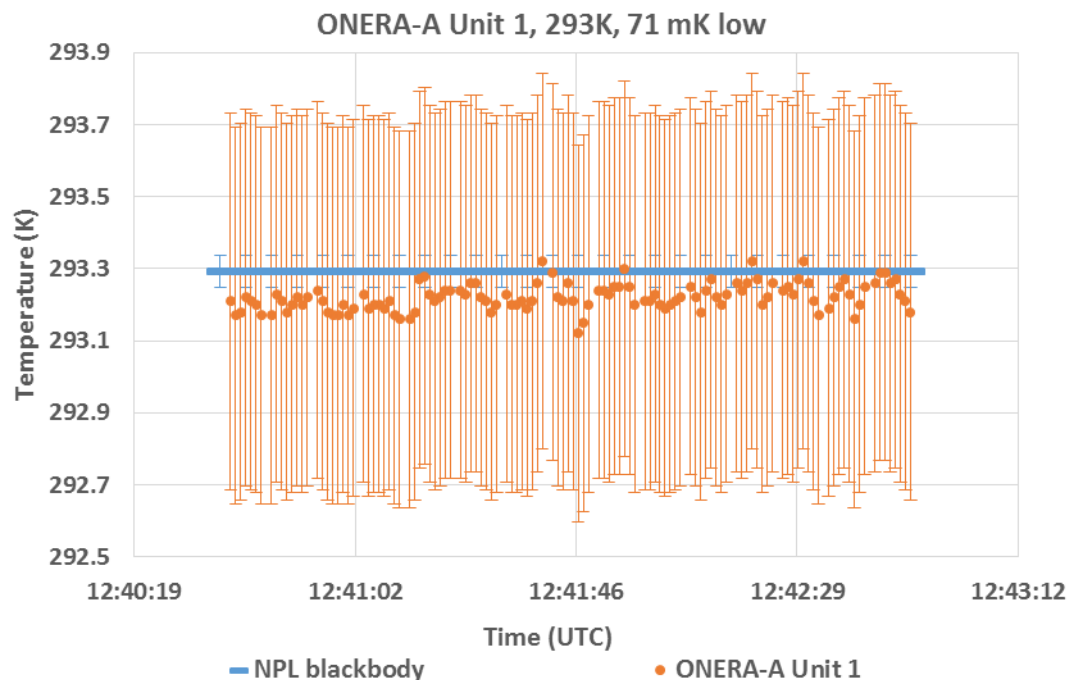


Figure 3.4.5: The KT19.85 II ONERA-A radiometer Unit 1 viewing the NPL blackbody maintained at about 20 °C. The deviation of the ONERA radiometer δT from the average blackbody temperature over the measurement interval was 71 mK.

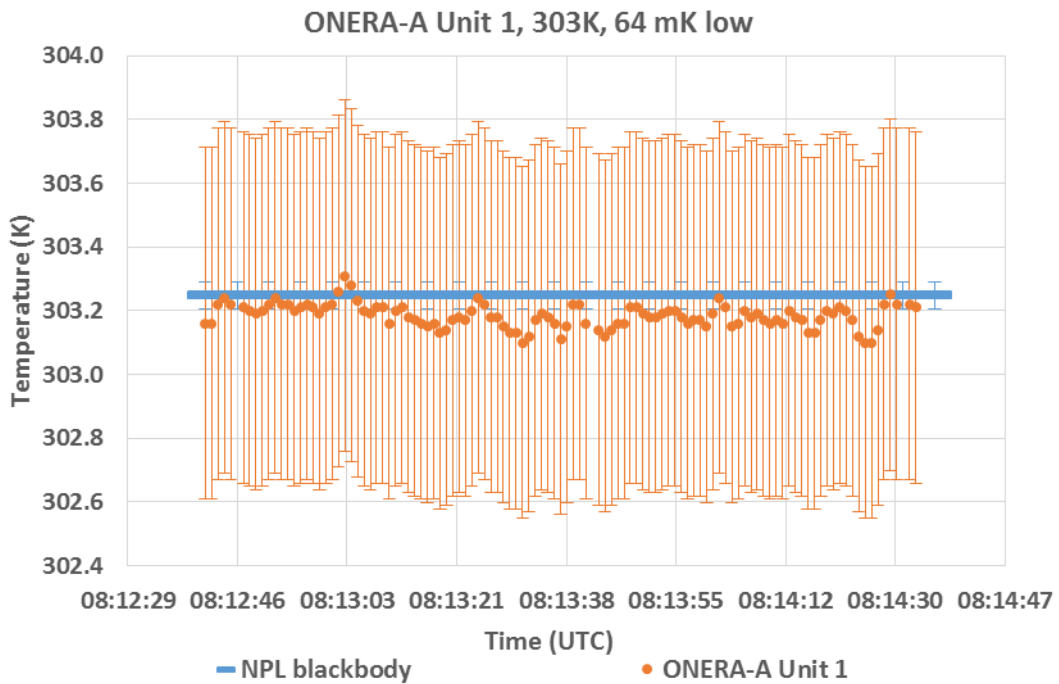


Figure 3.4.6: The KT19.85 II ONERA-A radiometer Unit 1 viewing the NPL blackbody maintained at about 30 °C. The deviation of the ONERA radiometer δT from the average blackbody temperature over the measurement interval was 64 mK.

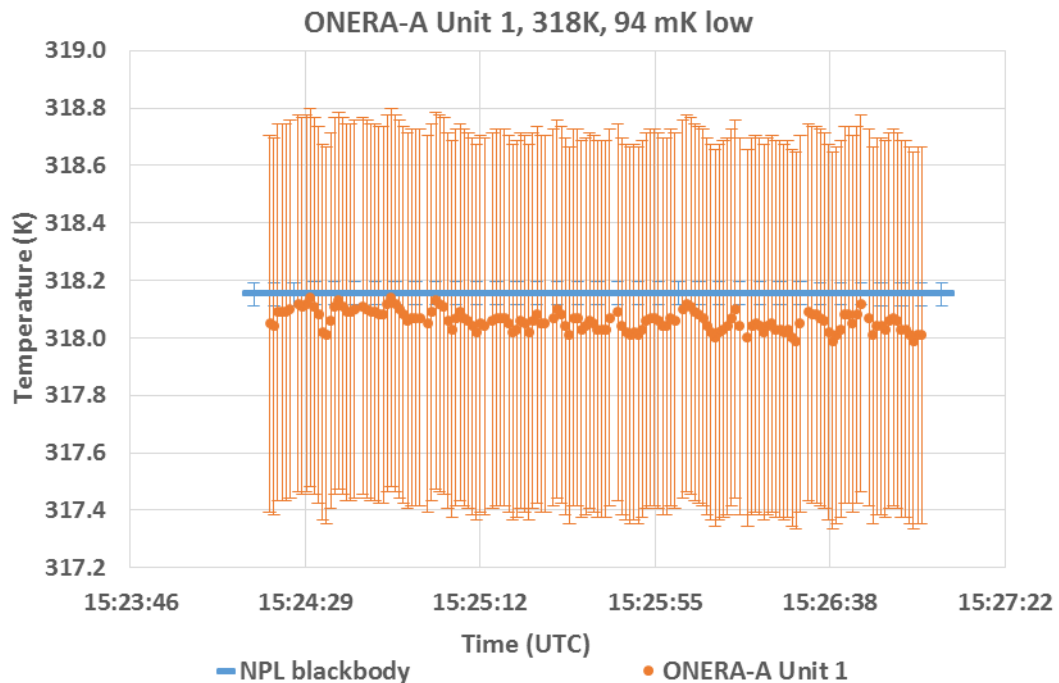


Figure 3.4.7: The KT19.85 II ONERA-A radiometer Unit 1 viewing the NPL blackbody maintained at about 45 °C. The deviation of the ONERA radiometer δT from the average blackbody temperature over the measurement interval was 94 mK.

3.4.3.2 Comparison of ONERA-A Unit 2 to the NPL reference blackbody

Figures 3.4.8 to 3.4.14 show the measurements completed by the ONERA-A radiometer unit 2 when it was viewing the NPL blackbody maintained at different temperatures. The uncertainty bars (shown in orange) in the Figures represent the uncertainty values provided by ONERA which correspond to the measurements shown in the Figures. Also shown in blue in these Figures are the values of the brightness temperature of the NPL reference blackbody along with their combined uncertainty values.

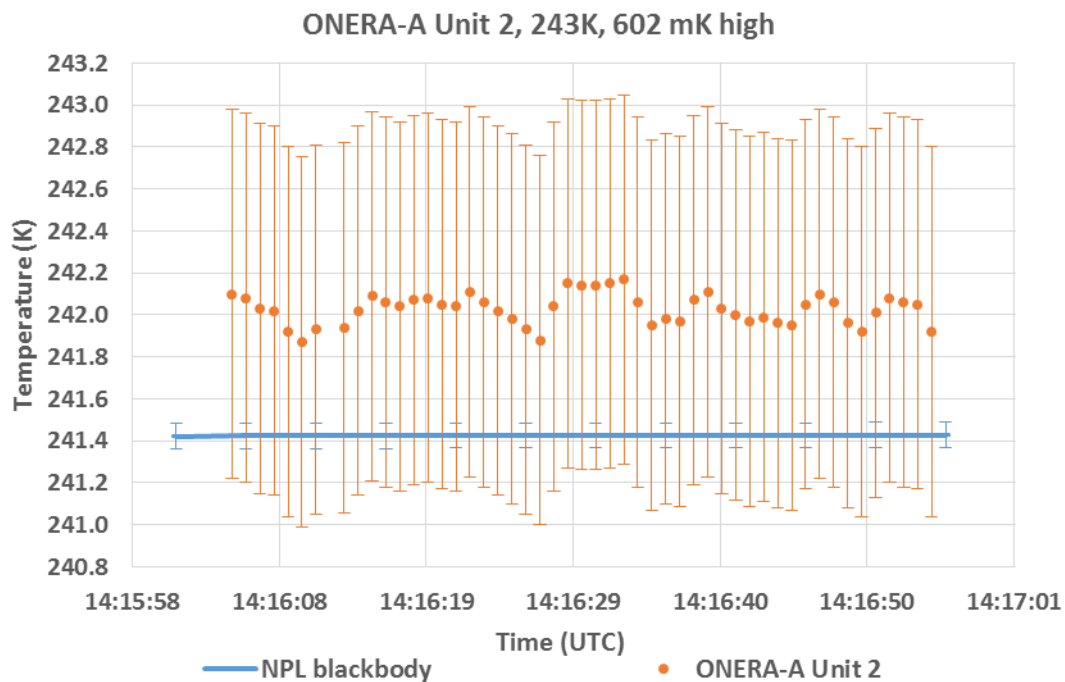


Figure 3.4.8: The KT19.85 II ONERA-A radiometer Unit 2 viewing the NPL blackbody maintained at about $-30\text{ }^{\circ}\text{C}$. The deviation of the ONERA radiometer δT from the average blackbody temperature over the measurement interval was 602 mK.

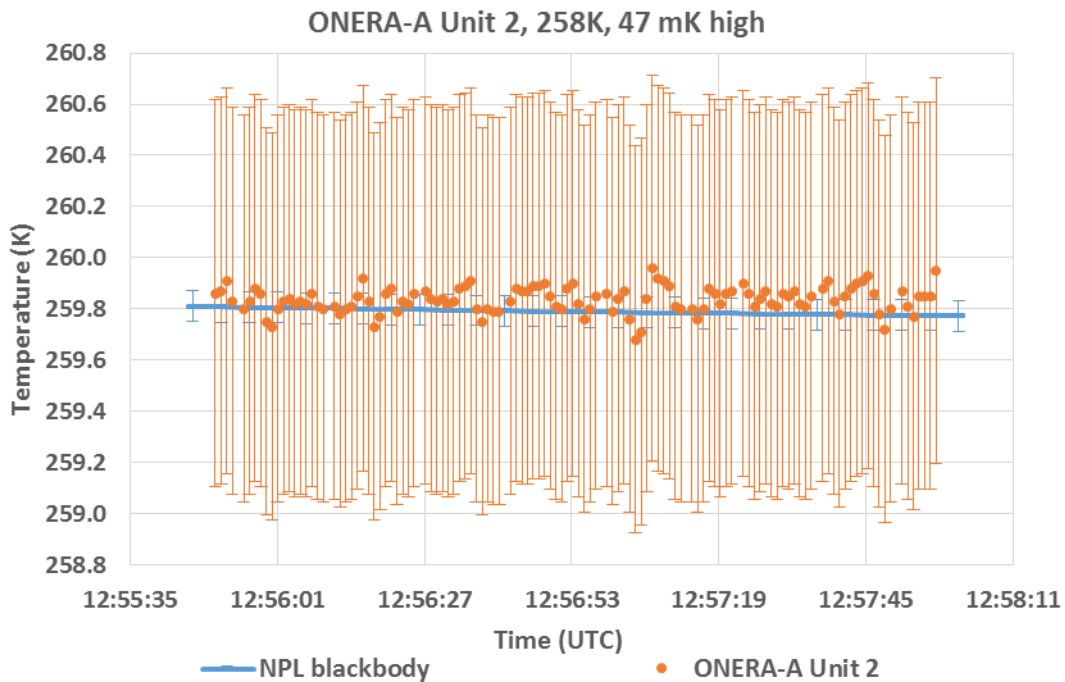


Figure 3.4.9: The KT19.85 II ONERA-A radiometer Unit 2 viewing the NPL blackbody maintained at about -15 °C. The deviation of the ONERA radiometer δT from the average blackbody temperature over the measurement interval was 47 mK.

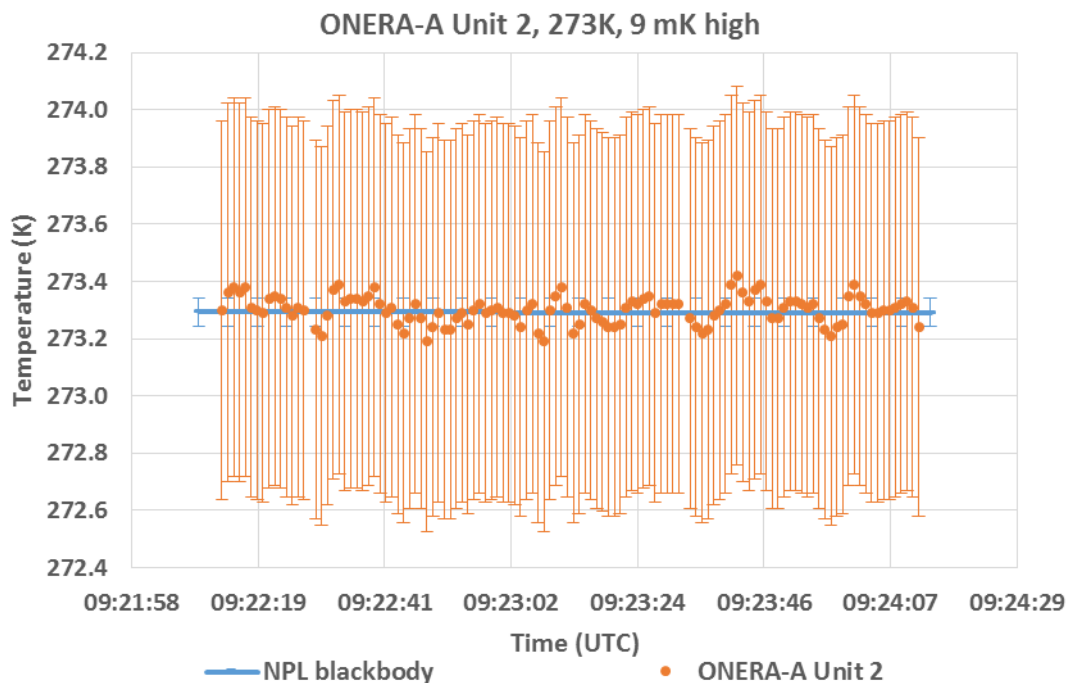


Figure 3.4.10: The KT19.85 II ONERA-A radiometer Heitronics Unit 2 viewing the NPL blackbody at 0 °C. The deviation of the ONERA radiometer δT from the average blackbody temperature over the measurement interval was 9 mK.

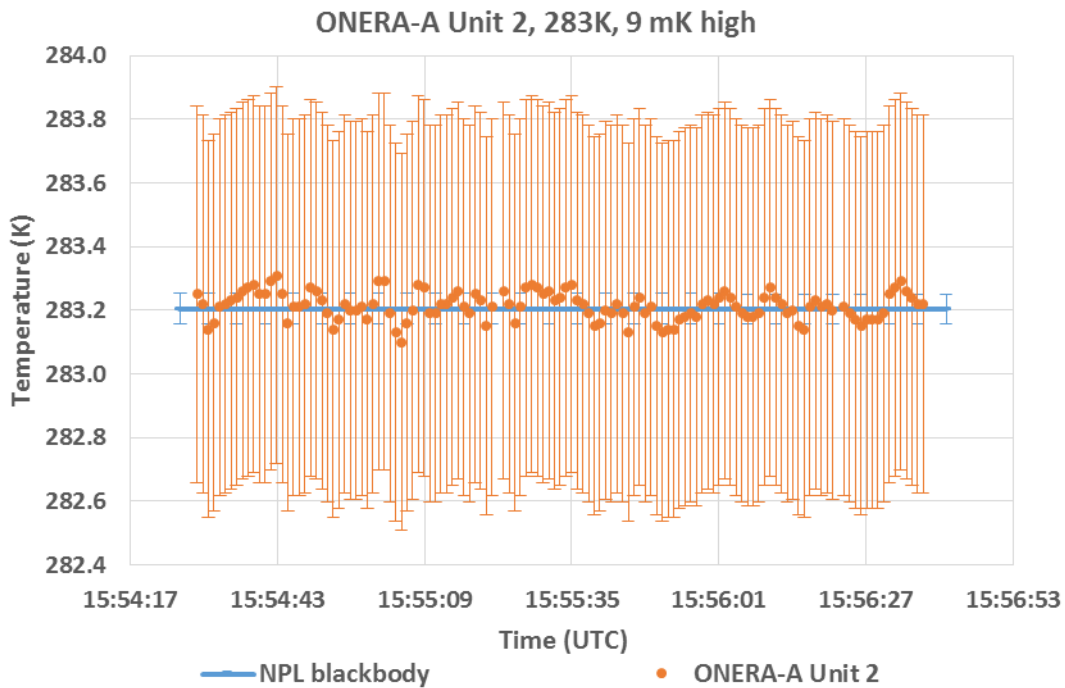


Figure 3.4.11: The KT19.85 II ONERA-A radiometer Unit 2 viewing the NPL blackbody maintained at about 10 °C. The deviation of the ONERA radiometer δT from the average blackbody temperature over the measurement interval was 9 mK.

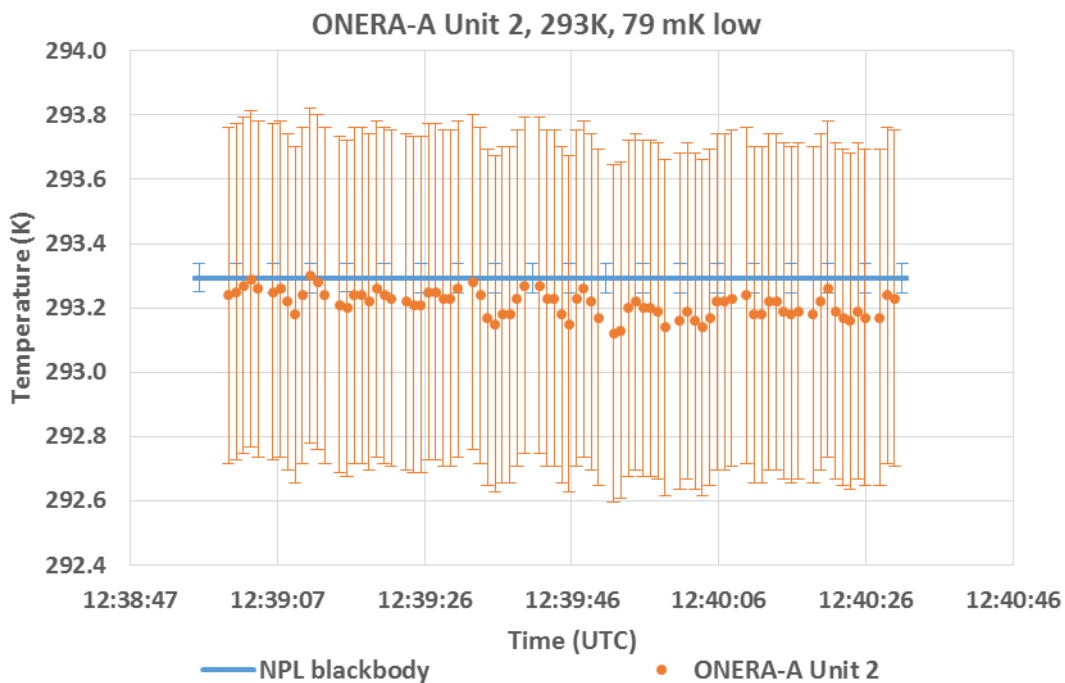


Figure 3.4.12: The KT19.85 II ONERA-A radiometer Unit 2 viewing the NPL blackbody maintained at about 20 °C. The deviation of the ONERA radiometer δT from the average blackbody temperature over the measurement interval was 79 mK.

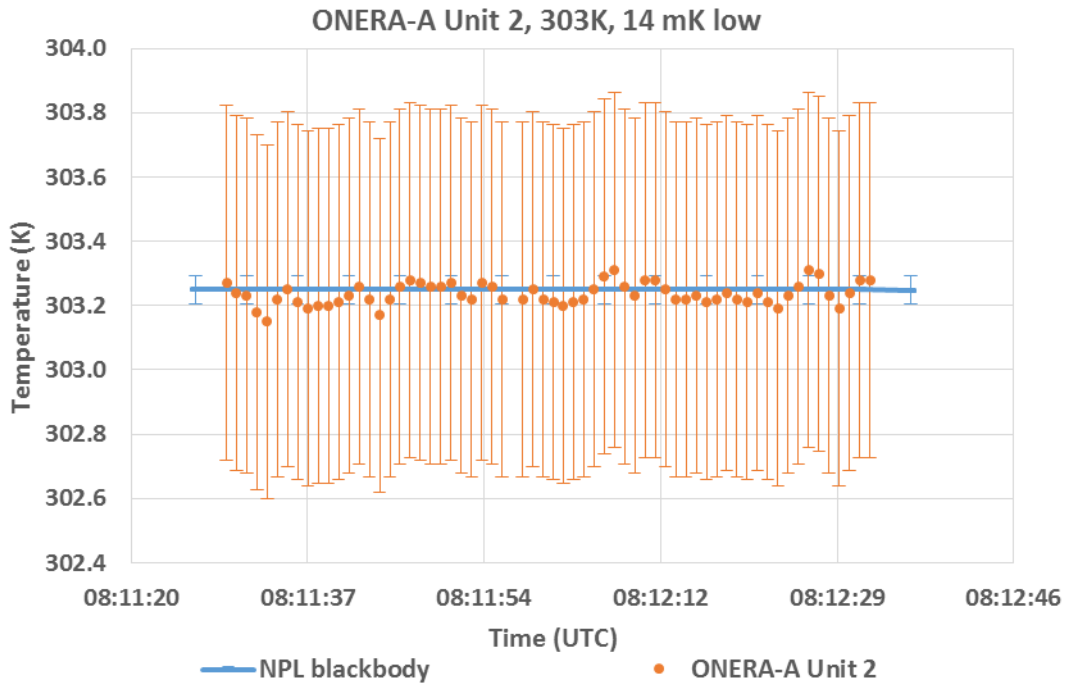


Figure 3.4.13: The KT19.85 II ONERA-A radiometer Unit 2 viewing the NPL blackbody maintained at about 30 °C. The deviation of the ONERA radiometer δT from the average blackbody temperature over the measurement interval was 14 mK.

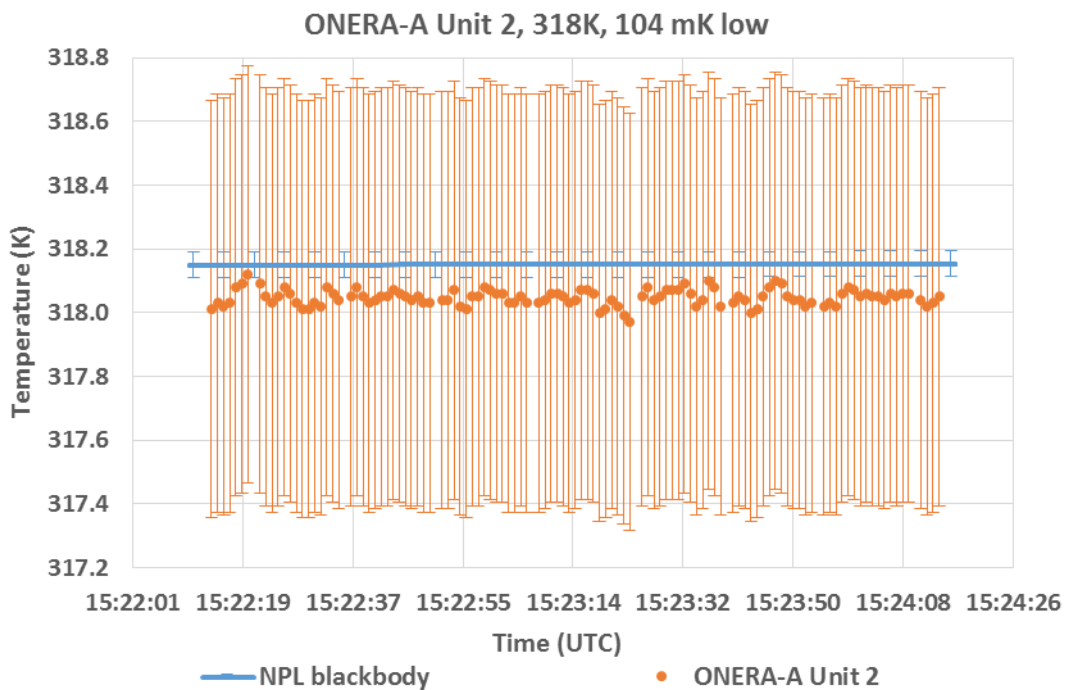


Figure 3.4.14: The KT19.85 II ONERA-A radiometer Unit 2 viewing the NPL blackbody maintained at about 45 °C. The deviation of the ONERA radiometer δT from the average blackbody temperature over the measurement interval was 104 mK.

3.4.3.3 Comparison of ONERA-A Unit 3 to the NPL reference blackbody

Figures 3.4.15 to 3.4.21 show the measurements completed by the ONERA-A radiometer unit 3 when it was viewing the NPL blackbody maintained at different temperatures. The uncertainty bars shown in orange in the figures represent the uncertainty values provided by ONERA which correspond to the measurements shown in the Figures. Also shown in blue in these Figures are the values of the brightness temperature of the NPL reference blackbody along with their combined uncertainty values.

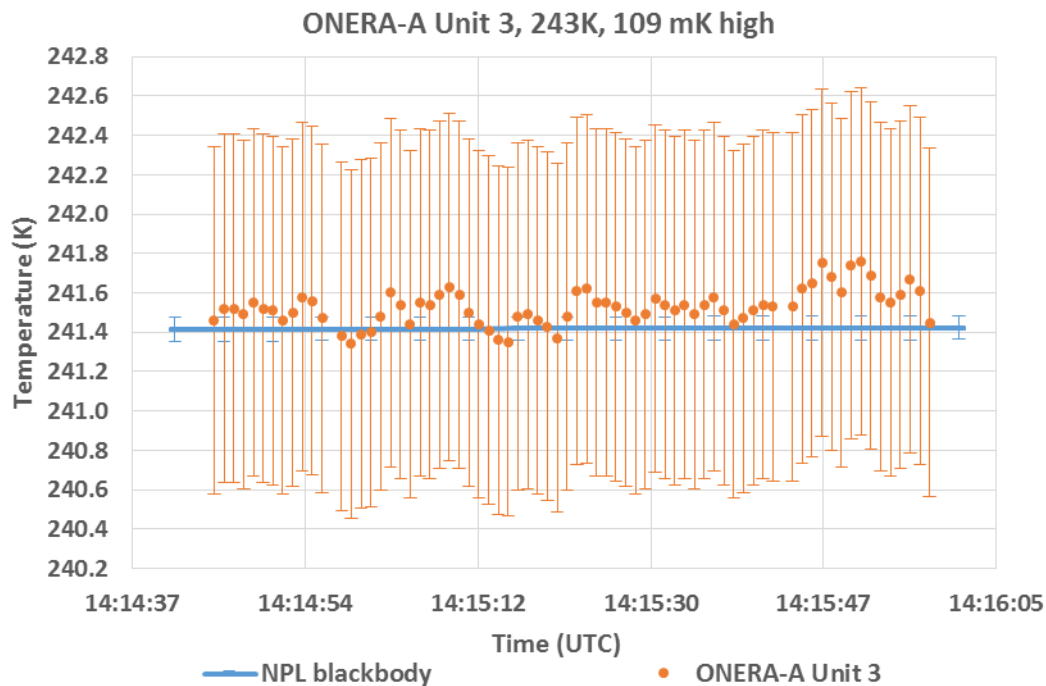


Figure 3.4.15: The KT19.85 II ONERA-A radiometer Unit 3 viewing the NPL blackbody maintained at about $-30\text{ }^{\circ}\text{C}$. The deviation of the ONERA radiometer δT from the average blackbody temperature over the measurement interval was 109 mK.

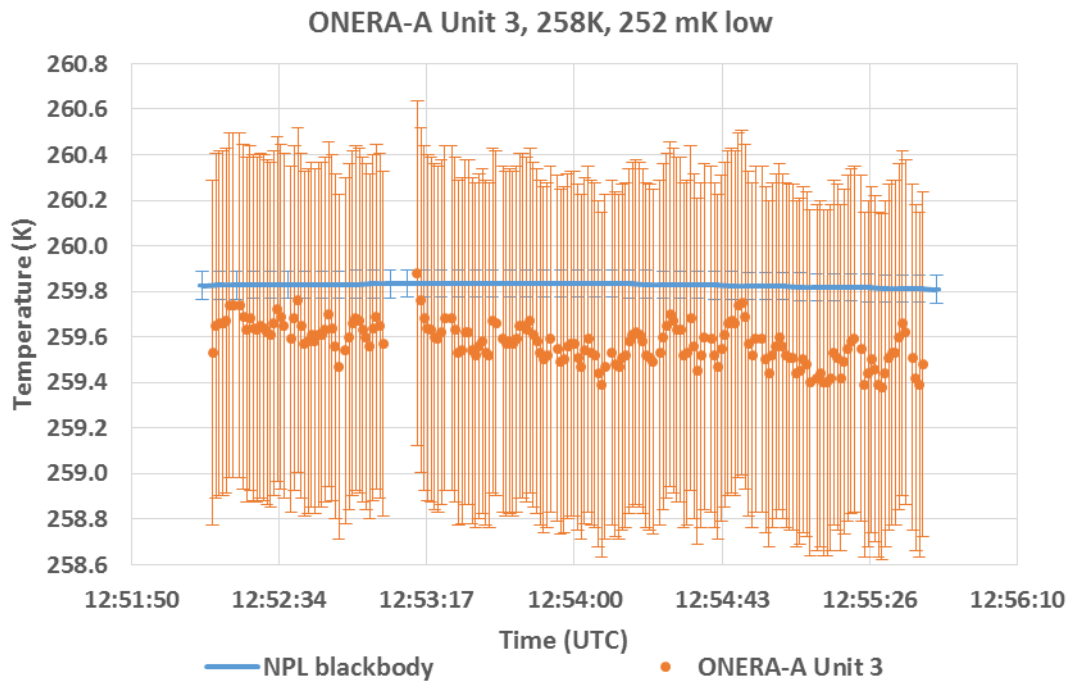


Figure 3.4.16: The KT19.85 II ONERA-A radiometer Unit 3 viewing the NPL blackbody maintained at about -15 C. The deviation of the ONERA radiometer δT from the average blackbody temperature over the measurement interval was 252 mK.

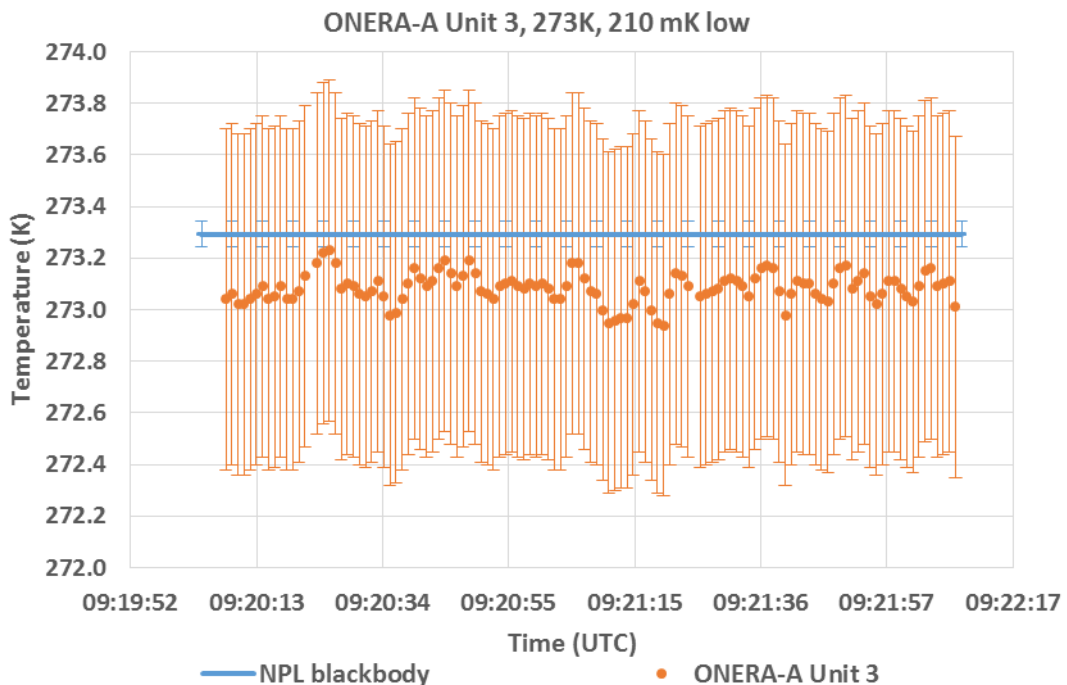


Figure 3.4.17: The KT19.85 II ONERA-A radiometer Unit 3 viewing the NPL blackbody maintained at about 0 °C. The deviation of the ONERA radiometer δT from the average blackbody temperature over the measurement interval was 210 mK.

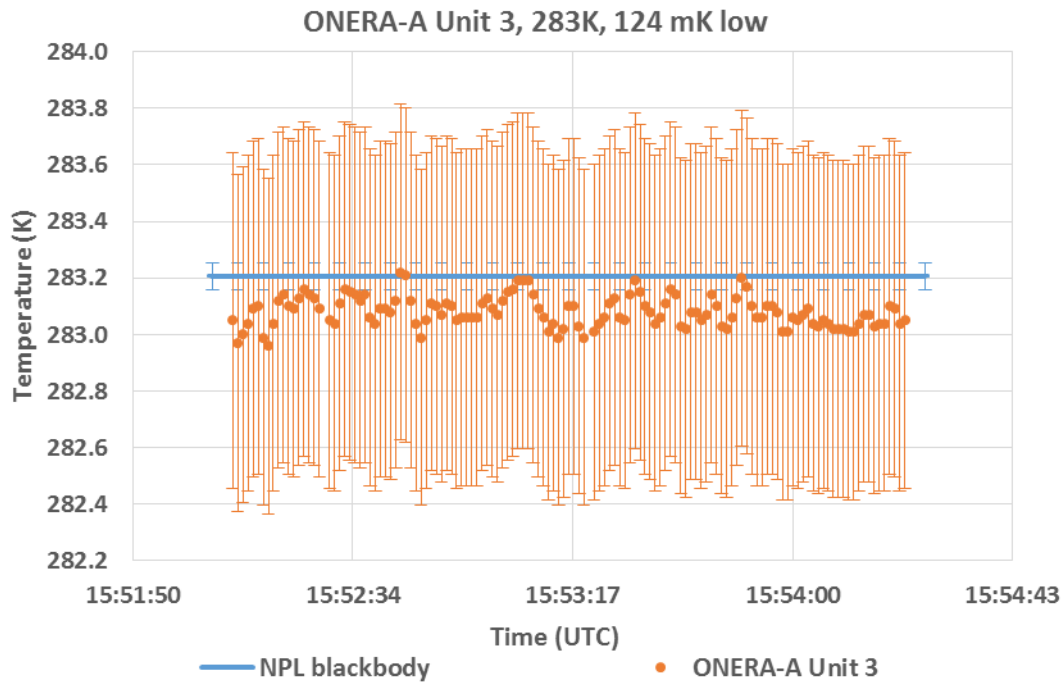


Figure 3.4.18: The KT19.85 II ONERA-A radiometer Unit 3 viewing the NPL blackbody maintained at about 10 °C. The deviation of the ONERA radiometer δT from the average blackbody temperature over the measurement interval was 124 mK.

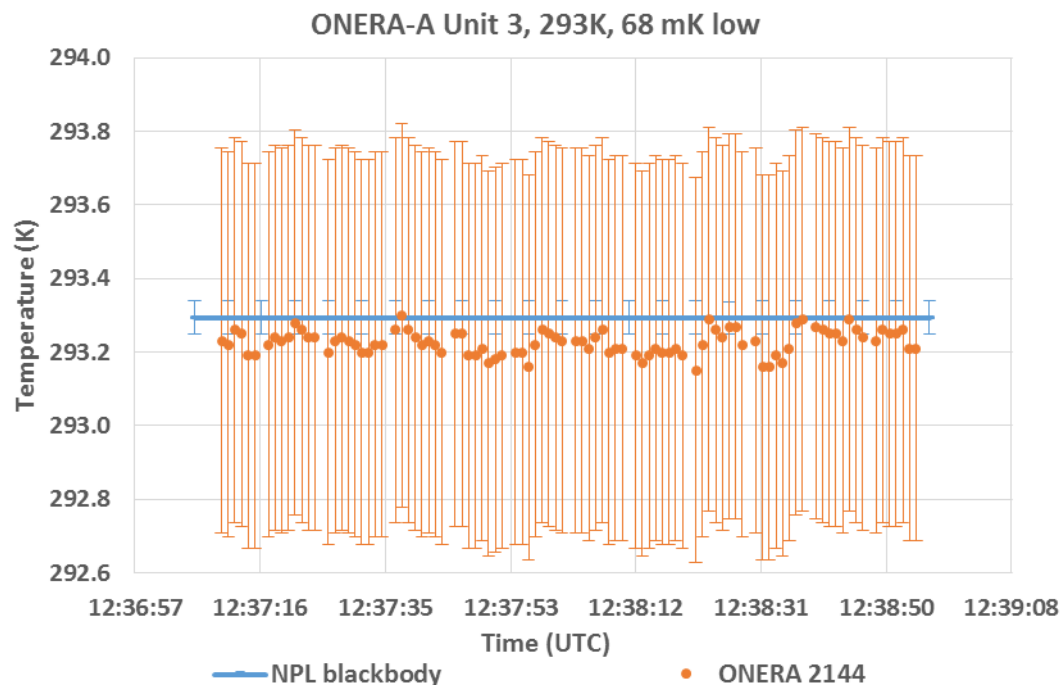


Figure 3.4.19: The KT19.85 II ONERA-A radiometer Unit 3 viewing the NPL blackbody maintained at about 20 °C. The deviation of the ONERA radiometer δT from the average blackbody temperature over the measurement interval was 68 mK.

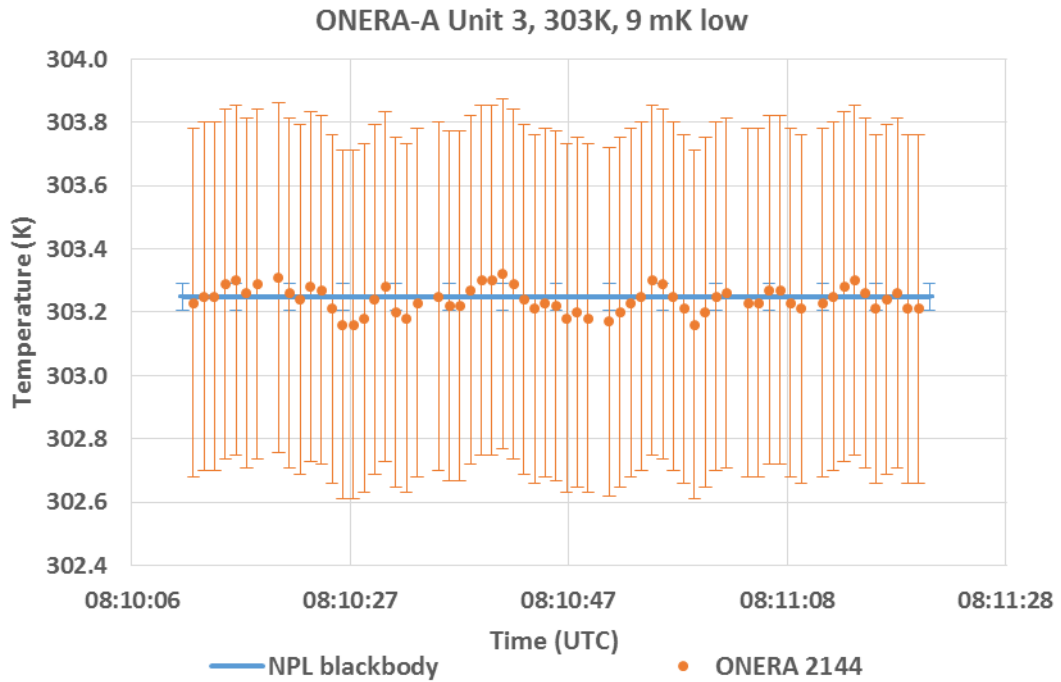


Figure 3.4.20: The KT19.85 II ONERA-A radiometer Unit 3 viewing the NPL blackbody maintained at about 30 °C. The deviation of the ONERA radiometer δT from the average blackbody temperature over the measurement interval was 9 mK.

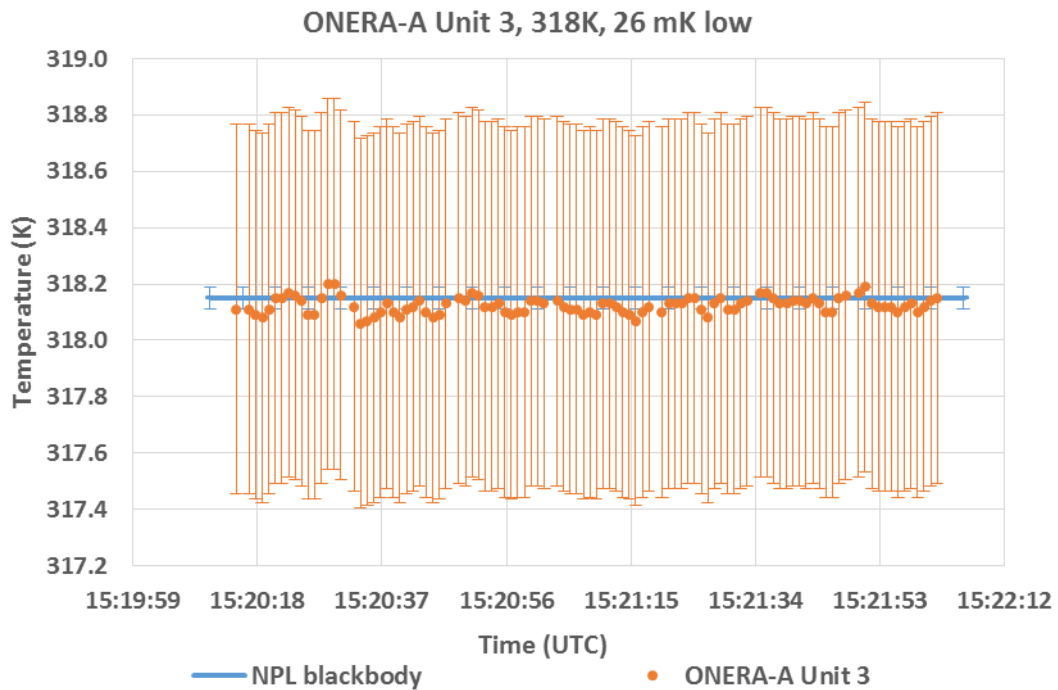


Figure 3.4.21: The KT19.85 II ONERA-A radiometer Unit 3 viewing the NPL blackbody maintained at about 45 °C. The deviation of the ONERA radiometer δT from the average blackbody temperature over the measurement interval was 26 mK.

3.4.3.4 Comparison of ONERA-B to the NPL reference blackbody

Figures 3.4.22 to 3.4.29 show the measurements completed by the ONERA-B Mikron spectroradiometer BOMEM MR354 when it was viewing the NPL blackbody maintained at different temperatures. The uncertainty bars shown in orange in the figures represent the uncertainty values provided by ONERA which correspond to the measurements shown in the Figures. Also shown in blue in these Figures are the values of the brightness temperature of the NPL reference blackbody along with their combined uncertainty values.

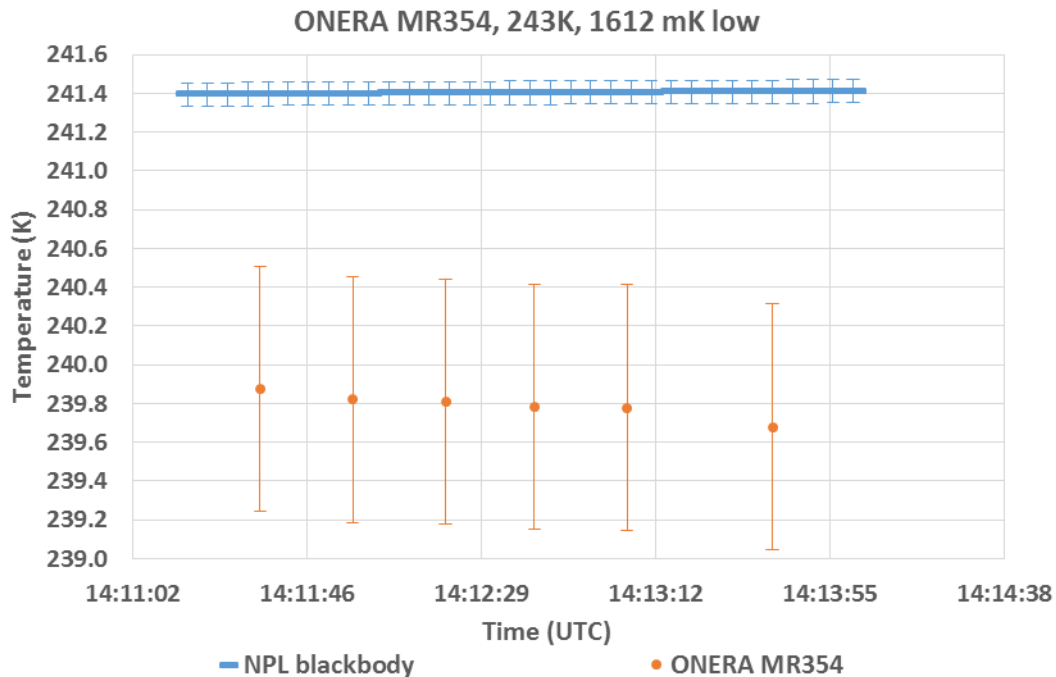


Figure 3.4.22: The ONERA-B Mikron spectroradiometer BOMEM MR354 viewing the NPL blackbody maintained at about -30 °C. The deviation of the ONERA spectroradiometer δT from the average blackbody temperature over the measurement interval was 1612 mK.

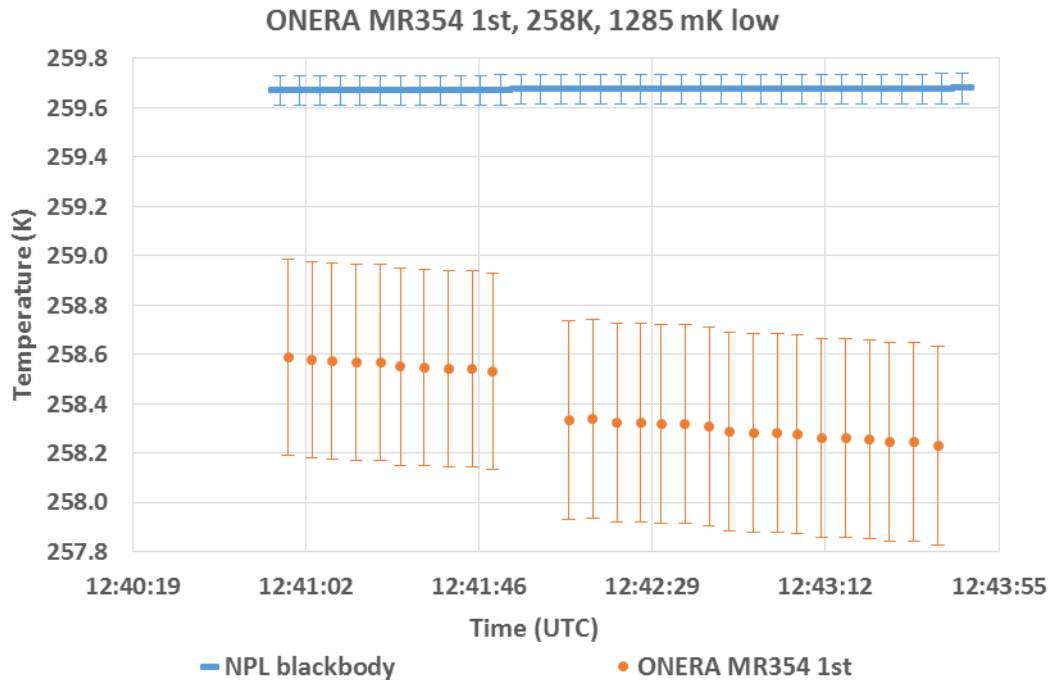


Figure 3.4.23: The ONERA-B Mikron spectroradiometer BOMEM MR354 viewing the NPL blackbody for the first measurement at $-15\text{ }^{\circ}\text{C}$. The deviation of the ONERA spectroradiometer from the average blackbody temperature over the measurement interval was 1285 mK.

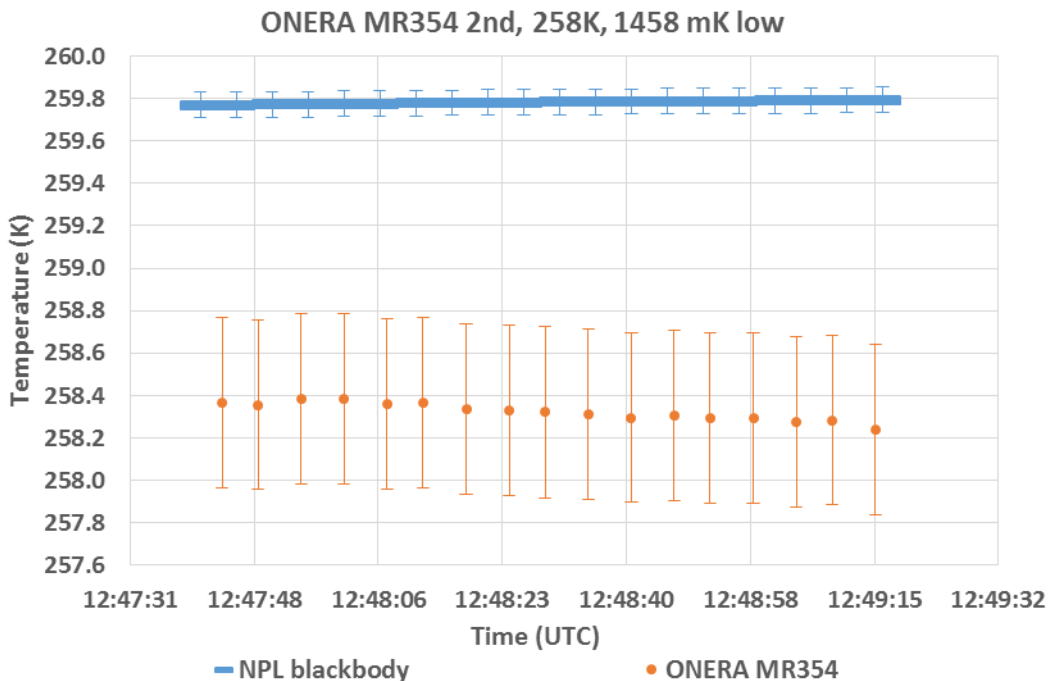


Figure 3.4.24: The ONERA-B Mikron spectroradiometer BOMEM MR354 viewing the NPL blackbody for the second measurement maintained at about $-15\text{ }^{\circ}\text{C}$. The deviation of the ONERA spectroradiometer from the average blackbody temperature over the measurement interval was 1458 mK.

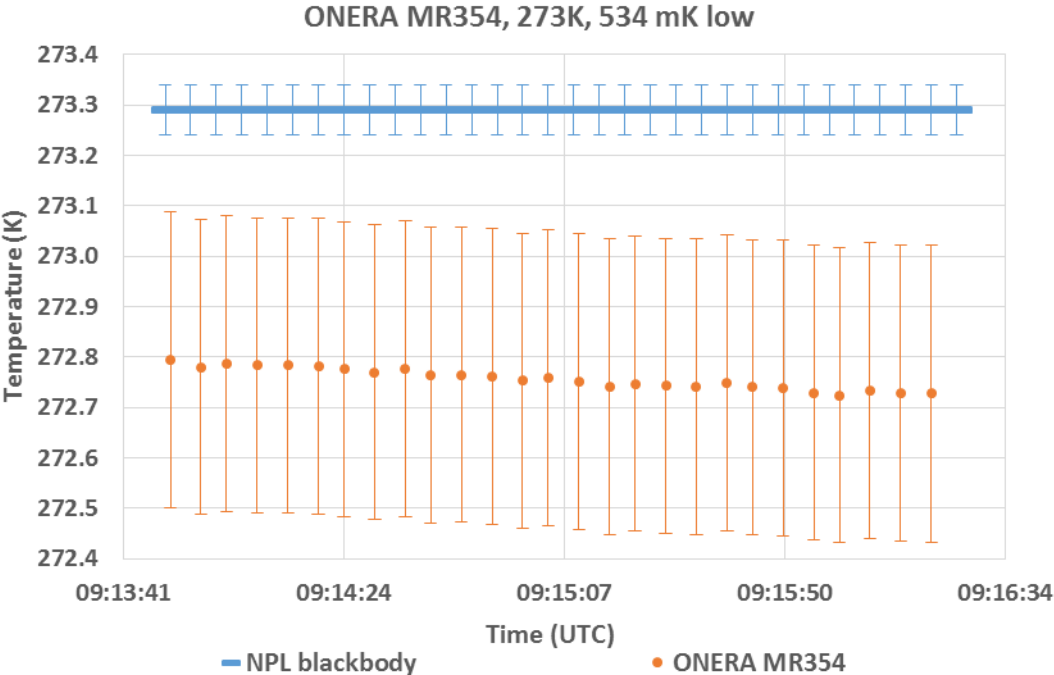


Figure 3.4.25: The ONERA-B Mikron spectroradiometer BOMEM MR354 viewing the NPL blackbody maintained at about 0 °C. The deviation of the ONERA spectroradiometer from the average blackbody temperature over the measurement interval was 534 mK.

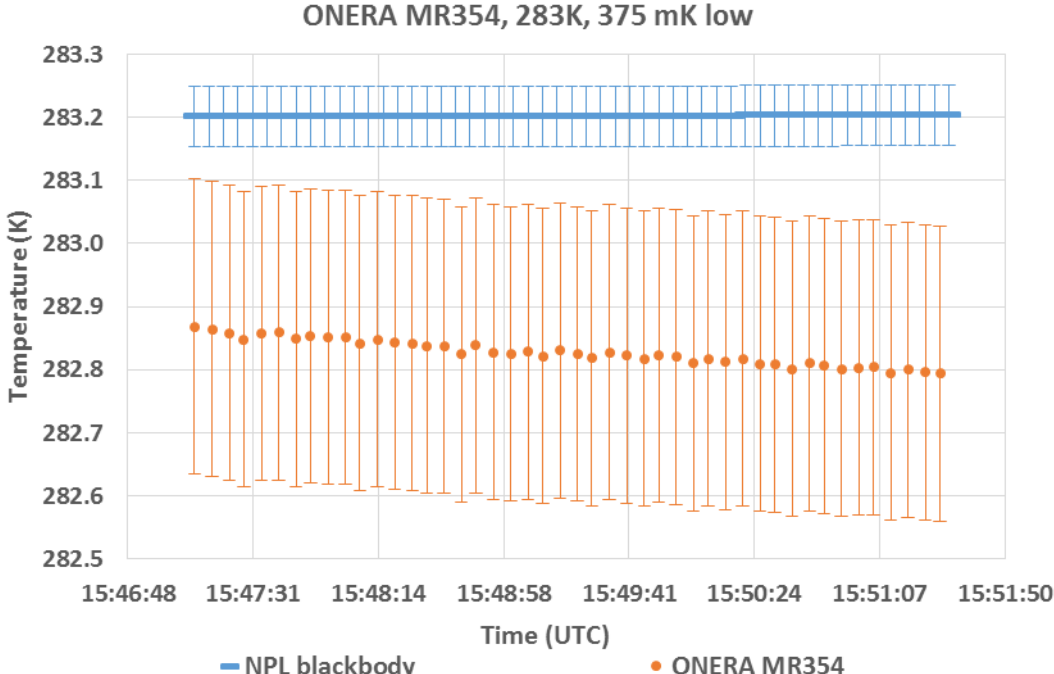


Figure 3.4.26: The ONERA-B Mikron spectroradiometer BOMEM MR354 viewing the NPL blackbody maintained at about 10 °C. The deviation of the ONERA spectroradiometer from the average blackbody temperature over the measurement interval was 375 mK.

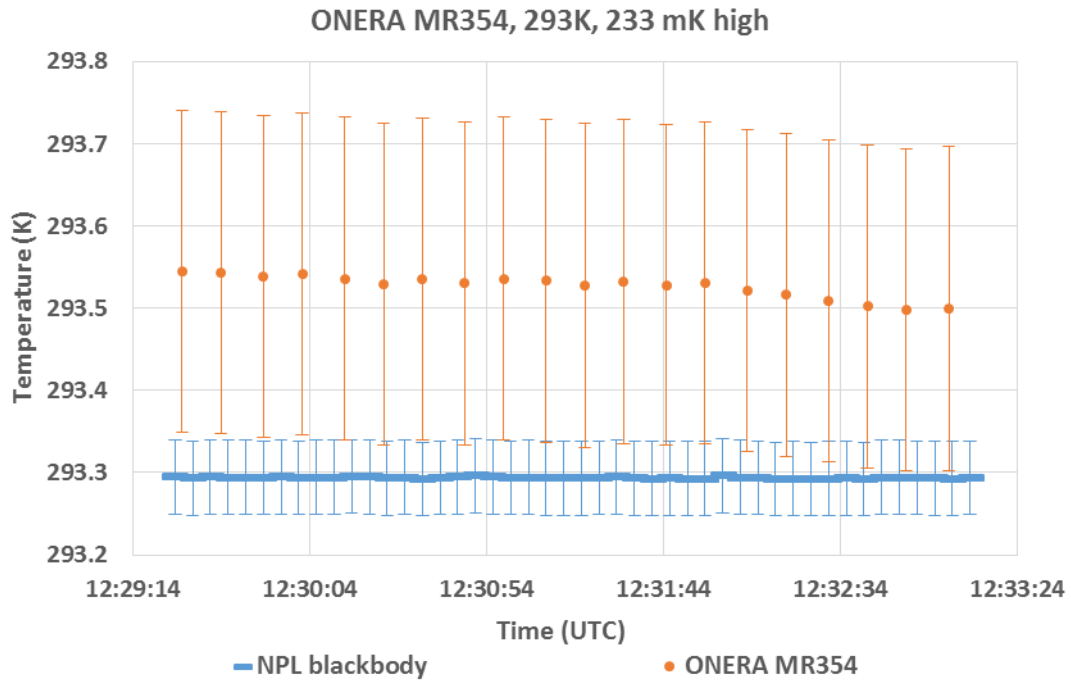


Figure 3.4.27: The ONERA-B Mikron spectroradiometer BOMEM MR354 viewing the NPL blackbody maintained at about 20 °C. The deviation of the ONERA spectroradiometer from the average blackbody temperature over the measurement interval was 233 mK.

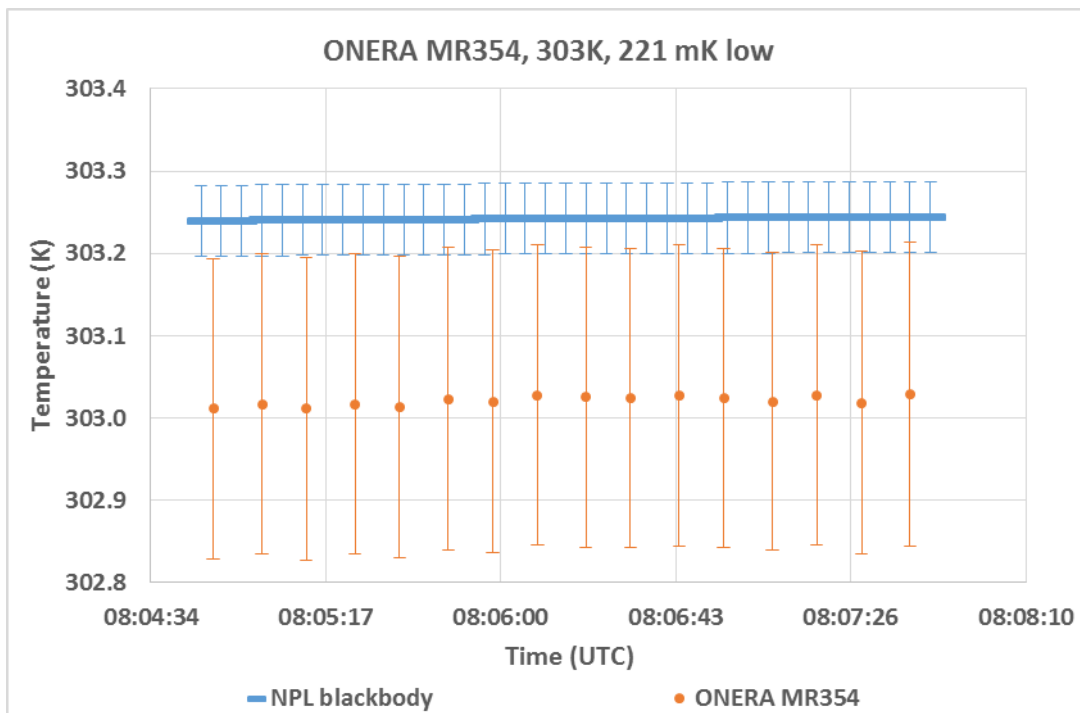


Figure 3.4.28: The ONERA-B Mikron spectroradiometer BOMEM MR354 viewing the NPL blackbody maintained at about 30 °C. The deviation of the ONERA spectroradiometer from the average blackbody temperature over the measurement interval was 221 mK.

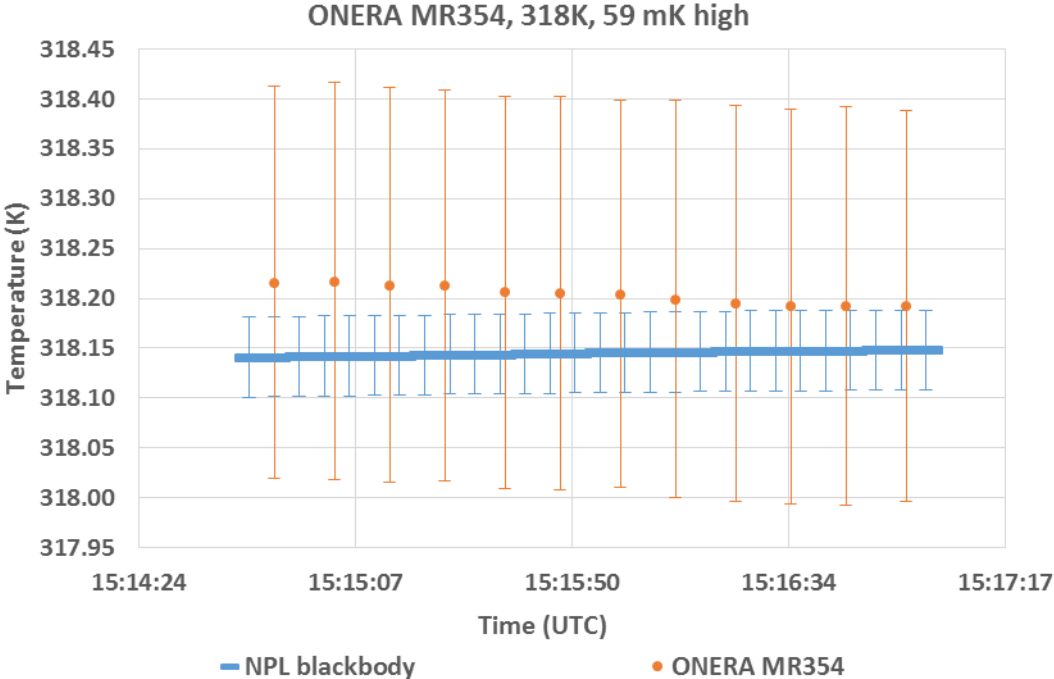


Figure 3.4.29: The ONERA-B Mikron spectroradiometer BOMEM MR354 viewing the NPL blackbody maintained at about 45 °C. The deviation of the ONERA spectroradiometer from the average blackbody temperature over the measurement interval was 59 mK.

3.5 MEASUREMENTS MADE BY CSIRO

Institute/organisation: CSIRO

Ocean Modelling Research Team, Research and Development Branch,
Bureau of Meteorology GPO Box 1289 Melbourne VIC 3001,
Level 11, 700 Collins Street, Docklands VIC 3008

Contact Name: Nicole Morgan

Email: Nicole.Morgan@csiro.au

3.5.1 Description of Radiometer and route of traceability

Make and type of Radiometer:

ISAR 5D

Outline Technical description of instrument:

Full information on this radiometer can be found in: Wimmer, W., and I. Robinson, 2016: The ISAR instrument uncertainty model. *J. Atmos. Oceanic Technol.* doi:10.1175/JTECH-D-16-0096.1, in press.

Establishment or traceability route for primary calibration including date of last realisation and breakdown of uncertainty:

Pre workshop calibration completed 22/05/2016.

Post workshop calibration completed 05/07/2016.

Operational methodology during measurement campaign:

Alignment was achieved using an alignment piece specifically designed for the dome nuts on the end to slot into. This is the same way the instrument is aligned during calibration and deployment.

The ISAR runs continuously and is post processed using calibration scripts which incorporate the uncertainty model, instrument data and pre and post calibrations to calculate the uncertainty.

Radiometer usage (deployment), previous use of instrument and planned applications.

This ISAR is installed on RV Investigator, Australia's blue water science vessel. It is part of the underway data collected on every voyage.

3.5.2 Uncertainty contributions associated with CSIRO's measurements at NPL

Table 3.5.1 shows the uncertainty budget associated with measurements made by the CSIRO radiometer.

Table 3.5.1: The uncertainty budget associated with measurements made by the CSIRO radiometer

e	Item	Uncertainty	Unit	Type
1	Detector linearity	<0.01%	K month ⁻¹	B
2	Detector noise	~0.002	Volts	A
3	Detector accuracy	±0.5	K	B
4	ADC	±1(±76.3)	LSB (μV)	B
5	ADC accuracy	±0.1%	Range	B
6	ADC zero drift	±6	μV °C ⁻¹	B
7	Reference voltage 16-bit ADC	±15	mV	B
8	Reference voltage 12-bit ADC	±20	mV	B
9	Reference resistor	1	%	B
10	Reference resistor temperature coefficient	±100	Ppm °C ⁻¹	B
11	BB emissivity	±0.000178	Emissivity	B
12	Sea surface emissivity	±0.07	Emissivity	B
13	Steinhart–Hart approximation	±0.01	K	B
14	Radiate transfer approximation	±0.001	K	B
15	Thermistor	±0.05	K	B
16	Thermistor noise	~0.002	V	A

Sources of uncertainties arising within the ISAR SST retrieval processor. A more detailed breakdown is available in the reference paper “The ISAR instrument uncertainty model”.

3.5.3 Comparison of CSIRO ISAR 5D to the NPL reference blackbody

Figures 3.5.1 to 3.5.7 show the measurements completed by the CSIRO radiometer ISAR 5D when it was viewing the NPL blackbody maintained at different temperatures. The uncertainty bars shown in orange in the figures represent the uncertainty values provided by CSIRO which correspond to the measurements shown in the Figures. Also shown in blue in these Figures are the values of the brightness temperature of the NPL reference blackbody along with their combined uncertainty values.

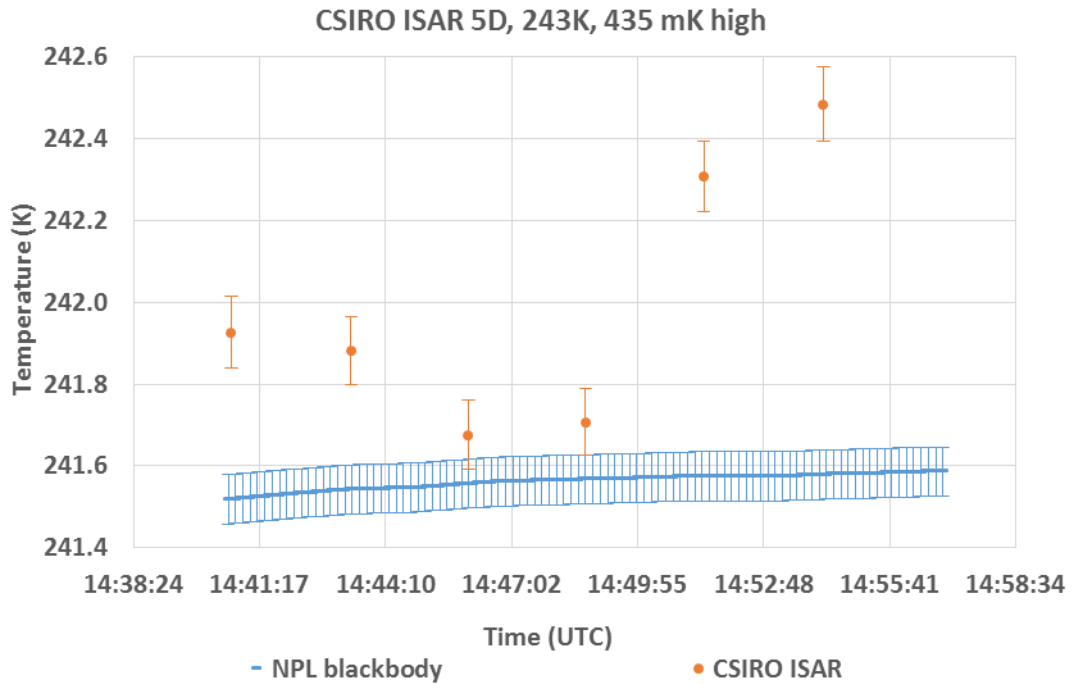


Figure 3.5.1: The ISAR 5D CSIRO radiometer viewing the NPL blackbody maintained at about -30 °C. The deviation of the CSIRO radiometer from the average blackbody temperature over the measurement interval was 435 mK.

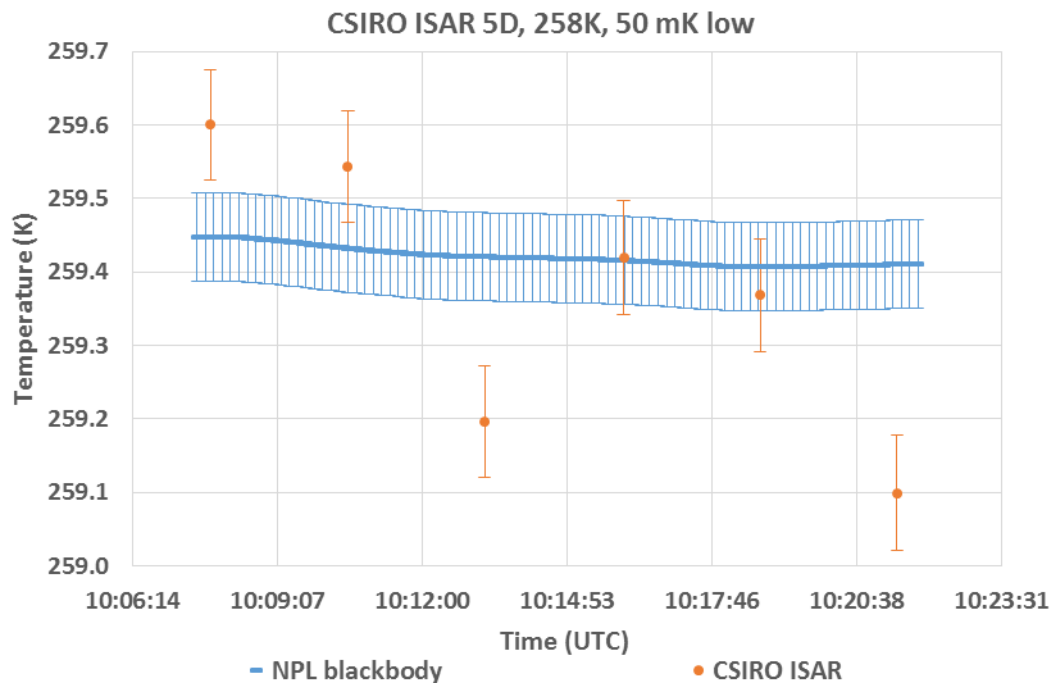


Figure 3.5.2: The ISAR 5D CSIRO radiometer viewing the NPL blackbody maintained at about -15 °C. The deviation of the CSIRO radiometer from the average blackbody temperature over the measurement interval was 50 mK.

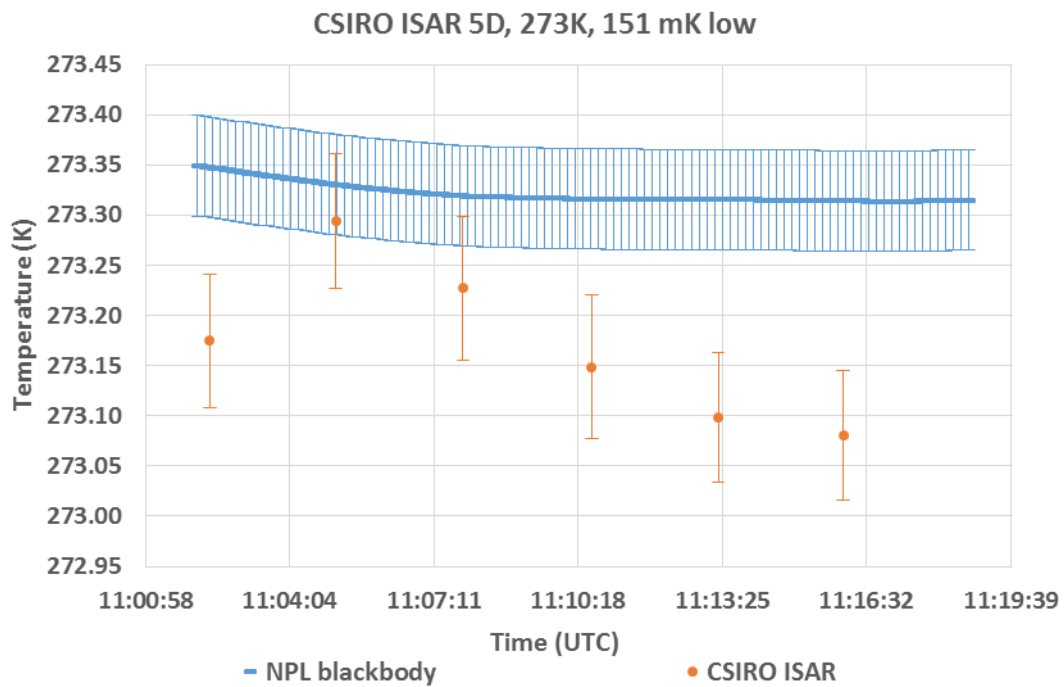


Figure 3.5.3: The ISAR 5D CSIRO radiometer viewing the NPL blackbody maintained at about 0 °C. The deviation of the CSIRO radiometer δT from the average blackbody temperature over the measurement interval was 151 mK

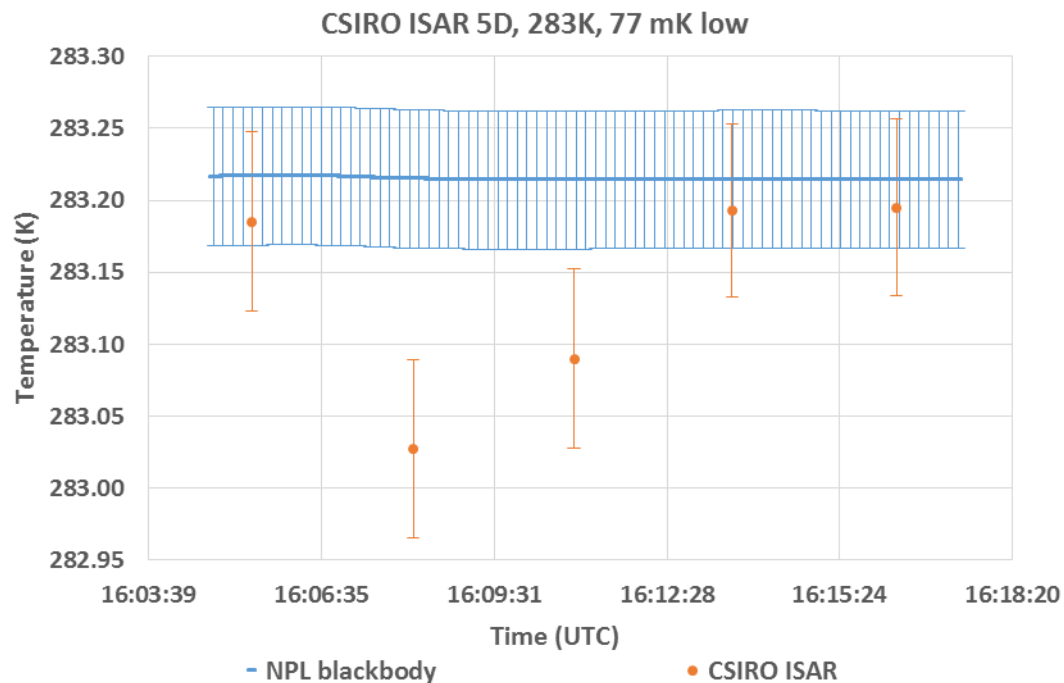


Figure 3.5.4: The ISAR 5D CSIRO radiometer viewing the NPL blackbody maintained at about 10 °C. The deviation of the CSIRO radiometer δT from the average blackbody temperature over the measurement interval was 77 mK.

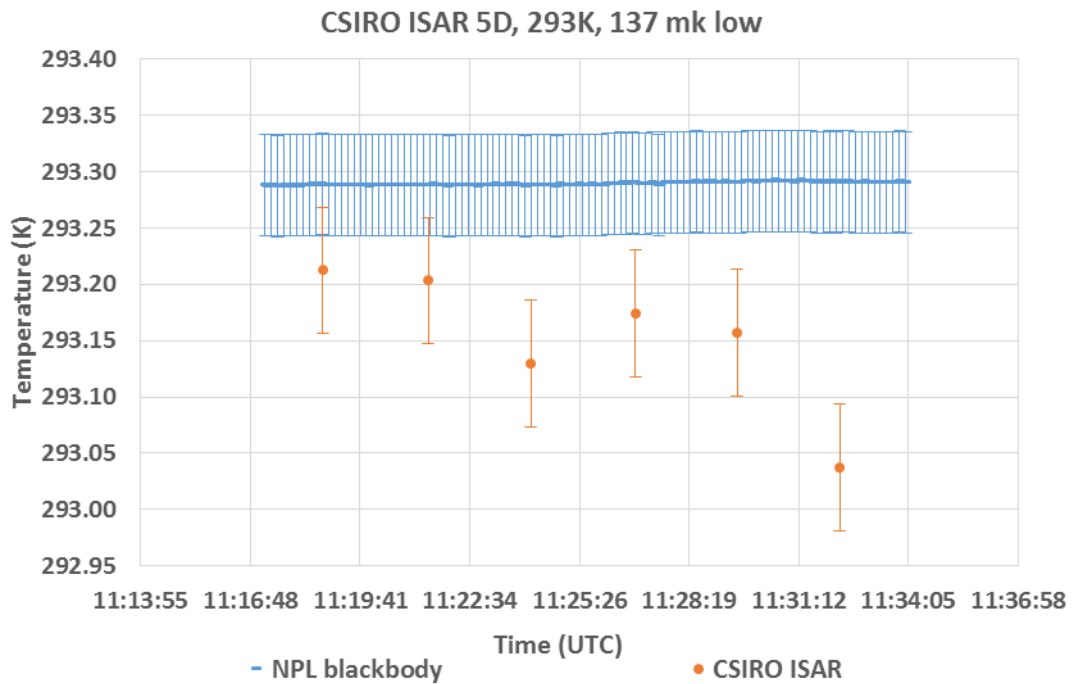


Figure 3.5.5: The ISAR 5D CSIRO radiometer viewing the NPL blackbody maintained at about 20 °C. The deviation of the CSIRO radiometer δT from the average blackbody temperature over the measurement interval was 137 mK.

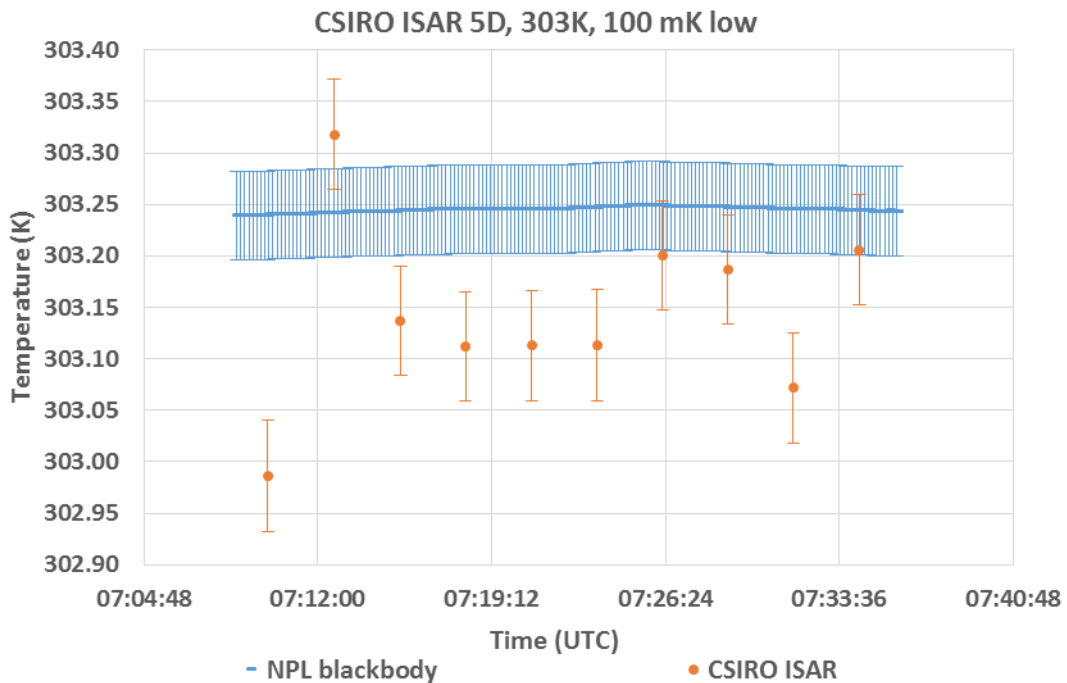


Figure 3.5.6: The ISAR 5D CSIRO radiometer viewing the NPL blackbody maintained at about 30 °C. The deviation of the CSIRO radiometer δT from the average blackbody temperature over the measurement interval was 100 mK.

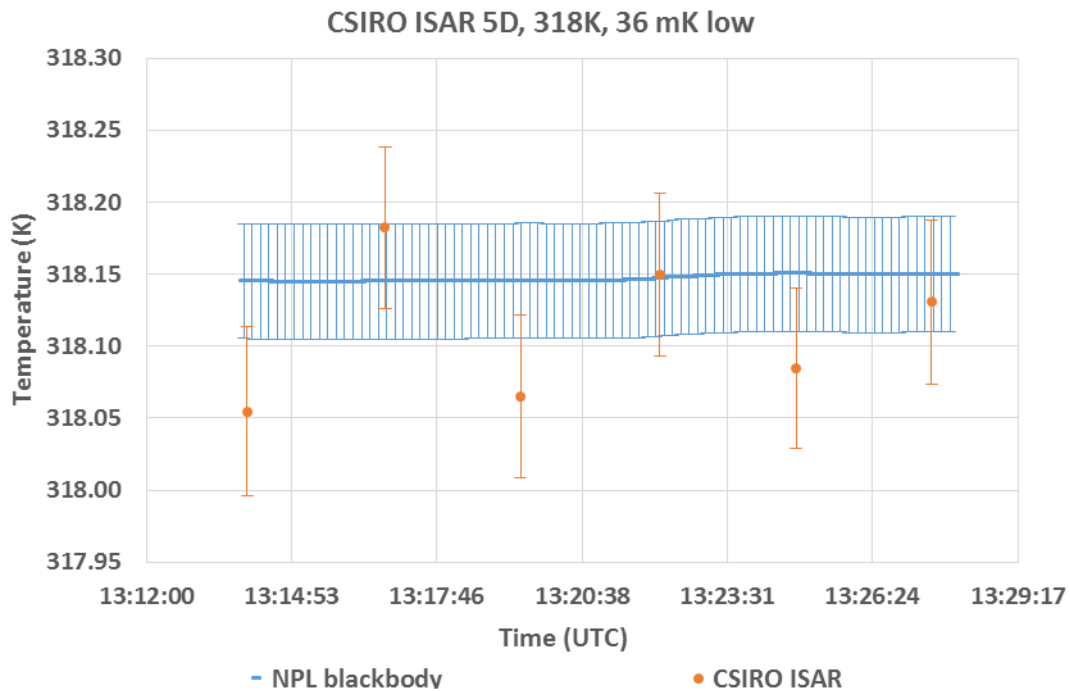


Figure 3.5.7: The ISAR 5D CSIRO radiometer viewing the NPL blackbody maintained at about 45 °C. The deviation of the CSIRO radiometer δT from the average blackbody temperature over the measurement interval was 36 mK.

3.6 MEASUREMENTS MADE BY STFC RAL

Science and Technology Facilities Council Rutherford Appleton Laboratory
 Chilton, Didcot, Oxon
 OX11 0QX, United Kingdom
 Contact Name: Tim Nightingale
 Email: Tim.Nightingale@stfc.ac.uk

3.6.1 Description of the radiometer and route of tracibility

Make and type of Radiometer:

Scanning Infrared Sea Surface Temperature Radiometer (SISTeR) manufactured by RAL Space.

Outline Technical description of instrument:

SISTeR is a chopped, self-calibrating filter radiometer manufactured by RAL Space. It has a single-element DLaTGS pyroelectric detector, a filter wheel containing up to six band-defining filters and two internal reference blackbodies, one operating at ambient temperature and the other heated to ~ 17 K above ambient. During operation the radiometer selects with a scan mirror successive views to each of the blackbodies and to the external scene in a repeated sequence. For Sea Surface Temperature (SST) measurements, the external measurements include views to the sea surface, and to the sky at the complementary angle. The instrument

field of view is approximately 13°. During the 2016 radiometer laboratory comparison, a filter centred at 10.8 µm was used.

Reference:

Further information on the SISTeR radiometer can be found in

<http://www.stfc.ac.uk/research/environment/sister/>

Establishment or traceability route for primary calibration including date of last realisation and breakdown of uncertainty.

The primary traceability route is through two rhodium iron thermometers, one embedded in each of the instrument's internal blackbodies. These thermometers are re-calibrated periodically against a secondary SPRT in a dedicated thermal block maintained by Oxford University. The SPRT calibration is traceable to NPL. The estimated re-calibration accuracy is approximately 4 mK. The last calibration of the internal blackbody thermometers used in the FRM4STS measurements took place in 2007/2008 and new calibration is scheduled.

There is circumstantial evidence that the hot blackbody thermometer calibration may have shifted since its last re-calibration, by about 50 mK. This will be confirmed by the next thermometer re-calibration.

The SISTeR calibration is validated against a CASOTS Mk 1 external blackbody, which has a copper cavity with Mankiewicz Nextel Velvet Coating 811-21 thermally controlled by a water bath. The temperature of the water bath is measured with a Fluke 5640 series thermistor probe, with a system accuracy of 4 mK, traceable to NIST.

A new calibrated thermistor probe and bridge was purchased in July 2016. When the two probes were inter-compared in the blackbody water bath, their measurements agreed comfortably to within their estimated uncertainties.

Operational methodology during measurement campaign:

SISTeR was aligned vertically to the NPL blackbody using stacks of paper on an adjustable table, and remained at the same height throughout. For each measurement it was positioned as close as possible to the blackbody. It was then aligned horizontally looking along the top of the instrument at the centre of the entrance aperture. Levelness was verified with a spirit level on the top of the instrument.

The SISCAL routine was used, which measures counts from the lab blackbody and each of the two internal blackbodies in turn.

Radiometer usage (deployment), previous use of instrument and planned applications:

The SISTeR radiometer was developed to collect SST validation data for the ATSR series of satellite radiometers. Latterly it supports the SLSTR and other satellite radiometers. The SISTeR instrument is currently deployed on the Queen Mary 2 cruise liner which is operated by Cunard Line. Deployments have been funded, at different times, by ESA, DECC and NERC. Typical routes are between Hamburg, Southampton and New York with side-trips from these ports, for example, to the Caribbean or to the Channel Islands. For four months of each year, from January to May, there is a round-the-world trip beginning and ending at Southampton.

3.6.2 Uncertainty contributions associated with STFC RAL's measurements at NPL

Uncertainty breakdown:

The uncertainties are given for both level 1 and level 3 data.

NPL lab measurements:

Level 1: Type A: 31 to 119 mK
 Type B: 12 to 128 mK
Level 3: Type A: 5 to 21 mK
 Type B: 12 to 127 mK

The lowest uncertainty values were at the highest temperature of the blackbody (45 °C) and the highest uncertainty values were at the coldest temperature of the blackbody (-31 °C).

Systematic inputs to the uncertainty model include the uncertainties on the instrument background radiance, the internal blackbody temperatures and emissivities, and the reflectance of the ocean surface.

Random inputs to the uncertainty model include the noise on measured thermometer counts, the noise on detector counts when viewing the internal blackbodies, and the variability of the measured sky radiances.

3.6.3 Comparison of RAL's SISTeR to the NPL reference blackbody

The photo below shows the STFC RAL SISTeR radiometer viewing the NPL reference blackbody.



The STFC RAL SISTeR radiometer viewing the NPL reference blackbody.

Figures 3.6.1 to 3.6.7 show the measurements completed by the STFC RAL SISTeR radiometer when it was viewing the NPL blackbody maintained at different temperatures. The uncertainty bars shown in orange in the figures represent the uncertainty values provided by STFC RAL which correspond to the measurements shown in the Figures. Also shown in blue in these Figures are the values of the brightness temperature of the NPL reference blackbody along with their combined uncertainty values.

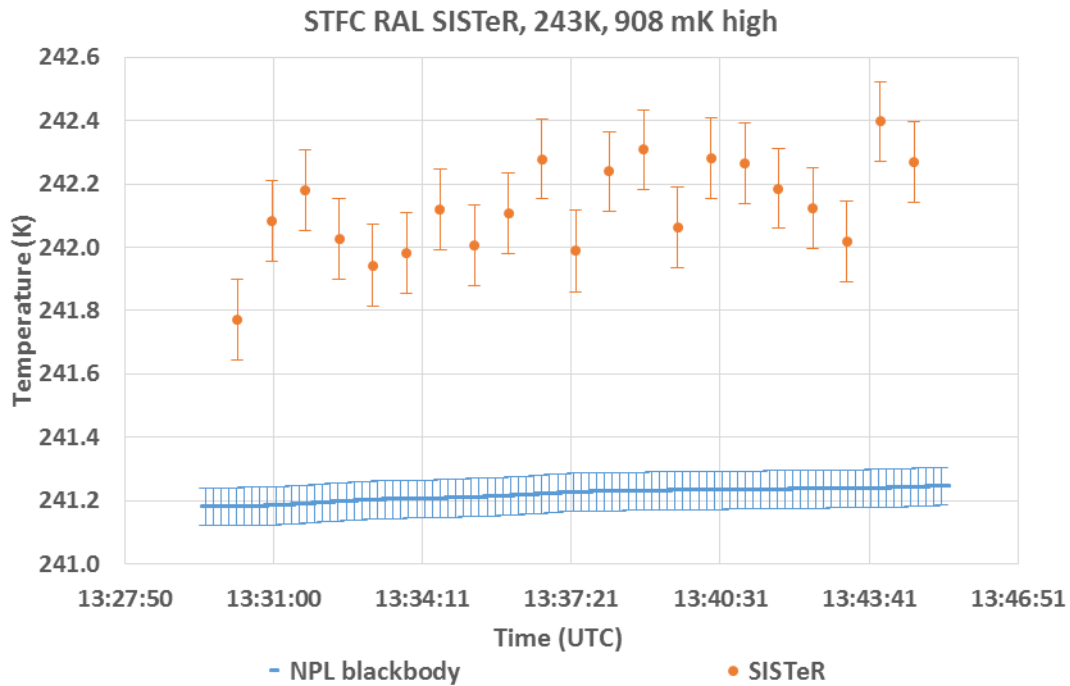


Figure 3.6.1: The SISTeR STFC RAL radiometer viewing the NPL blackbody maintained at about -30 °C. The deviation of the SISTeR radiometer from the average blackbody temperature over the measurement interval was 908 mK.

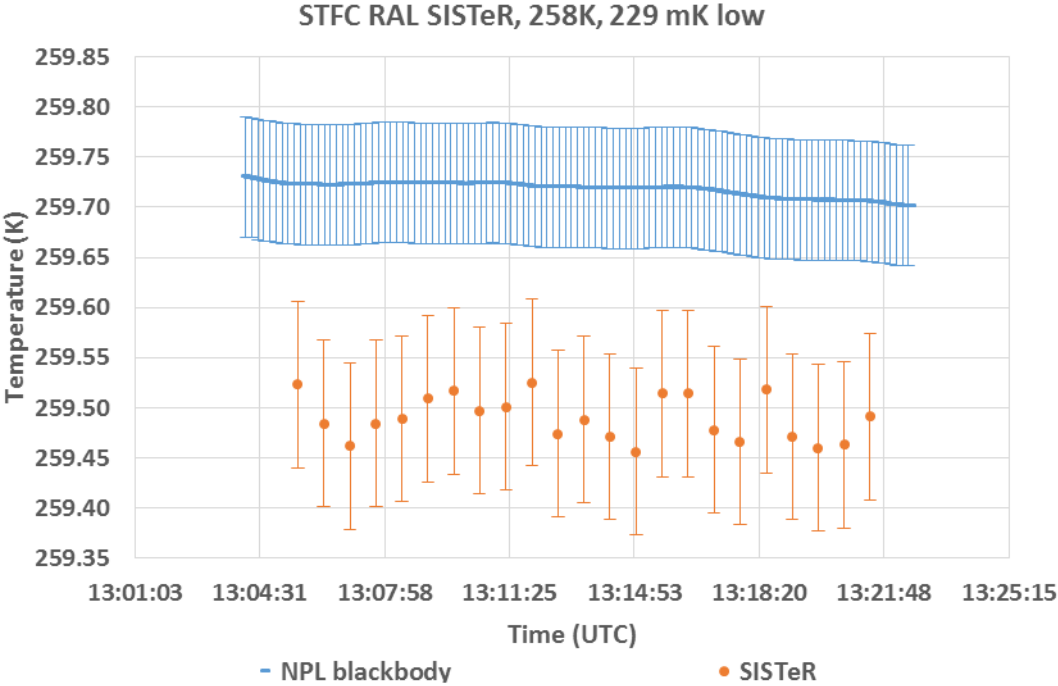


Figure 3.6.2: The SISTeR STFC RAL radiometer viewing the NPL blackbody maintained at about -15 °C. The deviation of the SISTeR radiometer from the average blackbody temperature over the measurement interval was 229 mK.

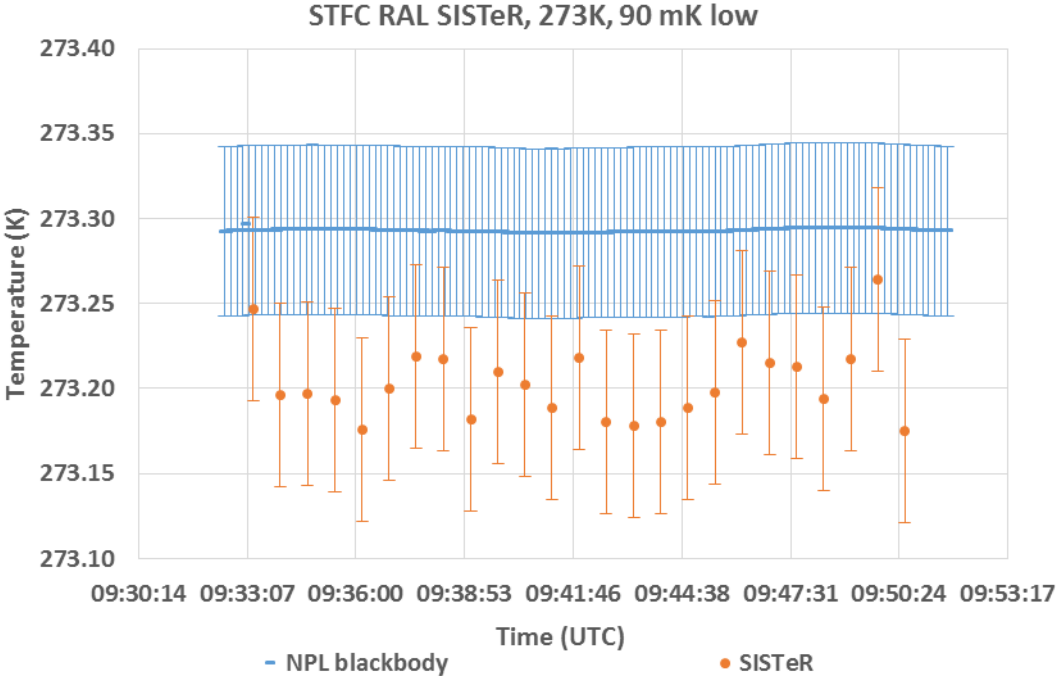


Figure 3.6.3: The SISTeR STFC RAL radiometer viewing the NPL blackbody maintained at about 0 °C. The deviation of the SISTeR radiometer from the average blackbody temperature over the measurement interval was 90 mK.

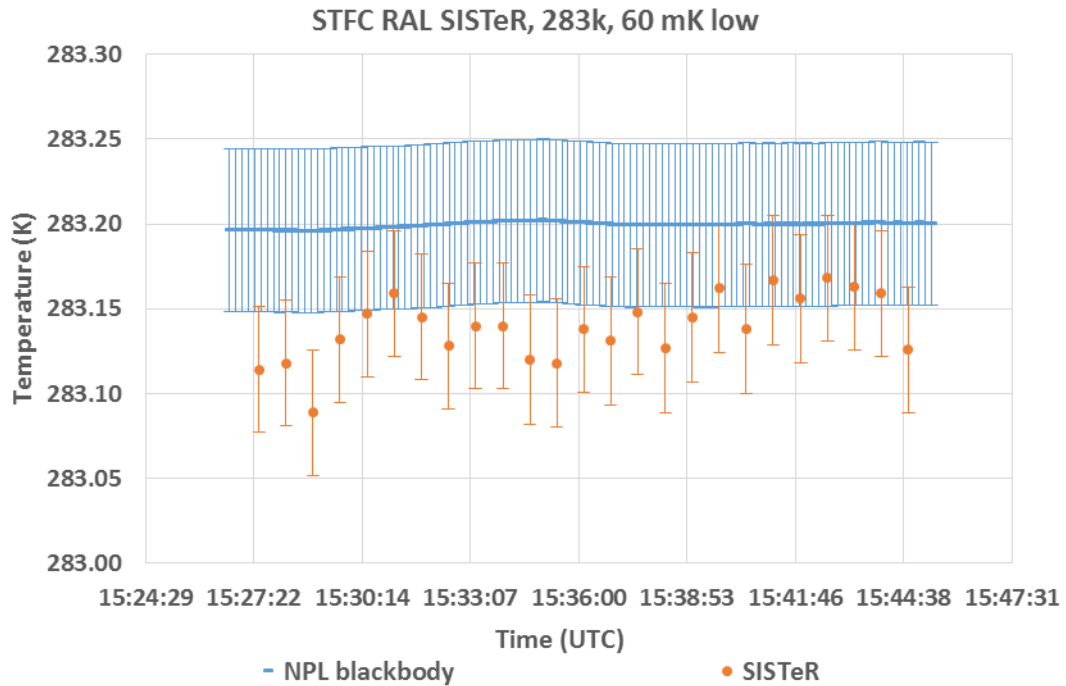


Figure 3.6.4: The SISTeR STFC RAL radiometer viewing the NPL blackbody maintained at about 10 °C. The deviation of the SISTeR radiometer from the average blackbody temperature over the measurement interval was 60 mK.

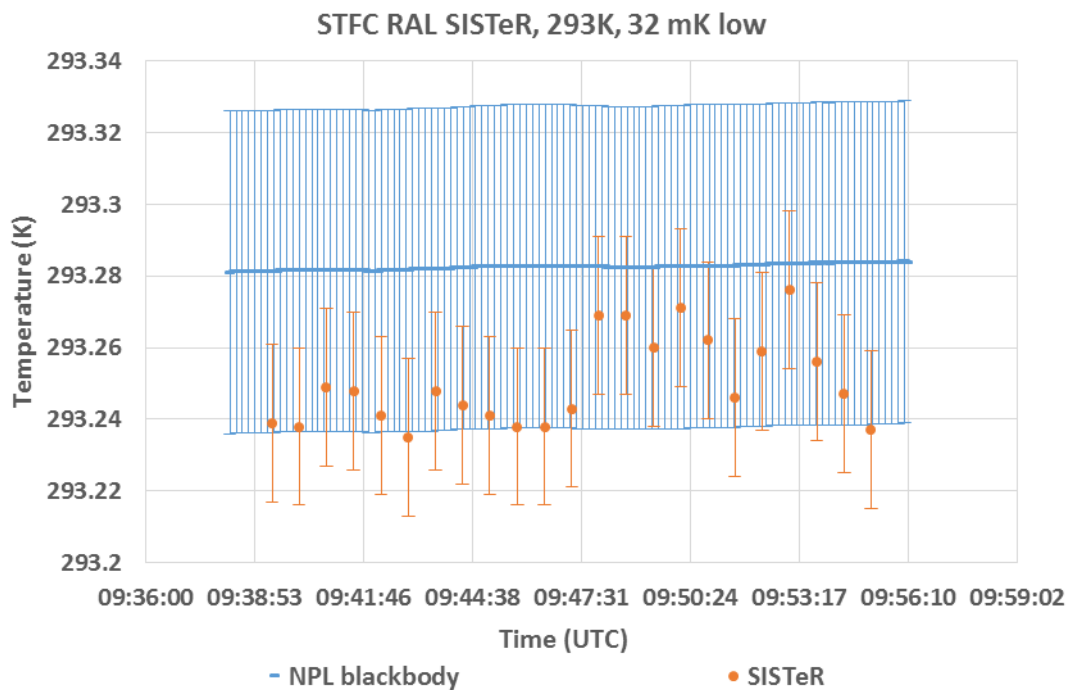


Figure 3.6.5: The SISTeR STFC RAL radiometer viewing the NPL blackbody maintained at about 20 °C. The deviation of the SISTeR radiometer from the average blackbody temperature over the measurement interval was 32 mK.

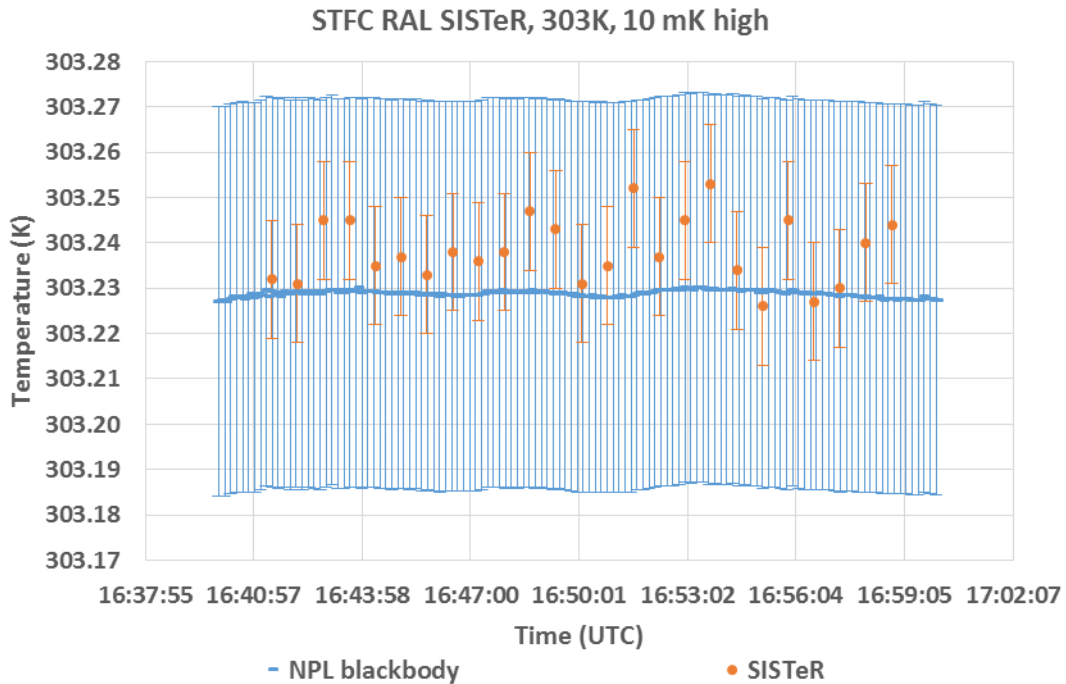


Figure 3.6.6: The SISTeR STFC RAL radiometer viewing the NPL blackbody maintained at about 30 °C. The deviation of the SISTeR radiometer from the average blackbody temperature over the measurement interval was 10 mK.

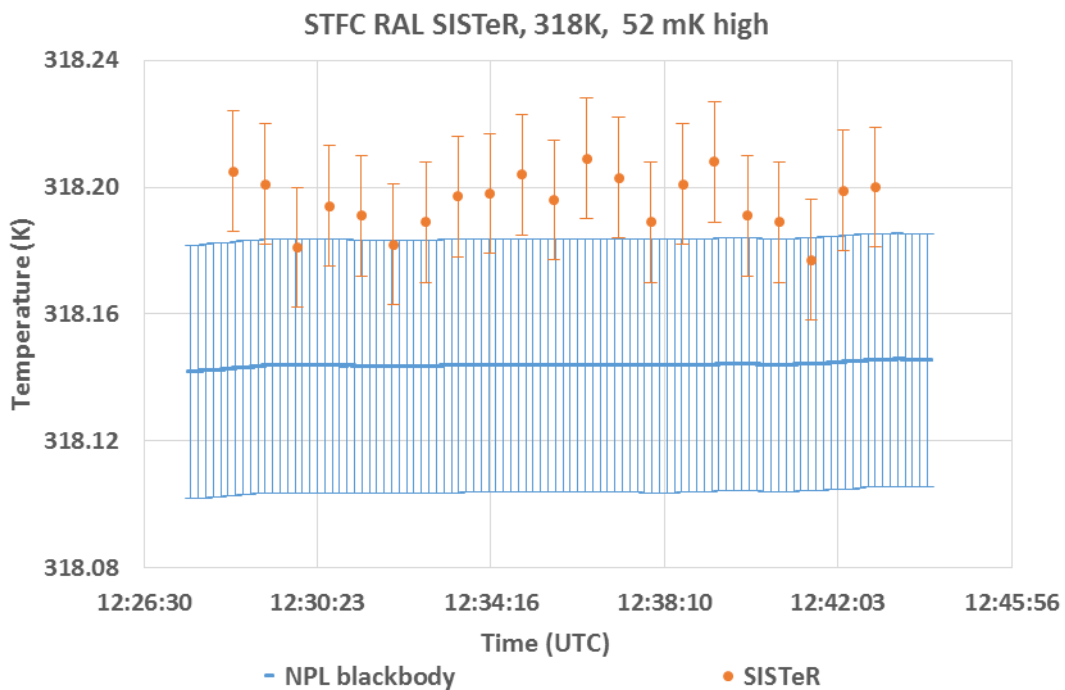


Figure 3.6.7: The SISTeR STFC RAL radiometer viewing the NPL blackbody maintained at about 45 °C. The deviation of the SISTeR radiometer δT from the average blackbody temperature over the measurement interval was 52 mK

3.7 MEASUREMENTS MADE BY SOUTHAMPTON UNIVERSITY

University of Southampton
 Ocean and Earth Science, National Oceanography Centre Southampton
 University of Southampton Waterfront Campus European Way Southampton
 SO14 3ZH United Kingdom
 Contact Name: Werenfrid Wimmer
 Email: w.wimmer@soton.ac.uk

3.7.1 Description of radiometer and route of traceability

Type: ISAR

Field of view: 3.5 degree half angle

Spectral band: 9.6-11.5 micrometer

Temperature resolution : 0.01 K

Uncertainty in measurements: 0.05 K + see paper (it's at least 0.05 as this is the uncertainty of the blackbody thermistors, but generally larger depending on emissivity and platform)

3.7.2 Uncertainty contributions associated with UoS' measurements at NPL

Table 3.7.1 shows the uncertainty budget associated with measurements made by the Southampton University radiometer

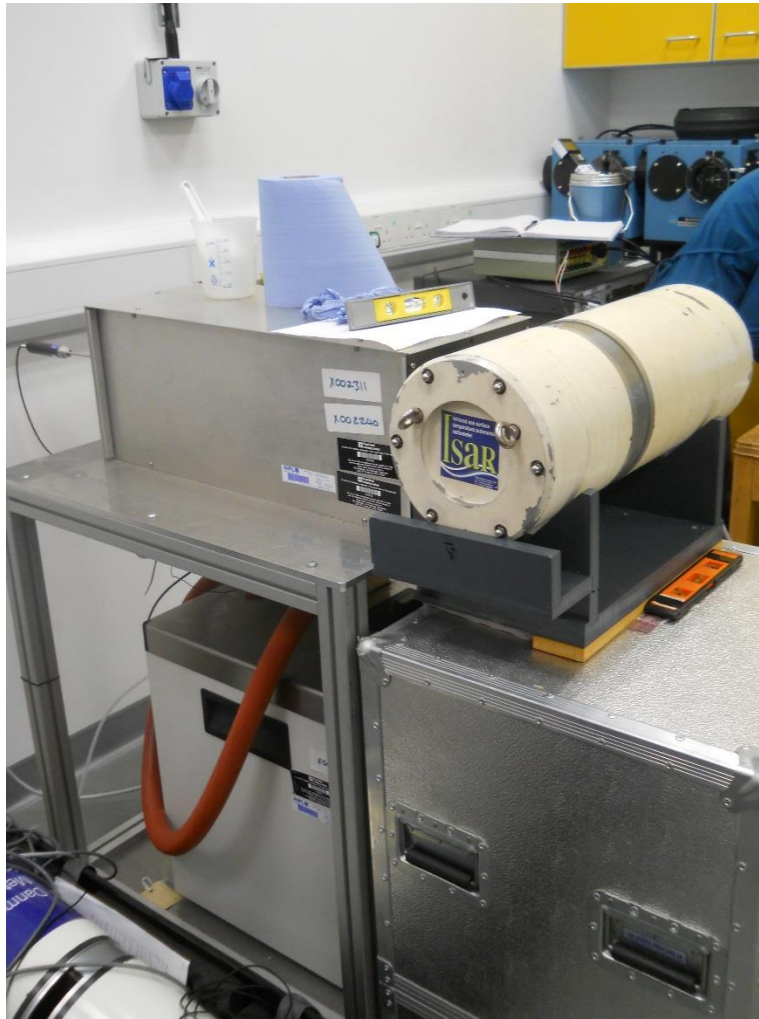
e	Item	Uncertainty	Unit	Type
1	Detector linearity	<0.01 %	K month ⁻¹	B
2	Detector noise	~0.002	Volts	A
3	Detector accuracy	±0.5	K	B
4	ADC	±1(±76.3)	LSB (μV)	B
5	ADC accuracy	±0.1%	Range	B
6	ADC zero drift	±6	μV °C ⁻¹	B
7	Reference voltage 16-bit ADC	±15	mV	B
8	Reference voltage 12-bit ADC	±20	mV	B
9	Reference resistor	1	%	B
10	Reference resistor temperature coefficient	±100	Ppm °C ⁻¹	B
11	BB emissivity	±0.000178	Emissivity	B
12	Sea surface emissivity	±0.07	Emissivity	B
13	Steinhart–Hart approximation	±0.01	K	B
14	Radiate transfer approximation	±0.001	K	B
15	Thermistor	±0.05	K	B
16	Thermistor noise	~0.002	V	A

Sources of uncertainties arising within the ISAR SST retrieval processor. A more detailed breakdown is available in the reference paper below.

Reference: Wimmer, W., and I. Robinson, 2016: The ISAR instrument uncertainty model. *J. Atmos. Oceanic Technol.* doi:10.1175/JTECH-D-16-0096.1, in press.

3.7.3 Comparison of UoS ISAR to NPL reference blackbody

The photo below shows the UoS ISAR radiometer viewing the NPL reference blackbody.



The STFC RAL SISTeR radiometer viewing the NPL reference blackbody.

Figures 3.7.1 to 3.7.7 show the measurements completed by the University of Southampton radiometer ISAR 5D when it was viewing the NPL blackbody maintained at different temperatures. The uncertainty bars shown in orange in the Figures represent the uncertainty values provided by UoS which correspond to the measurements shown in the Figures. Also shown in blue in these Figures are the values of the brightness temperature of the NPL reference blackbody along with their combined uncertainty values.

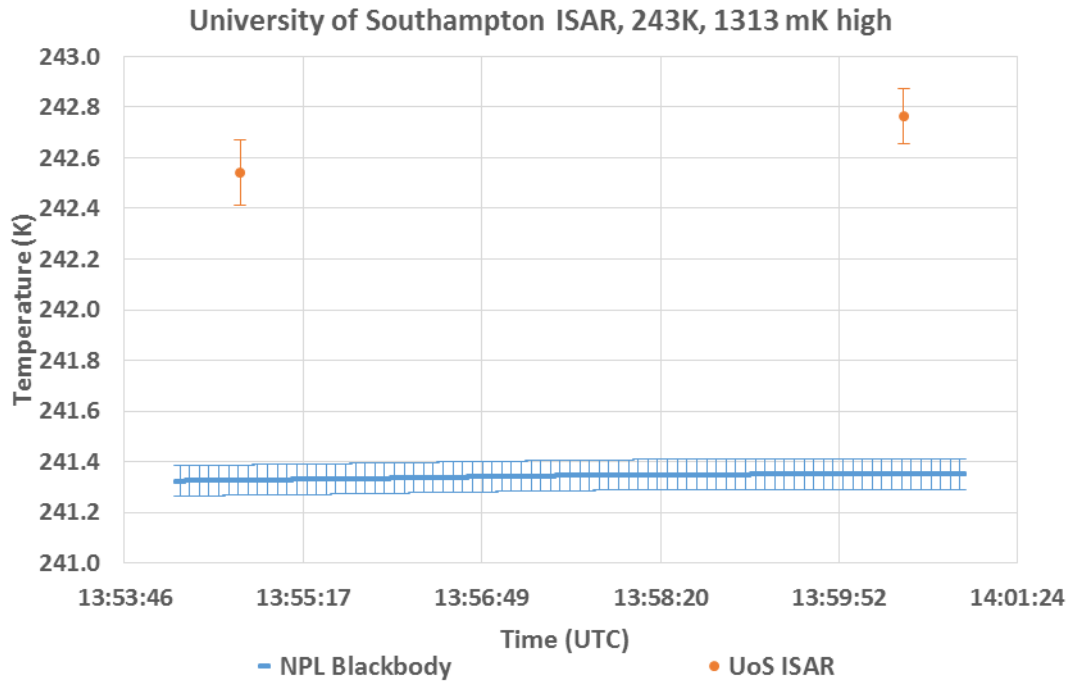


Figure 3.7.1: The University of Southampton ISAR radiometer viewing the NPL blackbody maintained at about -30 °C. The deviation of the ISAR radiometer from the average blackbody temperature over the measurement interval was 1313 mK

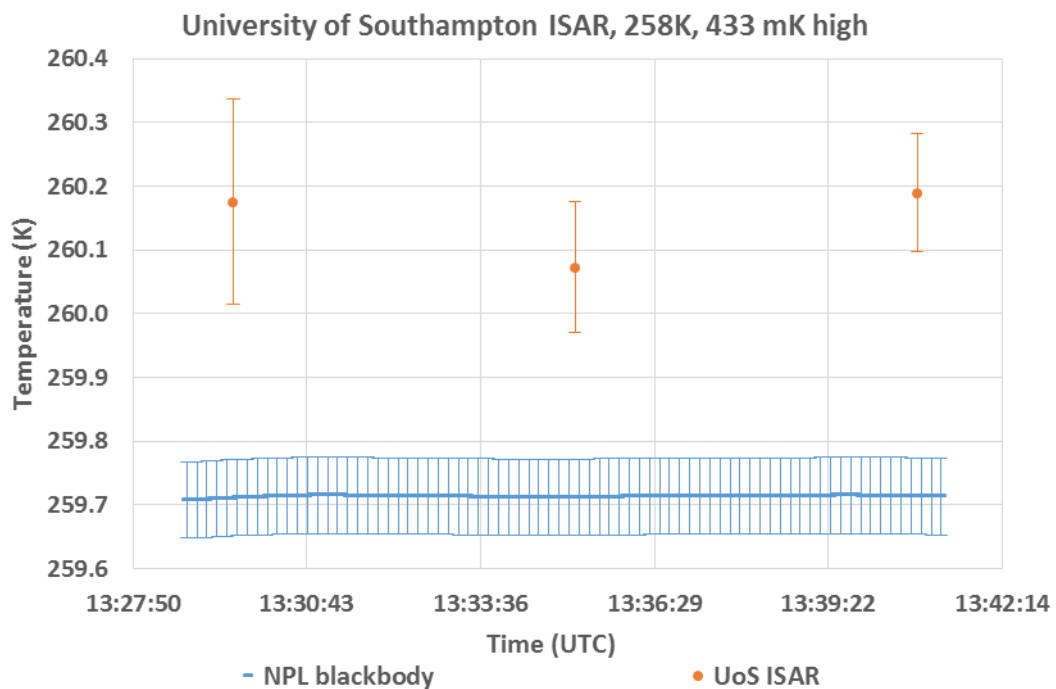


Figure 3.7.2: The University of Southampton ISAR radiometer viewing the NPL blackbody maintained at about -15 °C. The deviation of the ISAR radiometer from the average blackbody temperature over the measurement interval was 433 mK.

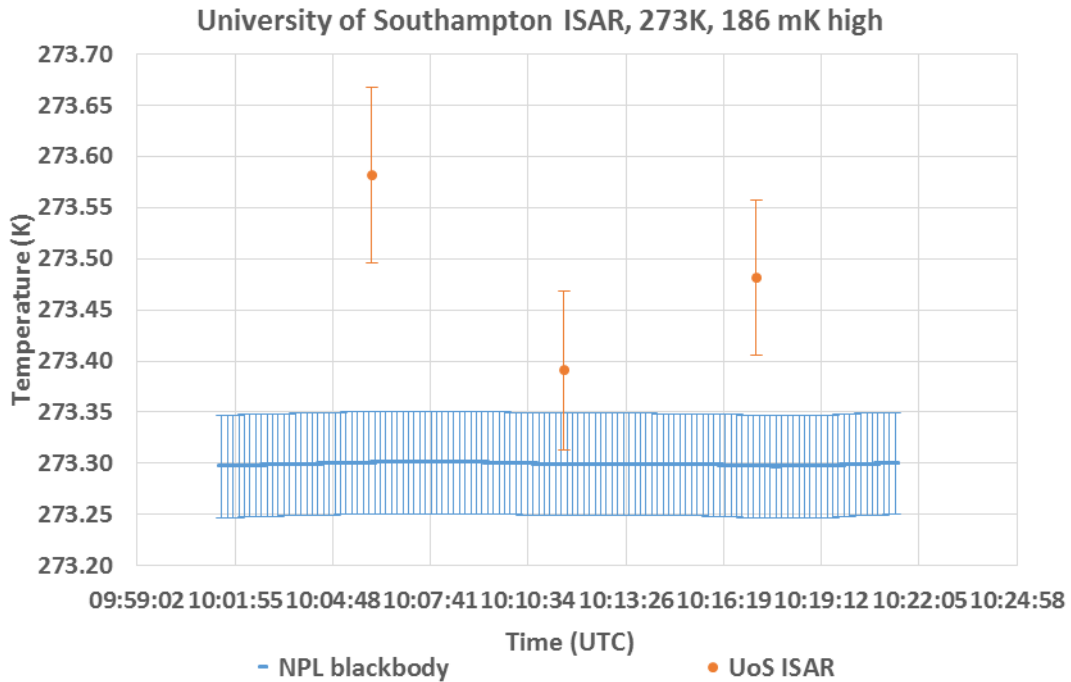


Figure 3.7.3: The University of Southampton ISAR radiometer viewing the NPL blackbody maintained at about 0 °C. The deviation of the ISAR radiometer from the average blackbody temperature over the measurement interval was 186 mK.

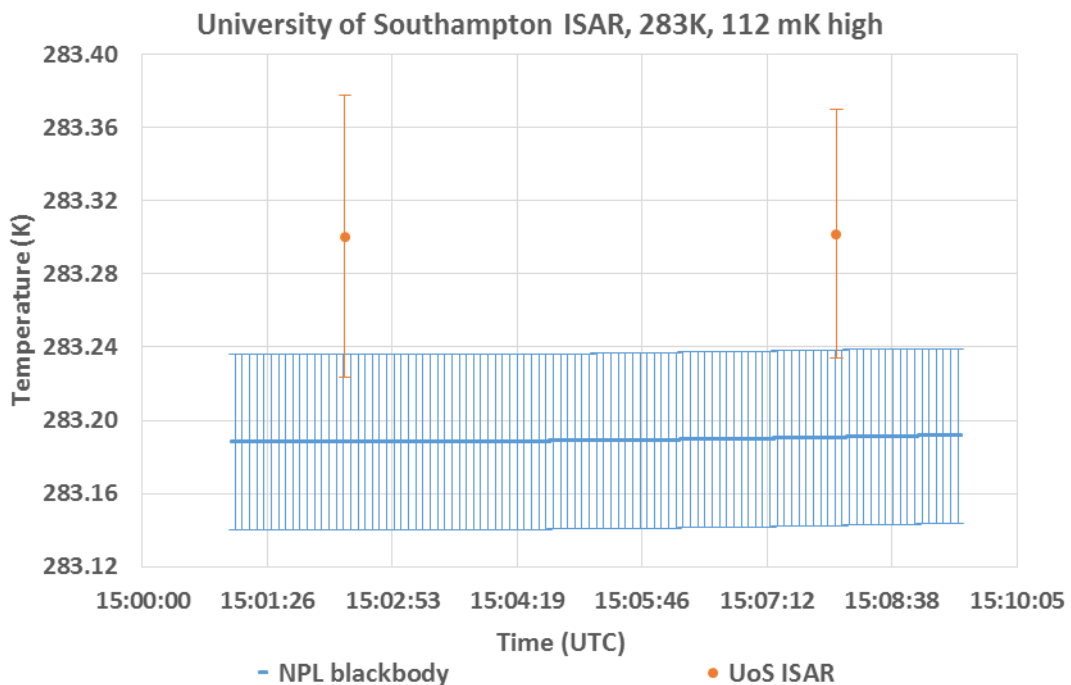


Figure 3.7.4: The University of Southampton ISAR radiometer viewing the NPL blackbody maintained at about 10 °C. The deviation of the ISAR radiometer from the average blackbody temperature over the measurement interval was 112 mK.

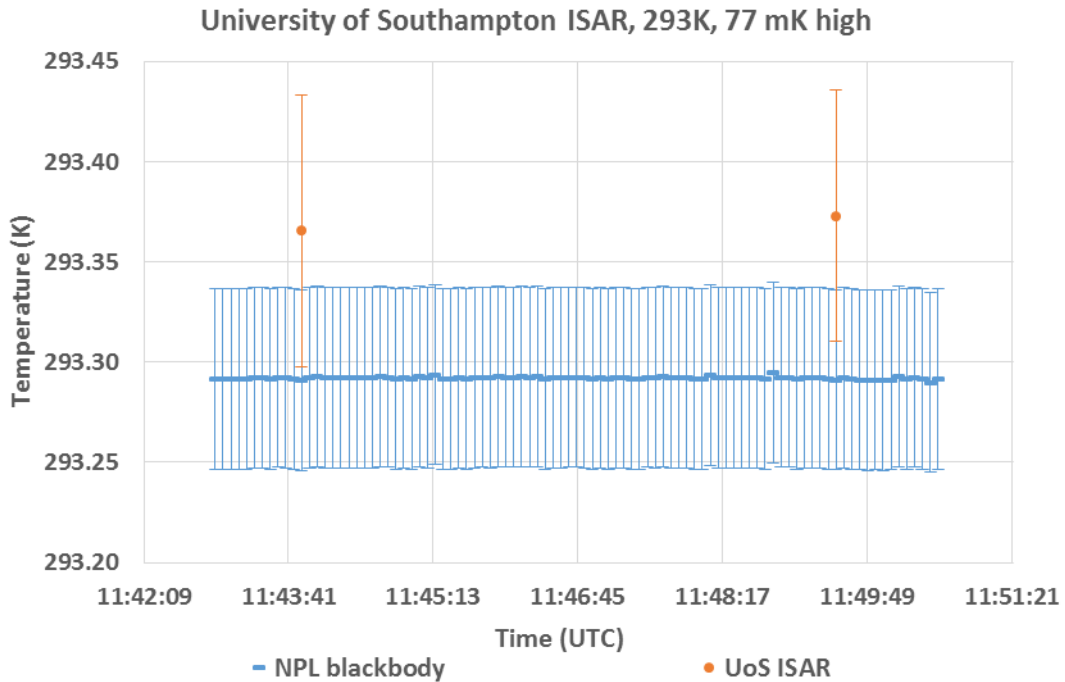


Figure 3.7.5: The University of Southampton ISAR radiometer viewing the NPL blackbody maintained at about 20 °C. The deviation of the ISAR radiometer from the average blackbody temperature over the measurement interval was 77 mK.

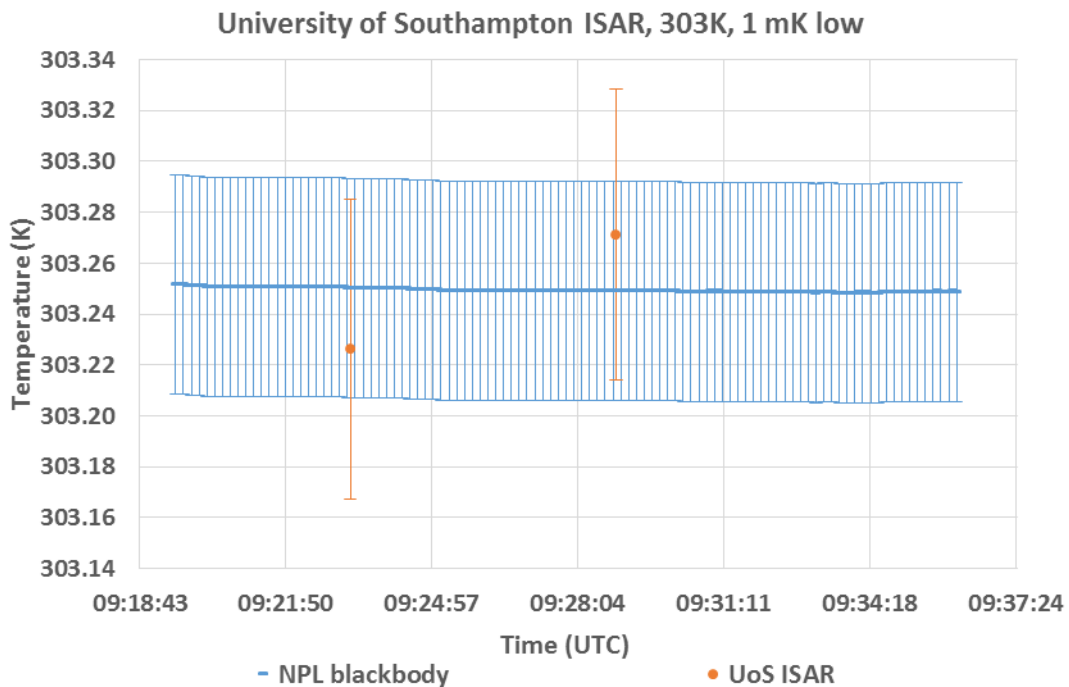


Figure 3.7.6: The University of Southampton ISAR radiometer viewing the NPL blackbody maintained at about 30 °C. The deviation of the ISAR radiometer from the average blackbody temperature over the measurement interval was 1 mK.

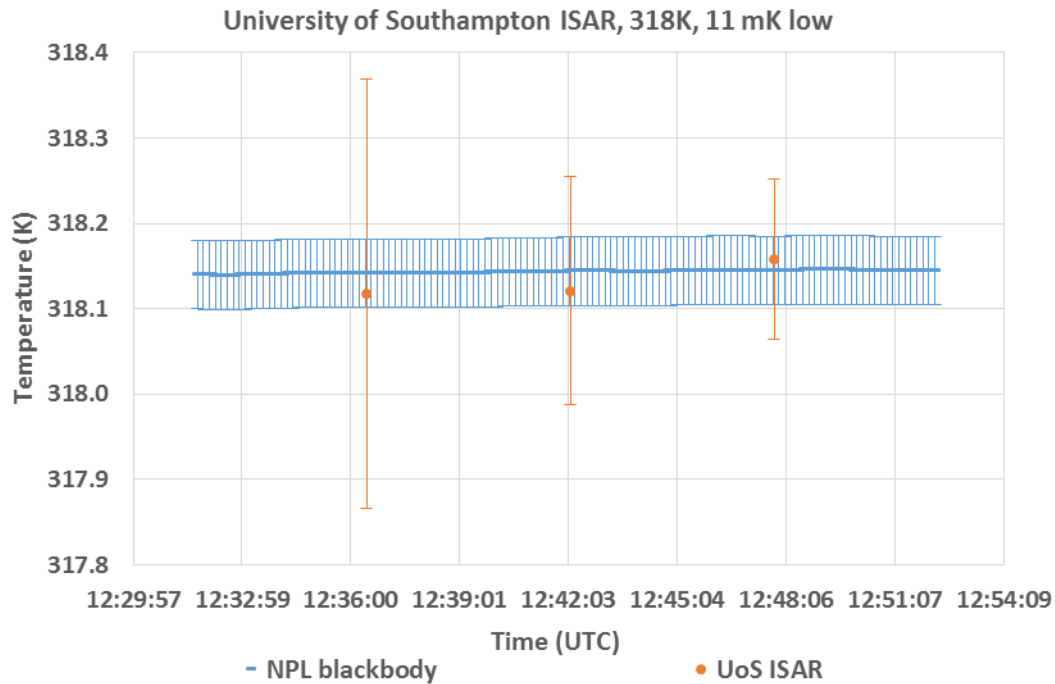


Figure 3.7.7: The University of Southampton ISAR radiometer viewing the NPL blackbody maintained at about 45 °C. The deviation of the ISAR radiometer from the average blackbody temperature over the measurement interval was 11 mK.

3.8 MEASUREMENTS MADE BY DMI

Danish Meteorological Institute
 Centre for Ocean and Ice, Lyngbyvej 100, 2100 København Ø
 Contact Name: Jacob Høyer
 Email: jlh@dmu.dk

3.8.1 Description of radiometers and route of traceability

3.8.1.1 Radiometer ISAR

Make and type of Radiometer: ISAR

The DMI TIR is an ISAR-5D, build by NOCS in 2012.

Outline Technical description of instrument: The radiometer is a self-calibrating radiometer, see Donlon, C., Robinson, I. S., Wimmer, W., Fisher, G., Reynolds, M., Edwards, R., & Nightingale, T. J. (2008). “An infrared sea surface temperature autonomous radiometer (ISAR) for deployment aboard volunteer observing ships (VOS)”. *Journal of Atmospheric and Oceanic Technology*, 25(1), 93-113.

Establishment or traceability route for primary calibration including date of last realisation and breakdown of uncertainty: The ISARS have been calibrated using the CASOTS blackbody, similar to the procedures used by Fred Wimmer, NOCS.

Operational methodology during measurement campaign:

The operational procedure for the DMI ISAR is to perform a calibration with the CASOTS blackbody, before and after any deployment over ice or water.

Radiometer usage (deployment), previous use of instrument and planned applications.

The DMI ISAR has been deployed at ships between Denmark and Greenland to observe SST. In addition, the DMI ISAR has participated in several field campaigns in the Arctic, to perform Ice surface temperature radiometer observations. The DMI ISAR has participated in the IST FICE campaign in March-April 2016.

3.8.1.2 Radiometer IR120

Make and type of Radiometer: Cambell Scientific IR120

The DMI IR120 was purchased from Cambell Scientific

Outline Technical description of instrument:

The radiometer is a broadband radiometer measuring within 8-14 μm with a 20 degree aperture. See: https://s.campbellsci.com/documents/eu/manuals/ir100_ir120.pdf

Establishment or traceability route for primary calibration including date of last realisation and breakdown of uncertainty:

The IR120 has been calibrated using the CASOTS blackbody.

Operational methodology during measurement campaign:

The operational procedure for the IR120 is to perform a calibration with the CASOTS, before and after any deployment over ice or water.

Radiometer usage (deployment), previous use of instrument and planned applications.

The IR120 has been used for several ice campaigns in Greenland and a similar instrument has been mounted on an automatic weather stations deployed From January-June 2015 and 2016

3.8.2 Uncertainty contributions associated with DMI's measurements at NPL

3.8.2.1 Uncertainty contributions ISAR

Table 3.8.1 shows the uncertainty budget associated with measurements made by the DMI ISAR radiometer.

Table 3.8.1 shows the uncertainty budget associated with measurements made by the DMI radiometer.

e	Item	Uncertainty	Unit	Type
1	Detector linearity	<0.01 %	K month ⁻¹	B
2	Detector noise	~0.002	Volts	A
3	Detector accuracy	±0.5	K	B
4	ADC	±1(±76.3)	LSB (μV)	B
5	ADC accuracy	±0.1%	Range	B
6	ADC zero drift	±6	μV °C ⁻¹	B
7	Reference voltage 16-bit ADC	±15	mV	B
8	Reference voltage 12-bit ADC	±20	mV	B
9	Reference resistor	1	%	B
10	Reference resistor temperature coefficient	±100	Ppm °C ⁻¹	B
11	BB emissivity	±0.000178	Emissivity	B
12	Sea surface emissivity	±0.07	Emissivity	B
13	Steinhart–Hart approximation	±0.01	K	B
14	Radiate transfer approximation	±0.001	K	B
15	Thermistor	±0.05	K	B
16	Thermistor noise	~0.002	V	A

Sources of uncertainties arising within the ISAR SST retrieval processor. A more detailed breakdown is available in the reference paper below.

Reference: Wimmer, W., and I. Robinson, 2016: The ISAR instrument uncertainty model. *J. Atmos. Oceanic Technol.* doi:10.1175/JTECH-D-16-0096.1, in press.

3.8.2.2 Camber Scientific IR120 radiometer

Aperture:	20 degrees.
Spectral band:	8-14 μm
Temperature resolution:	±0.01 °C
Uncertainty in measurement:	±0.2 °C
Typical Noise level at datalogger	0.05 °C RMS

3.8.3 Comparison of DMI's radiometers to the NPL reference blackbody.

3.8.3.1 Comparison of ISAR to the NPL reference blackbody

Figures 3.8.1 to 3.8.6 show the measurements completed by the DMI radiometer ISAR when it was viewing the NPL blackbody maintained at different temperatures. The uncertainty bars shown in orange in the Figures represent the uncertainty values provided by DMI which correspond to the measurements shown in the Figures. Also shown in blue in these Figures are the values of the brightness temperature of the NPL reference blackbody along with their combined uncertainty values.

Due to a limited schedule, a reliable temperature measurement was not made by DMI for the nominal temperature of -30 °C.

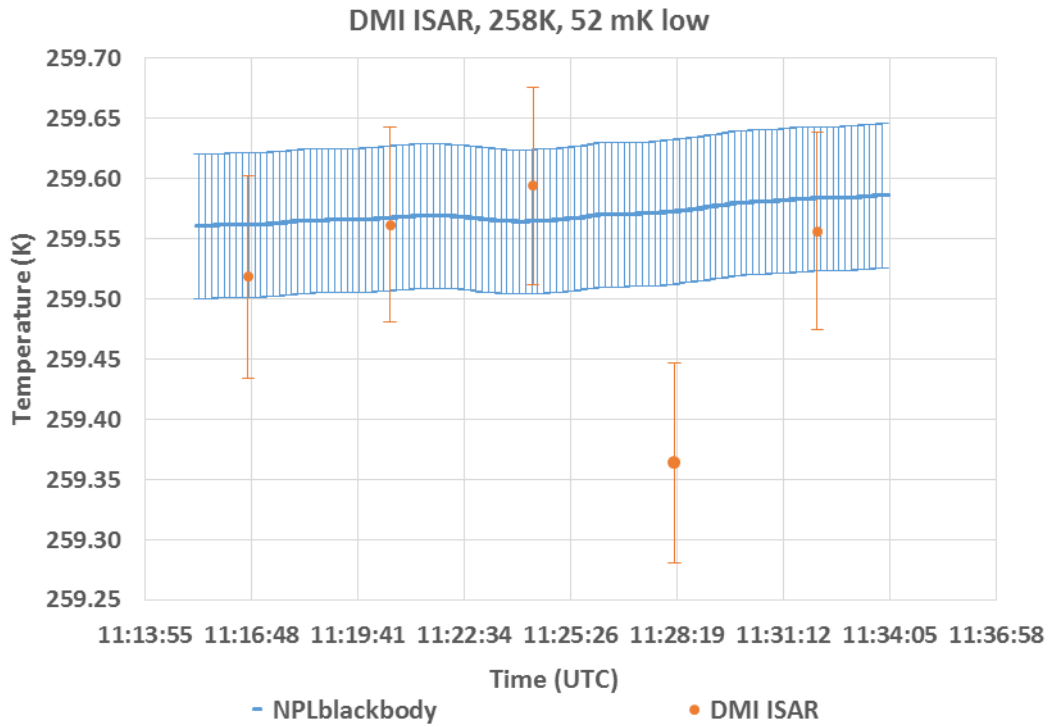


Figure 3.8.1: The DMI radiometer ISAR viewing the NPL blackbody maintained at -15 °C. The deviation of the ISAR radiometer from the average blackbody temperature over the measurement interval was 52 mK.

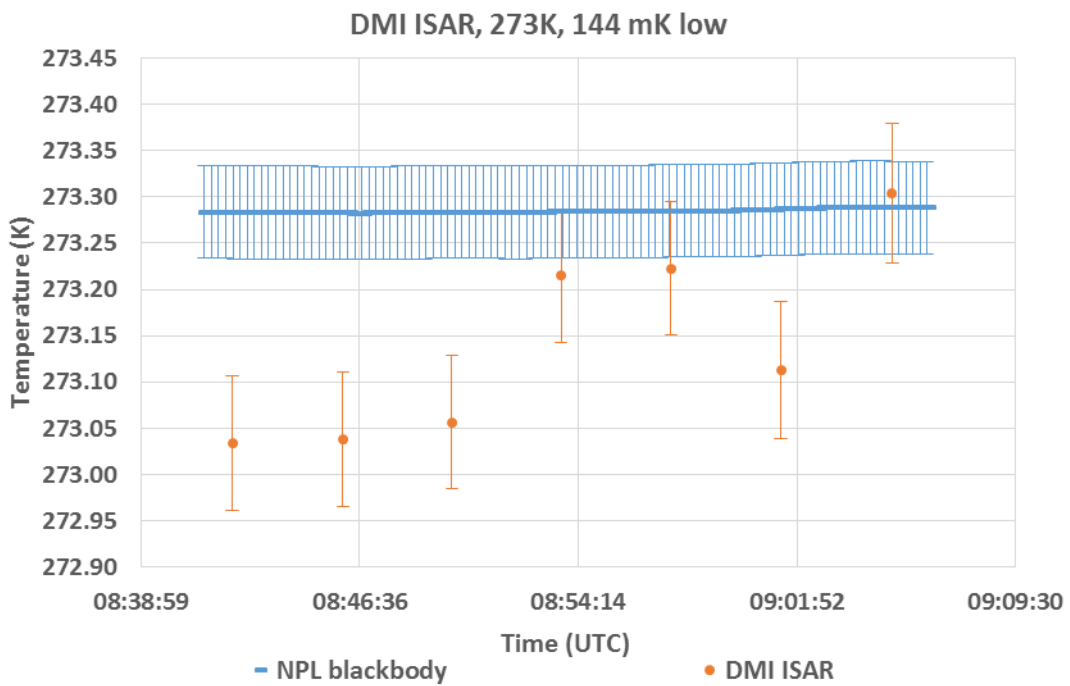


Figure 3.8.2: The DMI radiometer ISAR viewing the NPL blackbody maintained at 0 °C. The deviation of the ISAR radiometer from the average blackbody temperature over the measurement interval was 144 mK.

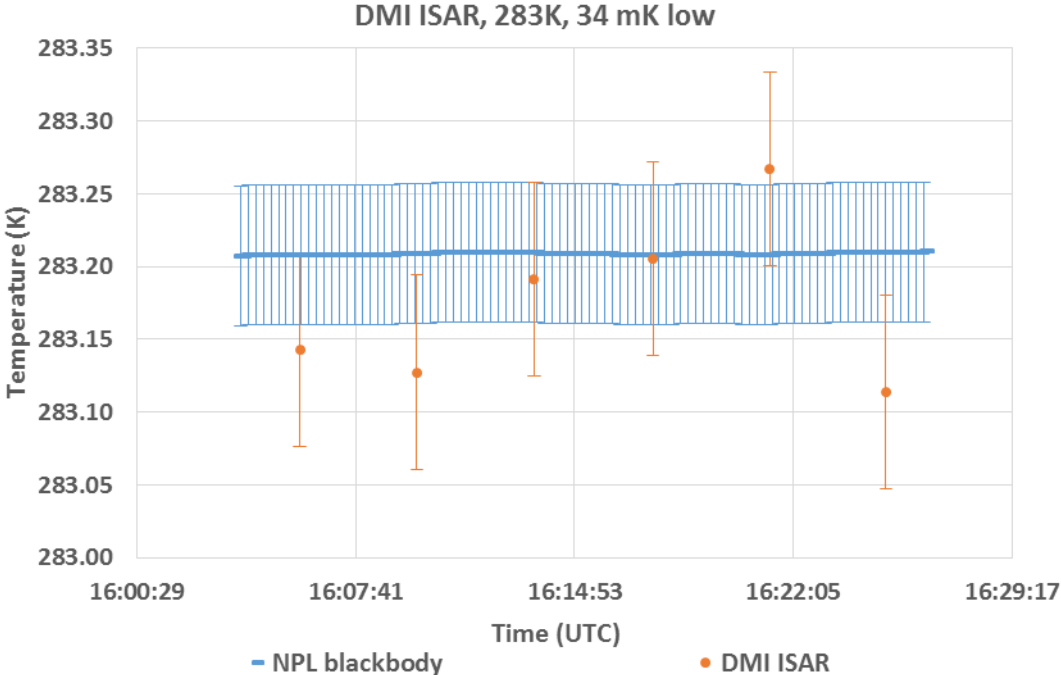


Figure 3.8.3: The DMI radiometer ISAR viewing the NPL blackbody maintained at 10 °C. The deviation of the ISAR radiometer from the average blackbody temperature over the measurement interval was 34 mK.

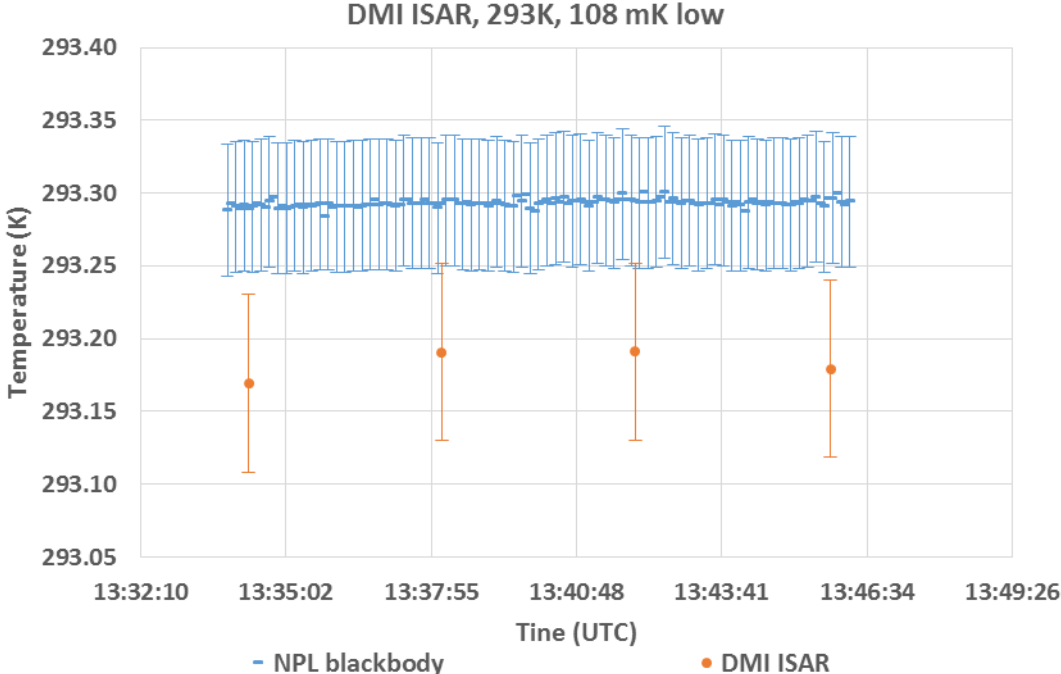


Figure 3.8.4: The DMI radiometer ISAR viewing the NPL blackbody maintained at 20 °C. The deviation of the ISAR radiometer from the average blackbody temperature over the measurement interval was 108 mK.

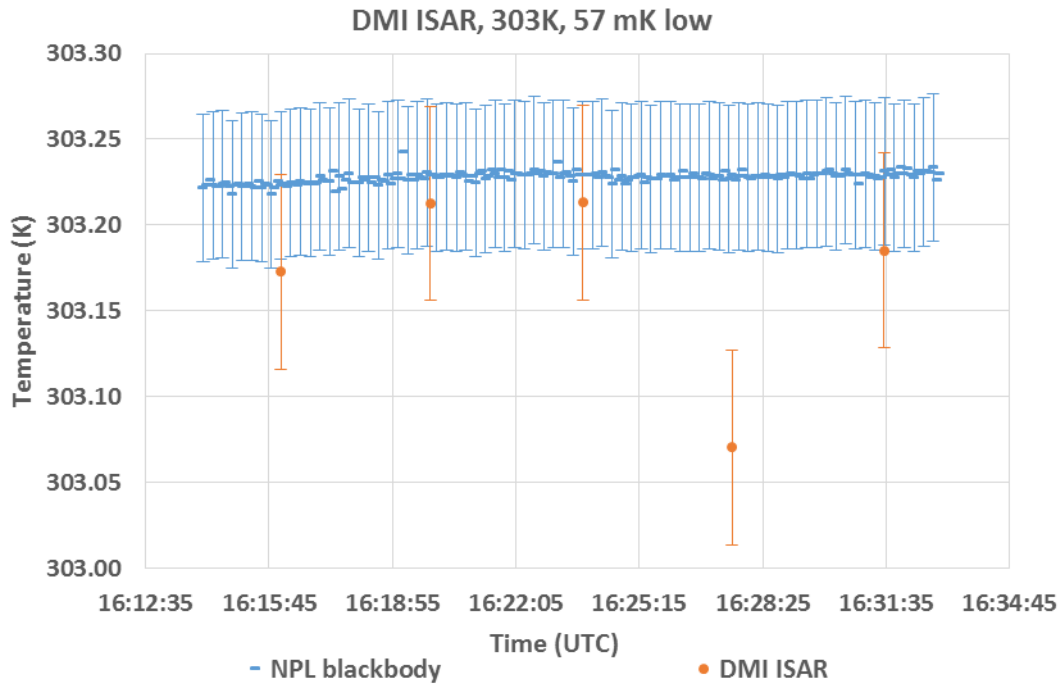


Figure 3.8.5: The DMI radiometer ISAR viewing the NPL blackbody maintained at 30 °C. The deviation of the ISAR radiometer from the average blackbody temperature over the measurement interval was 57 mK.

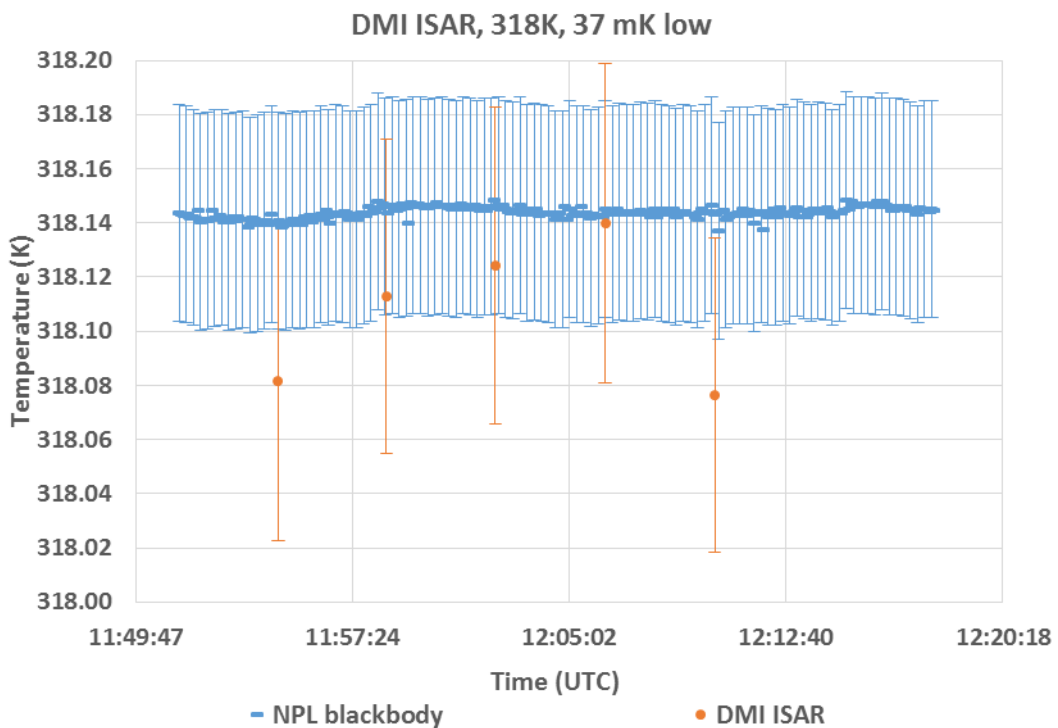


Figure 3.8.6: The DMI radiometer ISAR viewing the NPL blackbody maintained at 45 °C. The deviation of the ISAR radiometer from the average blackbody temperature over the measurement interval was 37 mK.

3.8.3.2 Comparison of IR120 radiometer to NPL reference blackbody

Figures 3.8.7, 3.8.8 and 3.8.9 show the measurements completed by the DMI radiometer IR120 when it was viewing the NPL blackbody maintained at different temperatures. The uncertainty bars shown in orange in the figures represent the uncertainty values provided by DMI which correspond to the measurements shown in the Figures. Also shown in blue in these Figures are the values of the brightness temperature of the NPL reference blackbody along with their combined uncertainty values.

Due to technical faults and a limited schedule, DMI were only able to make reliable temperature measurements of nominal blackbody temperatures of 10 °C, 20 °C and 30 °C using the IR120 radiometer.

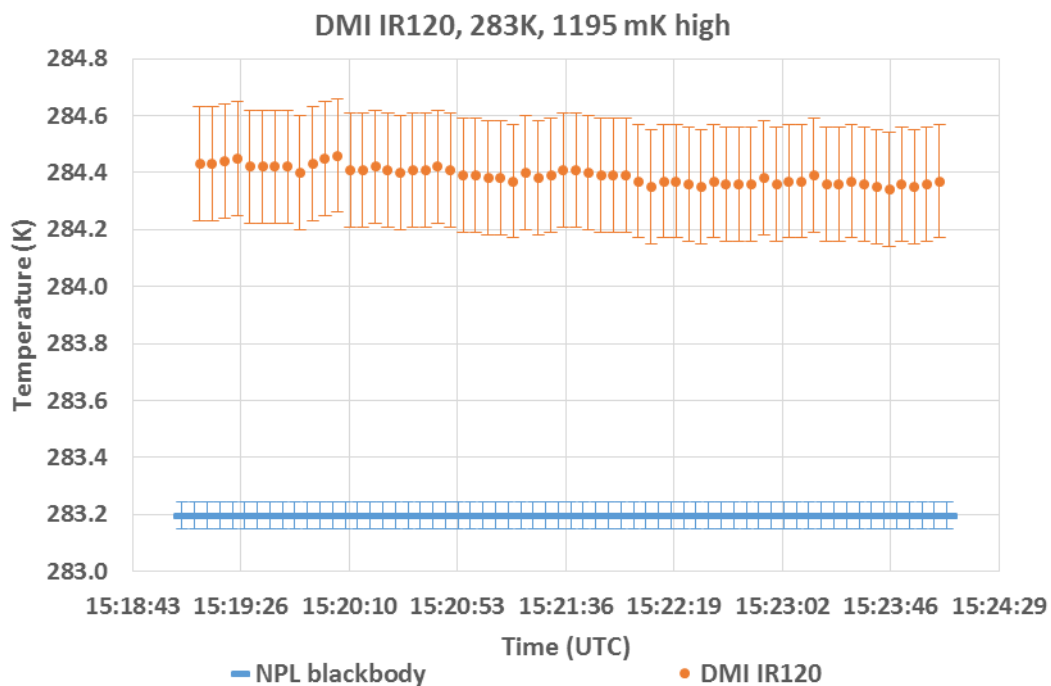


Figure 3.8.7: The DMI radiometer IR120 viewing the NPL blackbody maintained at 10 °C. The deviation of the ISAR radiometer from the average blackbody temperature over the measurement interval was 1195 mK.

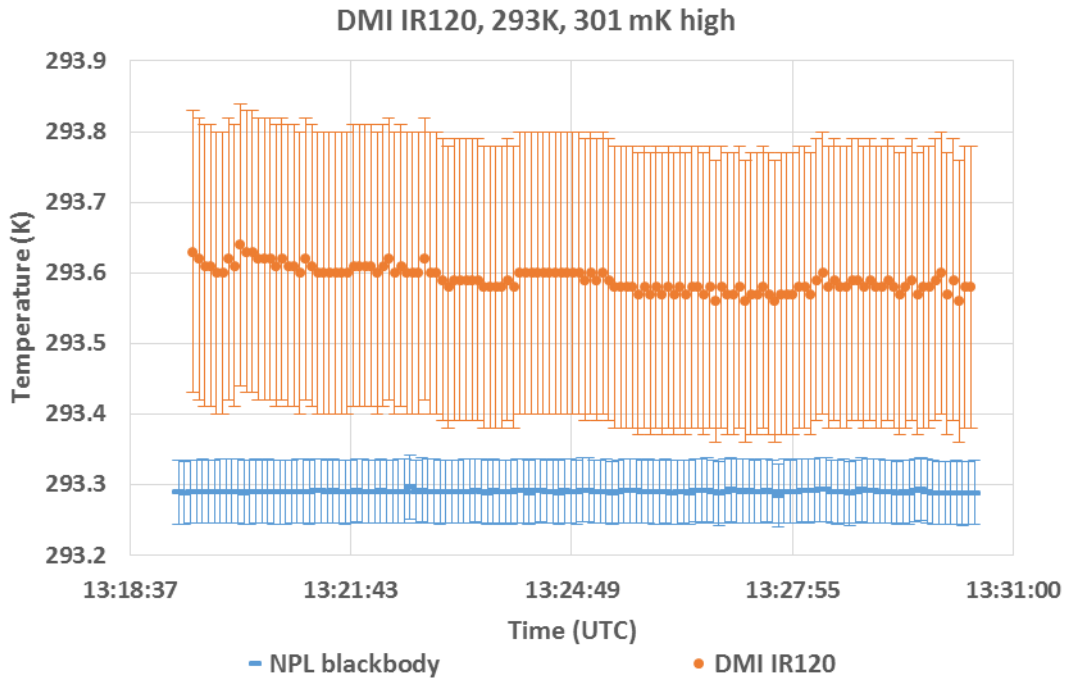


Figure 3.8.8: The DMI radiometer IR120 viewing the NPL blackbody maintained at 20 °C. The deviation of the ISAR radiometer from the average blackbody temperature over the measurement interval was 301 mK.

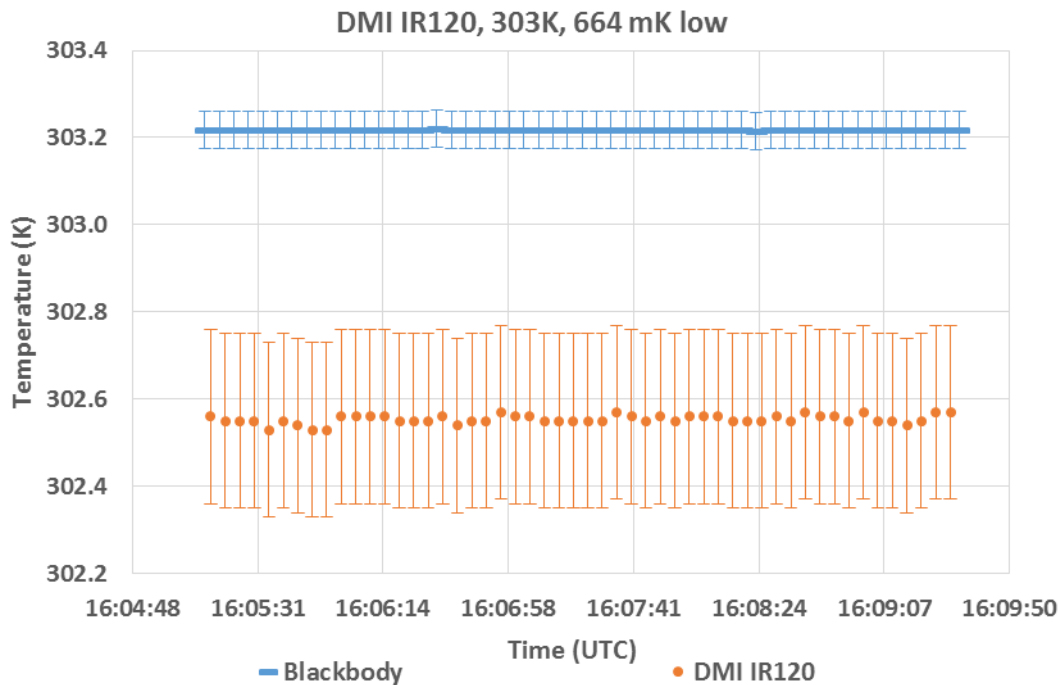


Figure 3.8.9: The DMI radiometer IR120 viewing the NPL blackbody maintained at 30 °C. The deviation of the ISAR radiometer from the average blackbody temperature over the measurement interval was 664 mK.

3.8.4 Additional comments from DMI regarding the radiometer lab comparison

DMI provided the following comments regarding the performance of their ISAR radiometer:

“We have discovered issues with one of our reference thermistors on the blackbody. It appears to have an offset at some time and have an enhanced variability at other times. This is a serious issue, as this is used to reference the KT15 target observations. It looks like it needs a hardware update. In any case, the DMI ISAR data should be used with care and a note to go with them. In addition, note that the radiometer performance for extreme target temperatures, relative to ambient may be degraded. Usually, the ambient temperature in e.g. ice experiments is similar to IST when measuring cold ice surfaces. This makes the ambient and heated blackbodies much more representable when correcting the measured brightness temperatures. We deliver total uncertainties based on the processing software provided by Werenfrid Wimmer of the University of Southampton”.

3.9 MEASUREMENTS MADE BY OUC, QINGDAO

Ocean University of China
238 Songling Road, Qingdao, 266100, China
Contact Name: Kailin Zhang
Email: zhangkl@ouc.edu.cn

3.9.1 Description of radiometers and route of traceability

3.9.1.1 The ISAR Radiometer

Make and type of Radiometer

Infrared Sea Surface Temperature Autonomous Radiometer (ISAR)

Outline Technical description of the radiometer:

Detector: Heitronics KT15.85 IIP 8115, Spectral bands: 9.6 μm to 11.5 μm ,

Calibration type: two internal blackbody (BB) cavities (Donlon et al. 2008)

Establishment or traceability route for primary calibration including date of last realisation and breakdown of uncertainty:

ISAR has undergone primary calibration by the manufacturer. Re-calibrations are performed before and after each measurement campaign using the blackbody manufactured by LR TECH INC. The overall uncertainty of ISAR is about 0.1 K. (Donlon et al. 2008; Wimmer et al. 2016)

Operational methodology during measurement campaign:

ISAR measures both the sea surface radiance and the downwelling atmosphere radiance which are calibrated by two reference blackbody cavities. During one measuring cycle, ISAR measures the ambient blackbody 30 times, the heated blackbody 30 times, the sky 10 times and

the sea 40 times. Using the self-calibration system in ISAR, SST is calculated for each measuring cycle (Donlon et al. 2008).

Radiometer usage (deployment), previous use of instrument and planned applications.

The ISAR has been deployed on the research vessel Dong Fang Hong II of Ocean University of China and continuously operating mainly in the China Seas since 2009.

References:

Donlon, C. J., I. S. Robinson, M. Reynolds, W. Wimmer, G. Fisher, R. Edwards, and T. J. Nightingale, 2008: An Infrared Sea Surface Temperature Autonomous Radiometer (ISAR) for Deployment aboard Volunteer Observing Ships (VOS), *J. Atmos. Oceanic Technol.*, 25, 93-113.

Wimmer, W., and I. Robinson, 2016: The ISAR instrument uncertainty model. *J. Atmos. Oceanic Technol.* doi:10.1175/JTECH-D-16-0096.1, in press.

3.9.1.2 The OUCFIRST Radiometer

Make and type of Radiometer

Ocean University of China First Infrared Radiometer for measurements of Sea Surface Temperature (OUCFIRST)

Outline Technical description of instrument:

Detector: Heitronics KT15.85 IIP 9928, Spectral bands: 9.6 μm to 11.5 μm ,

Calibration type: 2 internal blackbody (BB) cavities

Establishment or traceability route for primary calibration including date of last realisation and breakdown of uncertainty:

OUCFIRST is calibrated before and after each measurement campaign using the blackbody manufactured by LR TECH INC. The overall uncertainty of OUCFIRST is about 0.1 K.

Operational methodology during measurement campaign:

OUCFIRST has two measurement modes, one for lab calibration and the other one for outdoor measurement. For lab calibration, OUCFIRST measures the ambient blackbody 30 times, the heated blackbody 30 times and target blackbody 40 times. For outdoor mode, OUCFIRST measures the ambient blackbody 30 times, the heated blackbody 30 times, the sky 10 times and the sea 40 times. Using the self-calibration system in OUCFIRST, SST is calculated for each measuring cycle.

Radiometer usage (deployment), previous use of instrument and planned applications.

OUCFIRST is now under testing and has been deployed on the research vessel Dong Fang Hong II of Ocean University of China and operated for three campaigns in the China Seas in 2015 and 2016.

3.9.2 Uncertainty contributions associated with OUC's measurements at NPL**3.9.2.1 Uncertainty contributions ISAR**

Table 3.9.1 shows the uncertainty budget associated with measurements made by the ISAR OUC radiometer.

Table 3.9.1: The uncertainty budget associated with measurements made by the OUC radiometer

e	Item	Uncertainty	Unit	Type
1	Detector linearity	<0.01 %	K month ⁻¹	B
2	Detector noise	~0.002	Volts	A
3	Detector accuracy	±0.5	K	B
4	ADC	±1(±76.3)	LSB (μV)	B
5	ADC accuracy	±0.1 %	Range	B
6	ADC zero drift	±6	μV °C ⁻¹	B
7	Reference voltage 16-bit ADC	±15	mV	B
8	Reference voltage 12-bit ADC	±20	mV	B
9	Reference resistor	1	%	B
10	Reference resistor temperature coefficient	±100	Ppm °C ⁻¹	B
11	BB emissivity	±0.000178	Emissivity	B
12	Sea surface emissivity	±0.07	Emissivity	B
13	Steinhart–Hart approximation	±0.01	K	B
14	Radiate transfer approximation	±0.001	K	B
15	Thermistor	±0.05	K	B
16	Thermistor noise	~0.002	V	A

Sources of uncertainties arising within the ISAR SST retrieval processor. A more detailed breakdown is available in the reference paper: Wimmer, W., and I. Robinson, 2016: The ISAR instrument uncertainty model. *J. Atmos. Oceanic Technol.* doi:10.1175/JTECH-D-16-0096.1, in press.

3.9.2.2 Uncertainty contributions OUCFIRST

Uncertainty Contribution	Type A Uncertainty in Value / %	Type B Uncertainty in Value / (appropriate units)	Uncertainty in Brightness temperature K
Repeatability of measurement ⁽¹⁾	0.023 K /0.008%		0.023 K
Reproducibility of measurement ⁽²⁾	0.009 K /0.003%		0.009 K
Primary calibration ⁽³⁾		0.12 K	0.12 K
RMS total	0.025 K /0.008%	4 0.12 K	0.12 K

(1) Typical value of the standard deviation of 143 measurements at fixed black body temperature without re-alignment of radiometer.

(2) Typical value of difference between two runs of radiometer measurements at the same black body temperature including re-alignment.

(3) Typical value of difference between radiometer brightness temperature and ASSIST II Blackbody temperature.

3.9.3 Comparison of OUC's radiometers to the NPL reference blackbody

3.9.3.1 Comparison of ISAR to the NPL reference blackbody

Figures 3.9.1 to 3.9.7 show the measurements completed by the OUC ISAR radiometer when it was viewing the NPL blackbody maintained at different temperatures. The uncertainty bars shown in orange in the Figures represent the uncertainty values provided by OUC which correspond to the measurements shown in the Figures. Also shown in blue in these Figures are the values of the brightness temperature of the NPL reference blackbody along with their combined uncertainty values.

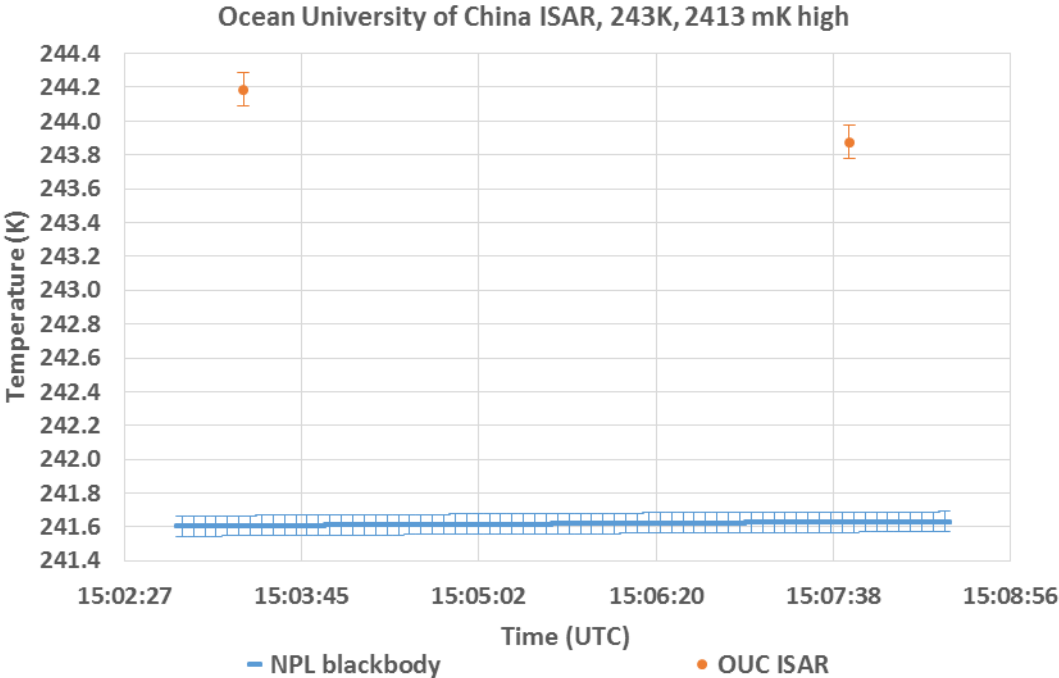


Figure 3.9.1: Measurements of the OUC ISAR radiometer when it was viewing the NPL blackbody maintained at about -30 °C. The deviation of the ISAR radiometer from the average blackbody temperature over the measurement interval was 2413 mK

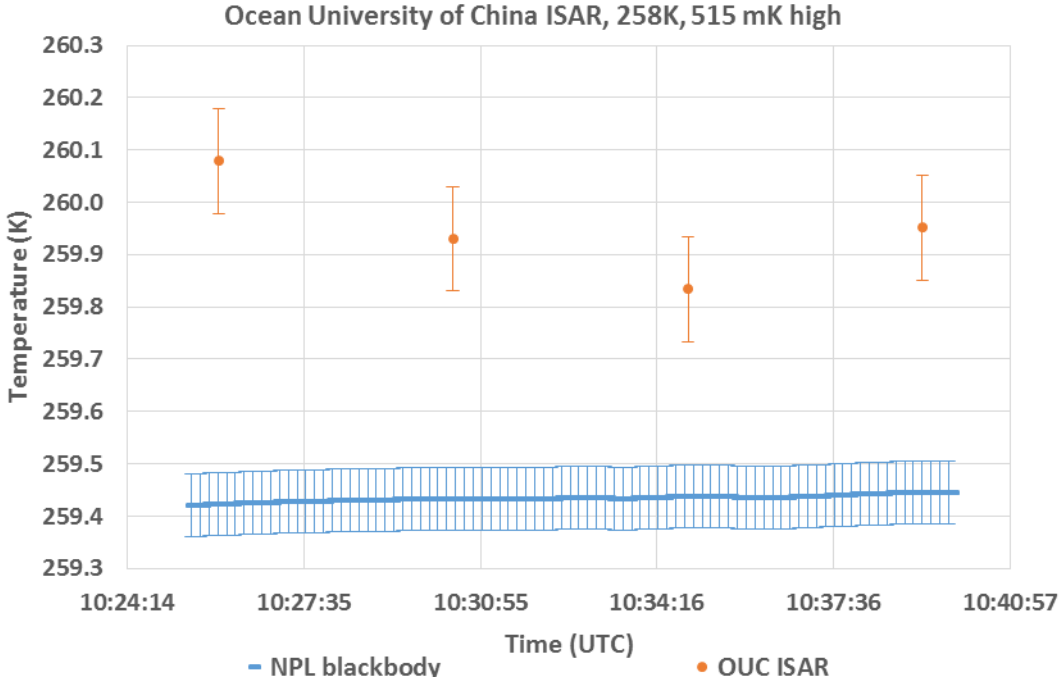


Figure 3.9.2: Measurements of the OUC ISAR radiometer when it was viewing the NPL blackbody maintained at about -15 °C. The deviation of the ISAR radiometer from the average blackbody temperature over the measurement interval was 515 mK

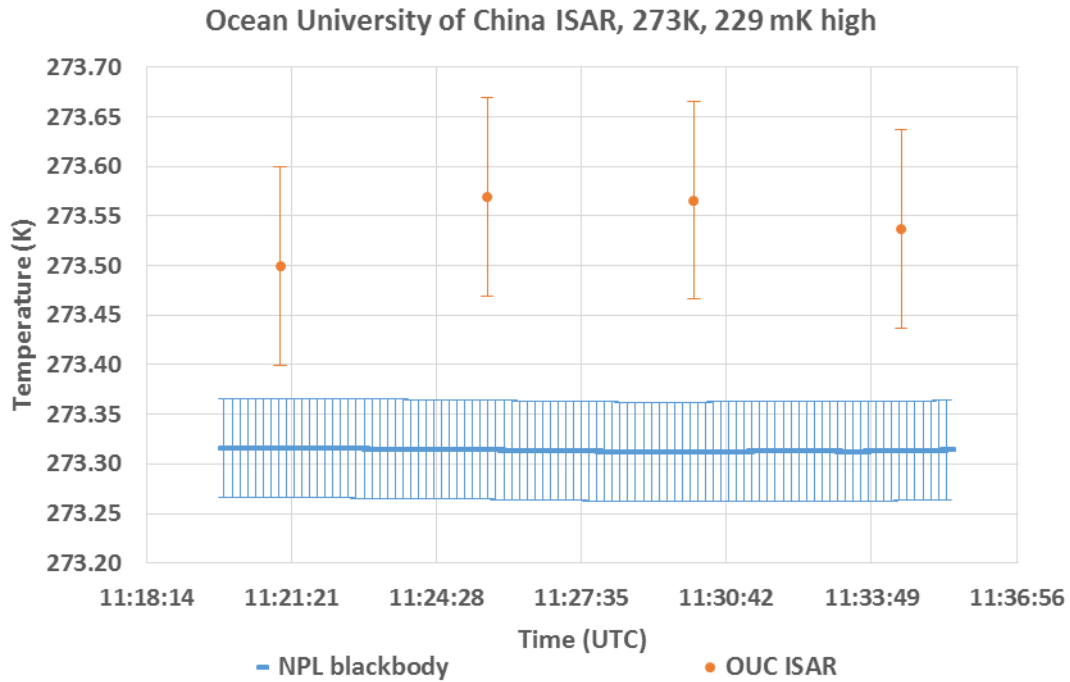


Figure 3.9.3: Measurements of the OUC ISAR radiometer when it was viewing the NPL blackbody maintained at about 0 °C. The deviation of the ISAR radiometer from the average blackbody temperature over the measurement interval was 229 mK.

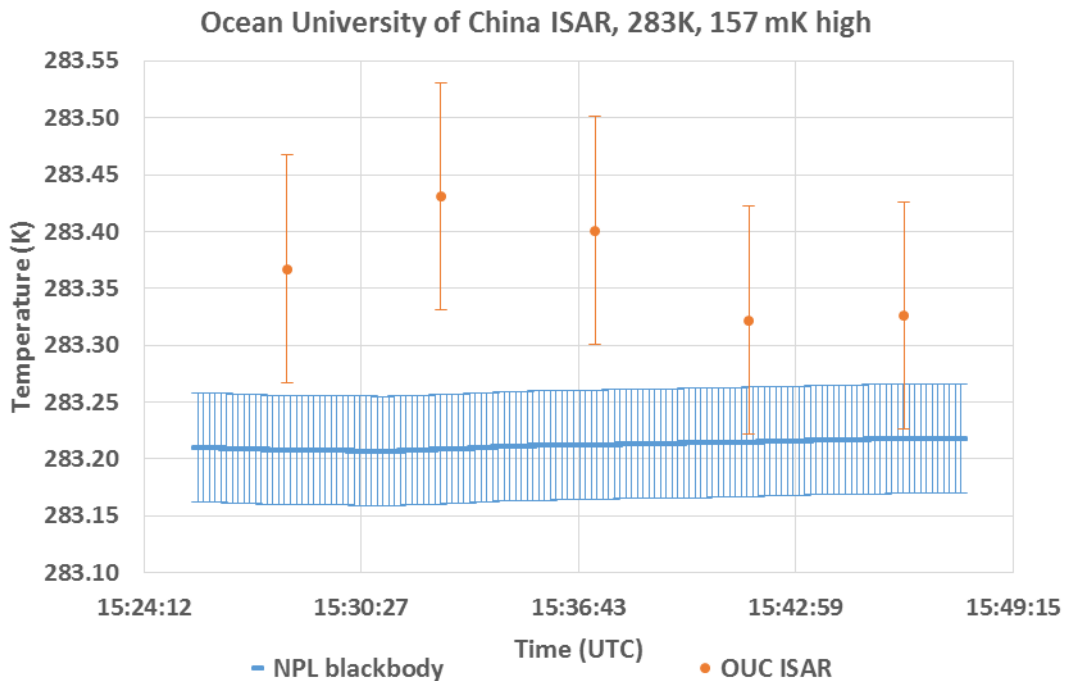


Figure 3.9.4: Measurements of the OUC ISAR radiometer when it was viewing the NPL blackbody maintained at about 10 °C. The deviation of the ISAR radiometer from the average blackbody temperature over the measurement interval was 157 mK.

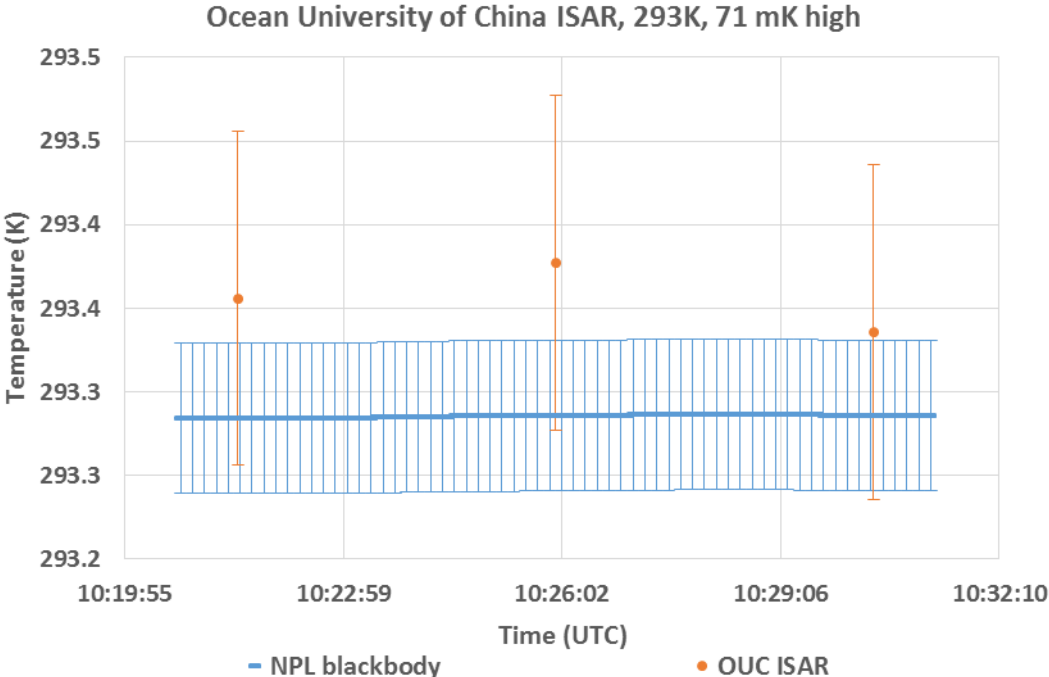


Figure 3.9.5: Measurements of the OUC ISAR radiometer when it was viewing the NPL blackbody maintained at about 20 °C. The deviation of the ISAR radiometer from the average blackbody temperature over the measurement interval was 71 mK

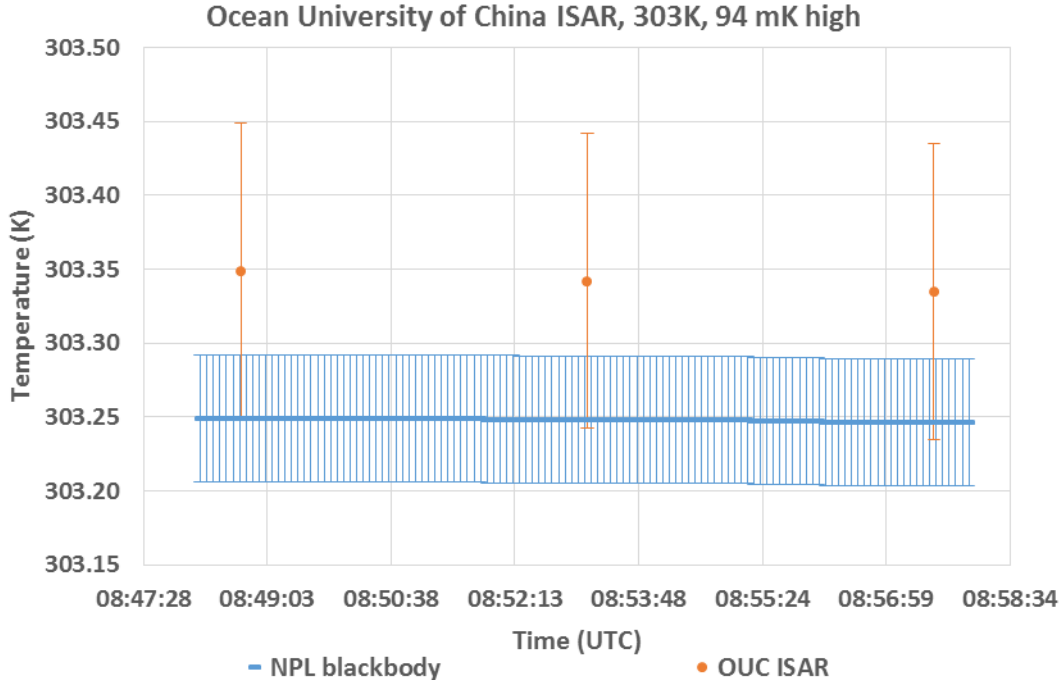


Figure 3.9.6: Measurements of the OUC ISAR radiometer when it was viewing the NPL blackbody maintained at about 30 °C. The deviation of the ISAR radiometer from the average blackbody temperature over the measurement interval was 94 mK.

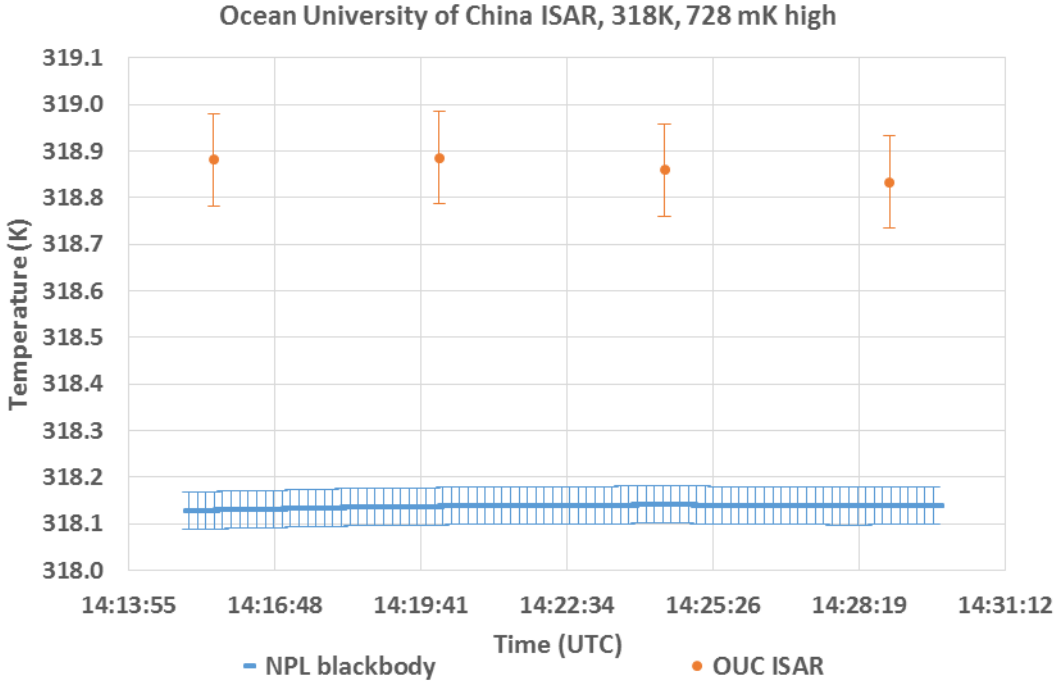


Figure 3.9.7: Measurements of the OUC ISAR radiometer when it was viewing the NPL blackbody maintained at about 45 °C. The deviation of the ISAR radiometer from the average blackbody temperature over the measurement interval was 728 mK.

3.9.3.2 Comparison of OUCFIRST radiometer to the NPL reference blackbody.

The photo below shows the OUCFIRST radiometer viewing the NPL reference blackbody.



The OUCFIRST radiometer viewing the NPL reference blackbody

Figures 3.9.8 to 3.9.14 show the measurements completed by the OUCFIRST radiometer when it was viewing the NPL blackbody maintained at different temperatures. The uncertainty bars shown in orange in the figures represent the uncertainty values provided by OUC which correspond to the measurements shown in the Figures. Also shown in blue in these Figures are the values of the brightness temperature of the NPL reference blackbody along with their combined uncertainty values.

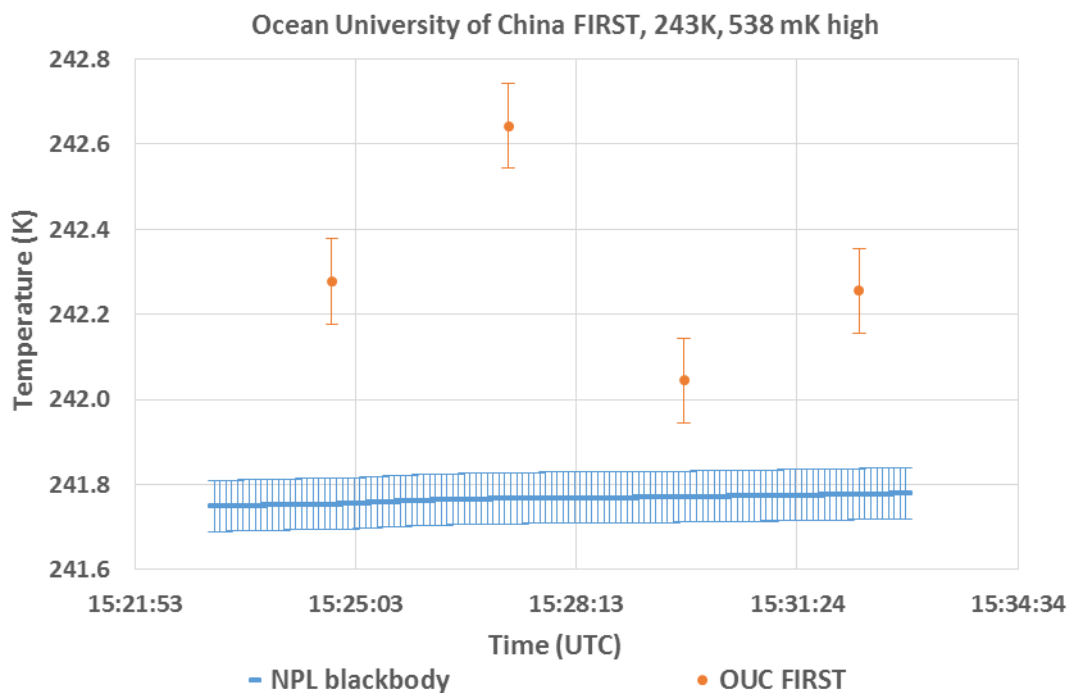


Figure 3.9.8: Measurements of the OUCFIRST radiometer when it was viewing the NPL blackbody maintained at about -30°C . The deviation of the OUC radiometer from the average blackbody temperature over the measurement interval was 538 mK.

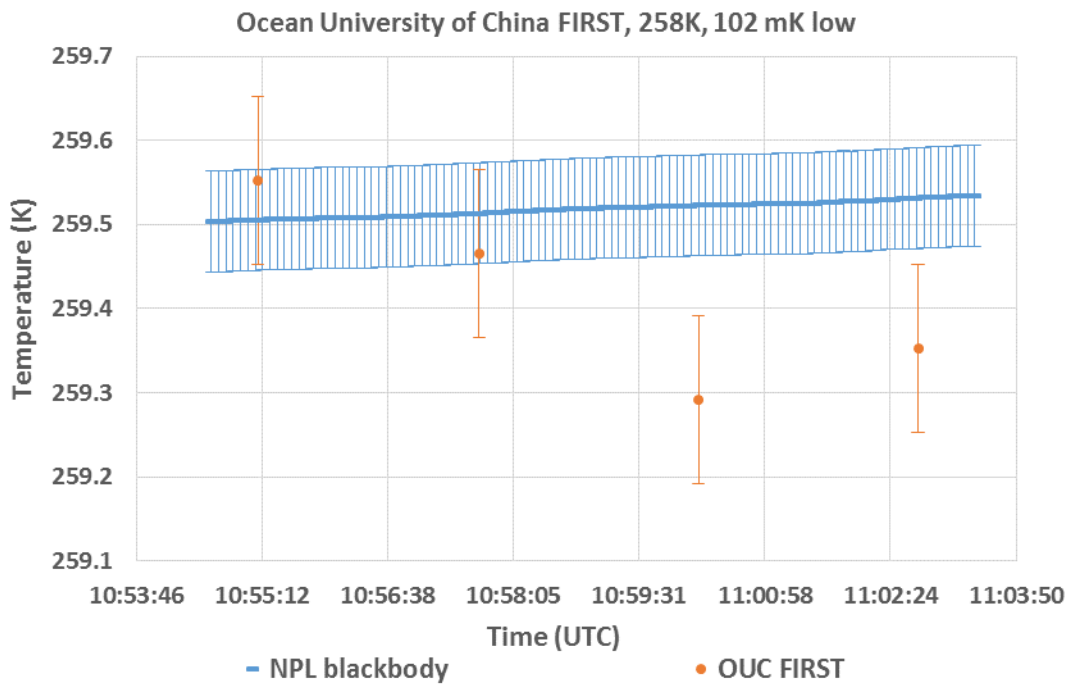


Figure 3.9.9: Measurements of the OUCFIRST radiometer when it was viewing the NPL blackbody maintained at about -15 °C. The deviation of the OUC radiometer from the average blackbody temperature over the measurement interval was 102 mK.

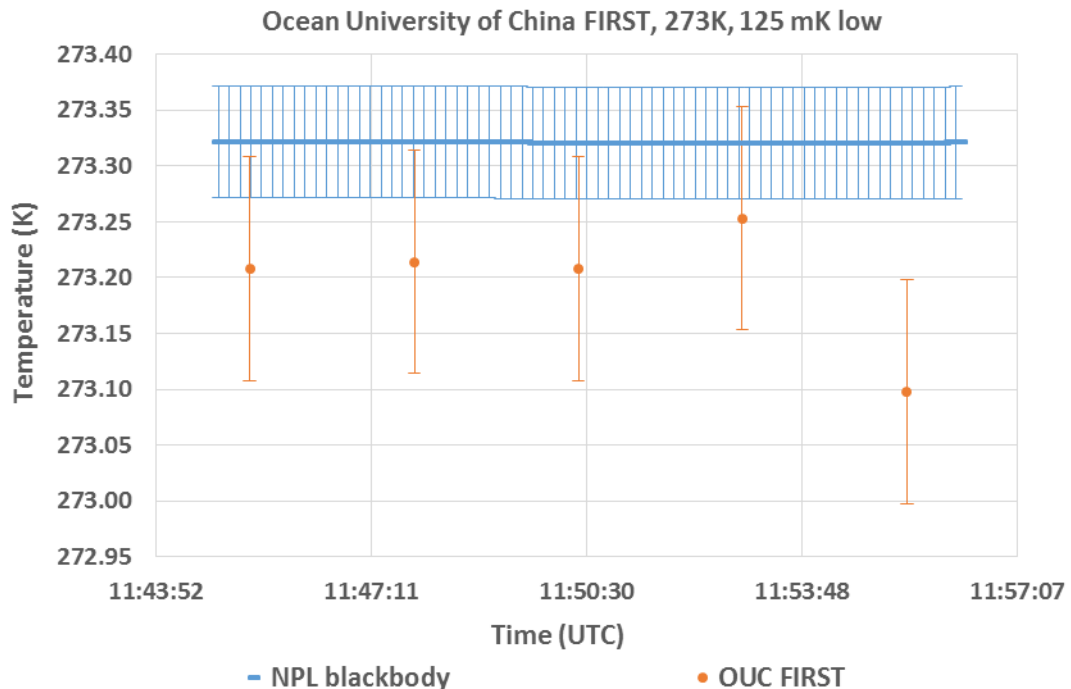


Figure 3.9.10: Measurements of the OUCFIRST radiometer when it was viewing the NPL blackbody maintained at about 0 °C. The deviation of the OUC radiometer from the average blackbody temperature over the measurement interval was 125 mK.

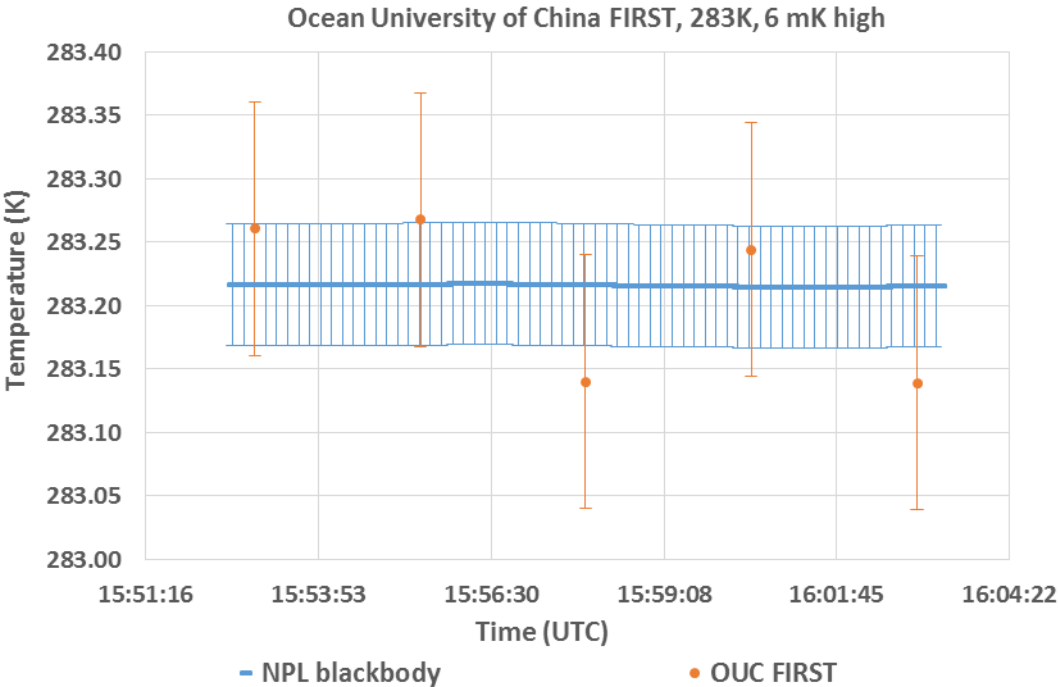


Figure 3.9.11: Measurements of the OUCFIRST radiometer when it was viewing the NPL blackbody maintained at about 10 °C. The deviation of the OUC radiometer from the average blackbody temperature over the measurement interval was 6 mK.

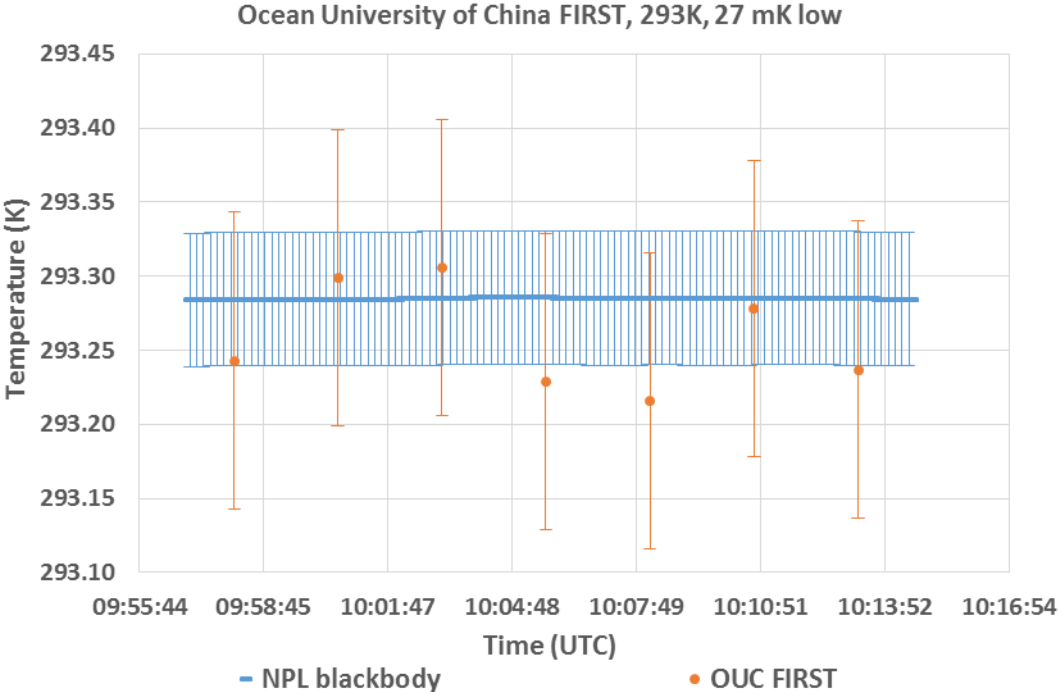


Figure 3.9.12: Measurements of the OUCFIRST radiometer when it was viewing the NPL blackbody maintained at about 20 °C. The deviation of the OUC radiometer from the average blackbody temperature over the measurement interval was 27 mK.

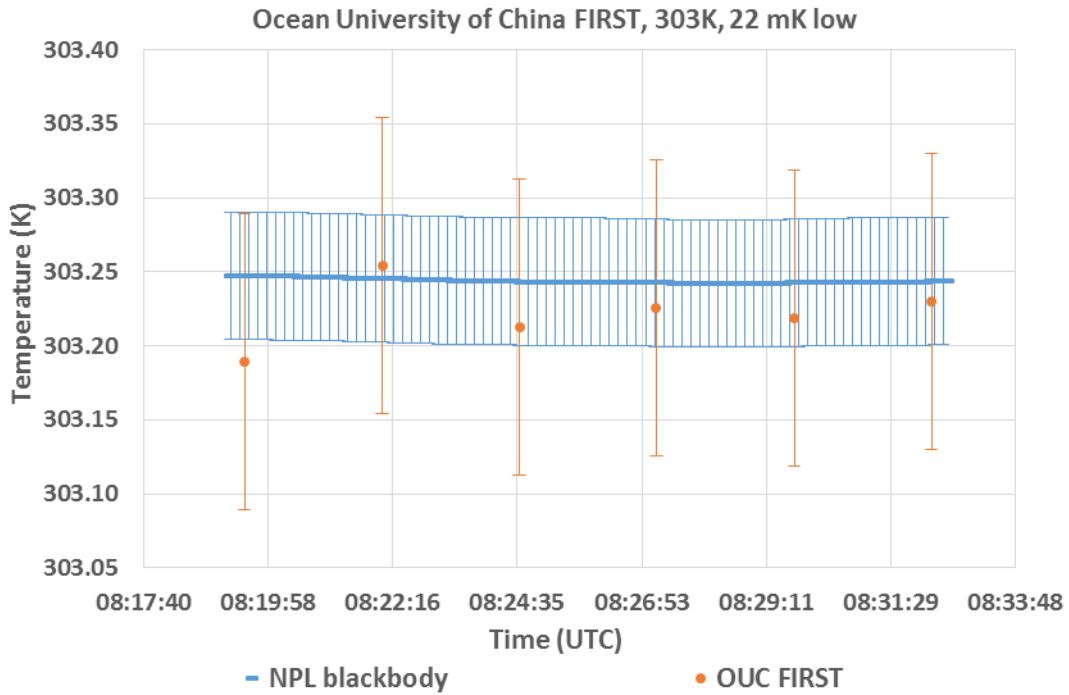


Figure 3.9.13: Measurements of the OUCFIRST radiometer when it was viewing the NPL blackbody maintained at about 30 °C. The deviation of the OUC radiometer from the average blackbody temperature over the measurement interval was 22 mK.

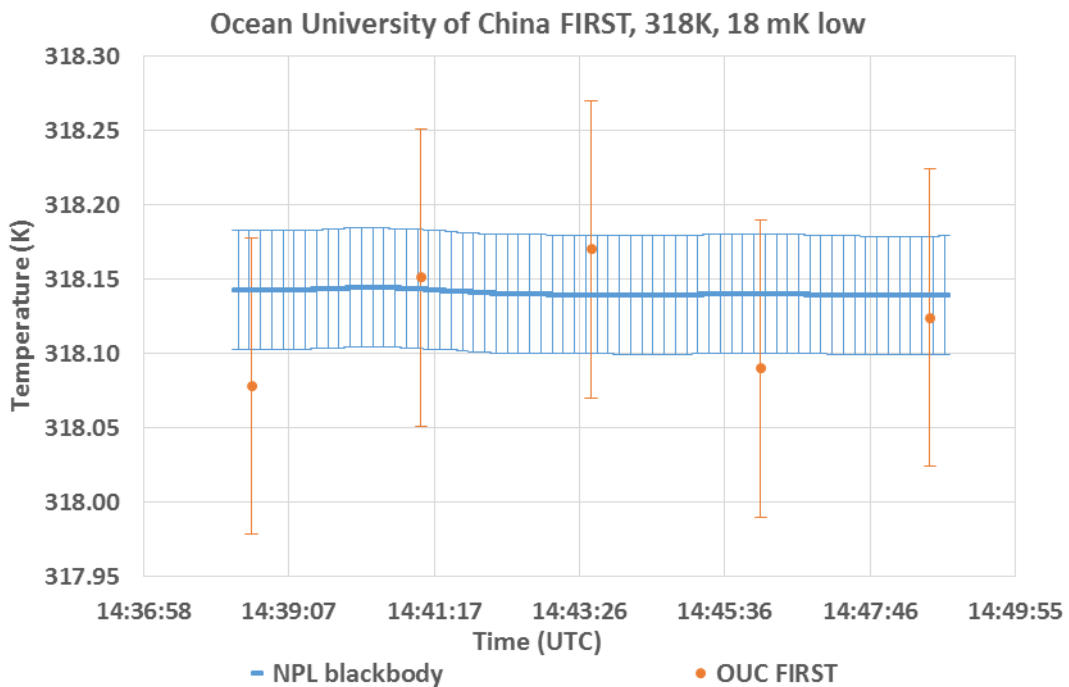


Figure 3.9.14: Measurements of the OUCFIRST radiometer when it was viewing the NPL blackbody maintained at about 45 °C. The deviation of the OUC radiometer from the average blackbody temperature over the measurement interval was 18 mK.

3.10 MEASUREMENTS MADE BY GOTA

Grupo de Observacion de la Tierra y la Atmosfera (GOTA)
 Departamento de Física Fundamental Experimental, Electrónica Sistemas
 Universidad de La Laguna Avda. Astrofísico Fco. Sanchez s/n 38200 La Laguna Tenerife,
 Canarias, Spain.

Contact Name: Manuel Arbelo

Email: marbelo@ull.es

3.10.1 Description of radiometer and route of traceability

Make and type of Radiometer: CIMEL Electronique CE312-2

Outline Technical description of instrument:

Type of detector: thermopile. 6 spectral bands: B1 8-13 μm , B2 11.0-11.7 μm , B3 10.3-11.0 μm , B4 8.9-9.3 μm , B5 8.5-8.9 μm , and B6 8.1-8.5 μm . The spectral characterisation of the instrument can be found in references 1, 2 and 3. Broad band: Germanium window and zinc sulphide filters. Narrow bands: interference filters. Field of view: 10°. The radiometer has a built-in radiance reference made of a concealable gold-coated mirror which enables comparison between the target radiance and the reference radiation from inside the detector cavity. The temperature of the detector is measured with a PRT, thus allowing compensation for the cavity radiation.

References:

1. Sicard, M., Spyak, P. R., Brogniez, G., Legrand, M., Abuhassan, N. K., Pietras, C., and Buis, J. P. (1999). Thermal infrared field radiometer for vicarious cross-calibration: characterization and comparisons with other field instruments. *Optical Engineering*, 38 (2), 345-356.
2. M. Legrand, C. Pietras, G. Brogniez, M. Haeffelin, N. K. Abuhassan and M. Sicard (2000). A high accuracy multiwavelength radiometer for in situ measurements in the thermal infrared. Part I: characterization of the instrument, *J. Atmos. Ocean Techn.*, 17, 1203-1214.
3. <http://www.cimel.fr/?instrument=radiometer-ir-climat-benchmark&lang=en>

Establishment or traceability route for primary calibration including date of last realisation and breakdown of uncertainty: The radiometer has not undergone a traceable primary calibration. The following uncertainty analysis was based on estimates, experience and laboratory measurements with our Landcal Blackbody Source P80P (May 23 to 26, 2016).

Type A

- Repeatability: typical value of the standard deviation of 10 measurements at fixed black body temperature without re-alignment of radiometer.

	B1	B2	B3	B4	B5	B6	Mean
K	0.04	0.10	0.09	0.09	0.11	0.10	0.09
%	0.01	0.03	0.04	0.03	0.04	0.04	0.03

- Reproducibility: typical value of difference between two runs of radiometer measurements at the same black body temperature including re-alignment.

	B1	B2	B3	B4	B5	B6	Mean
K	0.05	0.02	0.03	0.03	0.04	0.03	0.03
%	0.01	0.01	0.01	0.01	0.01	0.01	0.01

Total Type A uncertainty (RSS):

	B1	B2	B3	B4	B5	B6	Mean
K	0.06	0.10	0.09	0.09	0.12	0.10	0.09
%	0.01	0.03	0.04	0.03	0.04	0.04	0.03

Type B

- Linearity of radiometer: within temperature range of 278-303 K.

	B1	B2	B3	B4	B5	B6	Mean
K	0.09	0.11	0.10	0.10	0.11	0.10	0.10

- Primary calibration: typical value of difference between radiometer brightness temperature and Landcal Blackbody Source P80P temperature.

	B1	B2	B3	B4	B5	B6	Mean
K	0.9	0.4	0.3	0.4	0.3	0.2	0.4

- Drift since calibration: 0.0 K (as expected since very recent calibration measurements).

- Ambient temperature fluctuations: 0.3 K

- Size-of-Source Effect: not considered

- Atmospheric absorption/emission: not considered

Total Type B uncertainty (RSS):

	B1	B2	B3	B4	B5	B6	Mean
K	0.9	0.5	0.4	0.5	0.4	0.4	0.5

Type A + Type B uncertainty (RSS): 0.5 K

Operational methodology during measurement campaign: Calibration measurements were performed in the laboratory following, as close as possible, the procedures described in the Draft Protocol. The Landcal Blackbody Source P80P was set at four temperatures (278 K, 283 K, 293 K and 303 K) in two different runs. Enough time was allowed for the black body to reach equilibrium at each temperature. Radiometer was aligned with the black body cavity, and placed at a distance so that the field of view was smaller than the cavity diameter. Standard processing (see references above) was applied to the radiometer readouts to calculate the equivalent brightness temperature. The six bands of the CE312-2 instrument were used.

Radiometer usage (deployment), previous use of instrument and planned applications. Field measurements (hand held and tripod mounted) of land and sea surface temperature/emissivity. Validation of thermal infrared images from satellite sensors in Canary Islands as well as laboratory measurements of soil and vegetation emissivity. Planned validation of thermal infrared images from cameras on board UAVs in forest and crops in Macaronesian region.

3.10.2 Uncertainty contributions associated with GOTA's measurements at NPL

Uncertainty Contribution	Type A Uncertainty in Value / %	Type B Uncertainty in Value / (appropriate units)	Uncertainty in Brightness temperature K
Repeatability of measurement	0.03%		0.09 K
Reproducibility of measurement	0.01%		0.03 K
Primary calibration		0.4 K	0.4 K
Linearity of radiometer		0.10 K	0.1 K
Drift since calibration		-	-
Ambient temperature fluctuations		0.3 K	0.3 K
Size-of-Source Effect		-	-
Atmospheric absorption/emission		-	-
RMS total	0.03% / 0.09 K	0.5 K	0.5 K

Mean values for six bands (B1 - B6) are shown. Values for each band are in section 3.10.1.

3.10.3 Comparison of CE312-2 to NPL reference blackbody

Figures 3.10.1 to 3.10.7 show the measurements completed by the GOTA radiometer CIMEL Electronique CE312-2 when it was viewing the NPL blackbody maintained at different temperatures. The uncertainty bars, shown in orange, in the figures represent the uncertainty values provided by GOTA which correspond to the measurements shown in the Figures. Also shown in blue in these Figures are the values of the brightness temperature of the NPL reference blackbody along with their combined uncertainty values.

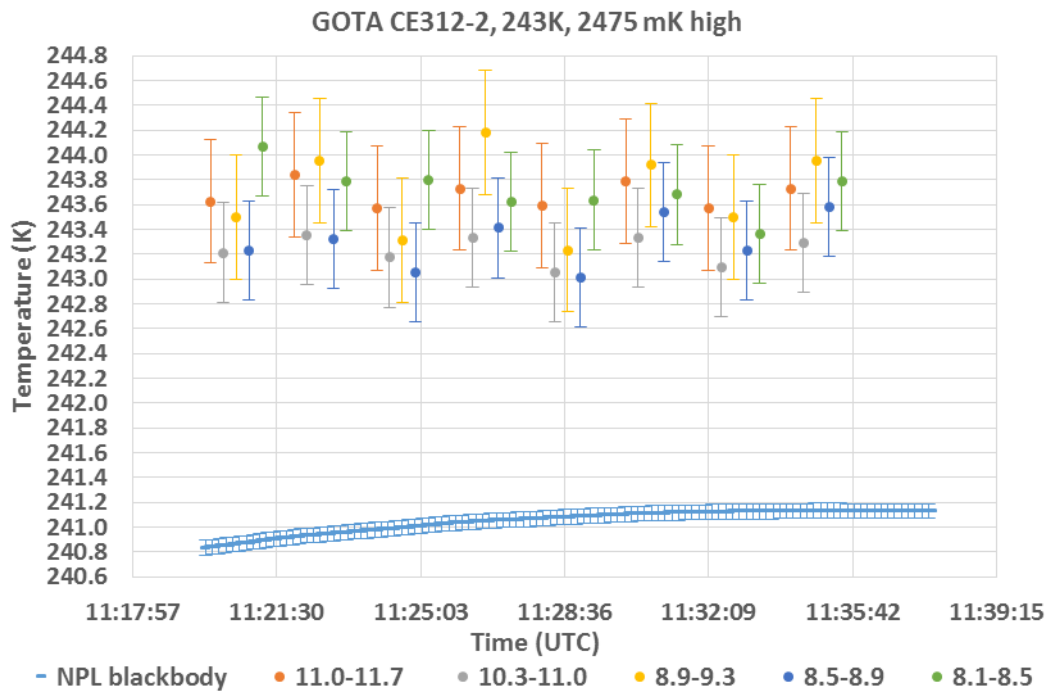


Figure 3.10.1: Measurements of the GOTA CIMEL CE312-2 radiometer viewing the NPL blackbody maintained at about -30 °C.

Table 3.10.1 shown below, indicates the deviation δT of the different radiometer channels from the average blackbody temperature, over the measurement interval for a nominal blackbody temperature of -30 °C.

Table 3.10.1: The deviation of the different radiometer channels δT from the average blackbody temperature, over the measurement interval for a nominal blackbody temperature of -30 °C.

Channel (μm)	δT (mK)
11.0-11.7	2632
10.3-11.0	2182
8.9-9.3	2645
8.5-8.9	2248
8.1-8.5	2670

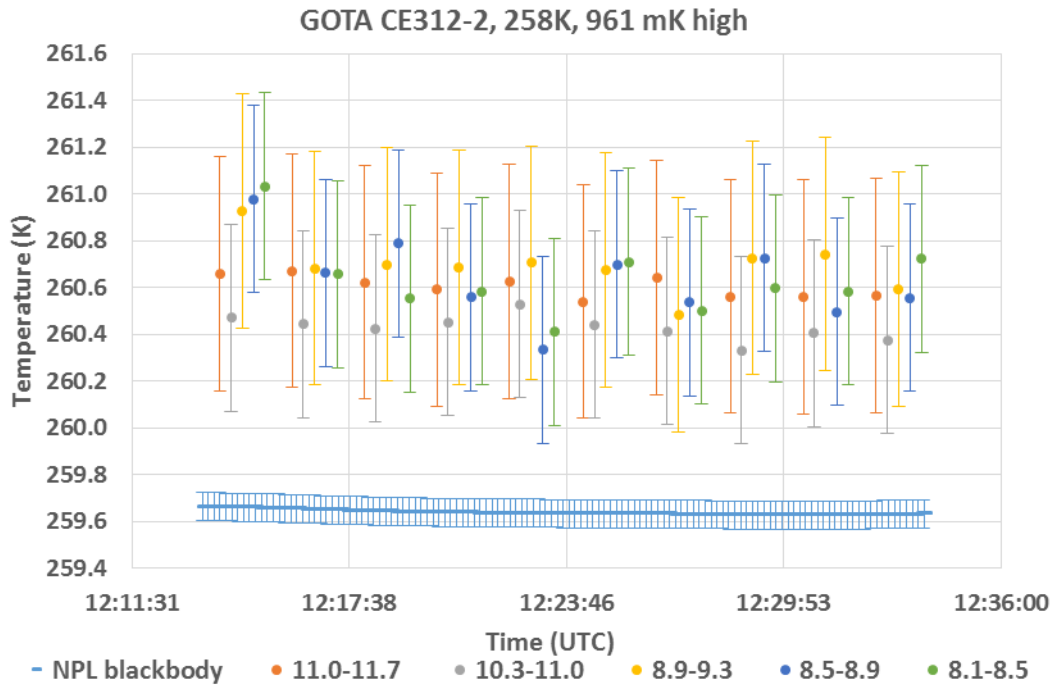


Figure 3.10.2: Measurements of the GOTA CIMEL CE312-2 radiometer viewing the NPL blackbody maintained at about -15 °C.

Table 3.10.2, shown below, indicates the deviation of the different radiometer channels δT from the average blackbody temperature, over the measurement interval for a nominal blackbody temperature of -15 °C.

Table 3.10.2: The deviation of the different radiometer channels δT from the average blackbody temperature, over the measurement interval for a nominal blackbody temperature of -15 °C.

Channel (μm)	δT (mK)
11.0-11.7	966
10.3-11.0	791
8.9-9.3	1055
8.5-8.9	996
8.1-8.5	998

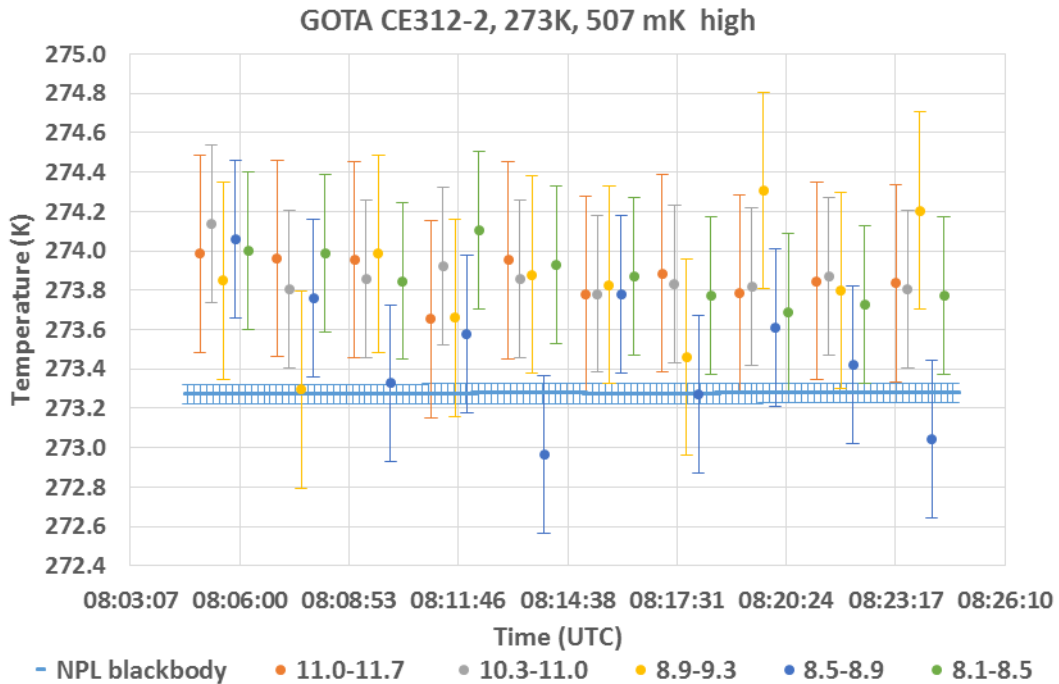


Figure 3.10.3: Measurements of the GOTA CIMEL CE312-2 radiometer viewing the NPL blackbody maintained at about 0 °C.

Table 3.10.3, shown below, indicates the deviation of the different radiometer channels δT from the average blackbody temperature, over the measurement interval for a nominal blackbody temperature of 0 °C.

Table 3.10.3: The deviation of the different radiometer channels δT from the average blackbody temperature, over the measurement interval for a nominal blackbody temperature of 0 °C.

Channel (μm)	δT (mK)
11.0-11.7	589
10.3-11.0	593
8.9-9.3	552
8.5-8.9	207
8.1-8.5	596

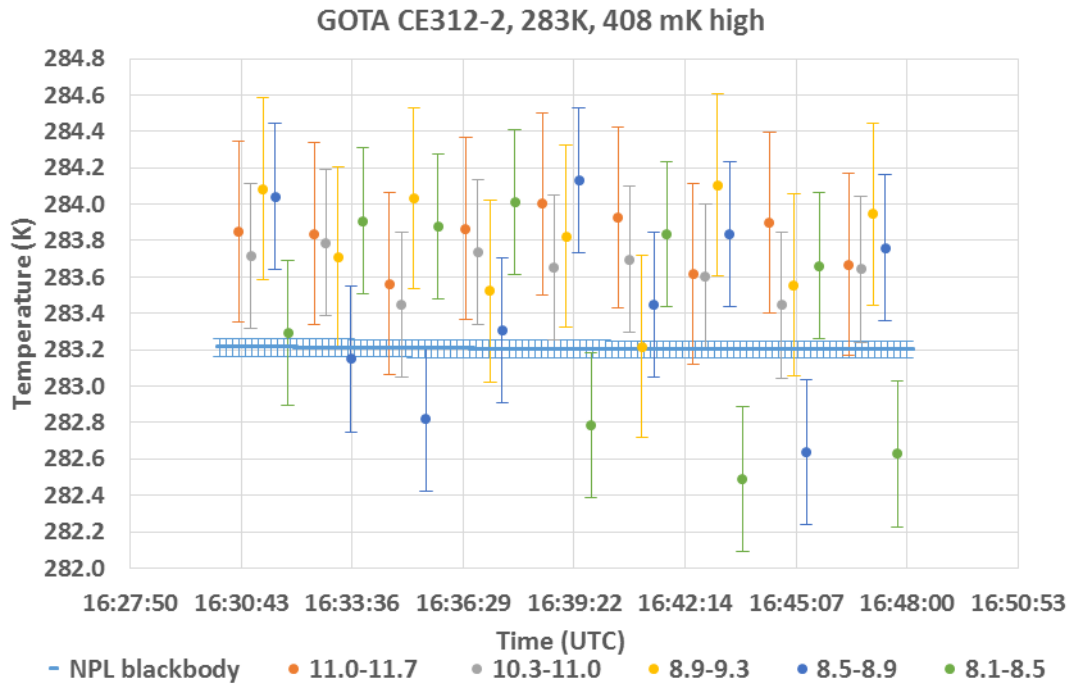


Figure 3.10.4: Measurements of the GOTA CIMEL CE312-2 radiometer viewing the NPL blackbody maintained at about 10°C.

Table 3.10.4, shown below, indicates the deviation of the different radiometer channels δT from the average blackbody temperature, over the measurement interval for a nominal blackbody temperature of 10 °C.

Table 3.10.4: The deviation of the different radiometer channels δT from the average blackbody temperature, over the measurement interval for a nominal blackbody temperature of 10 °C.

Channel (μm)	δT (mK)
11.0-11.7	599
10.3-11.0	432
8.9-9.3	572
8.5-8.9	255
8.1-8.5	184

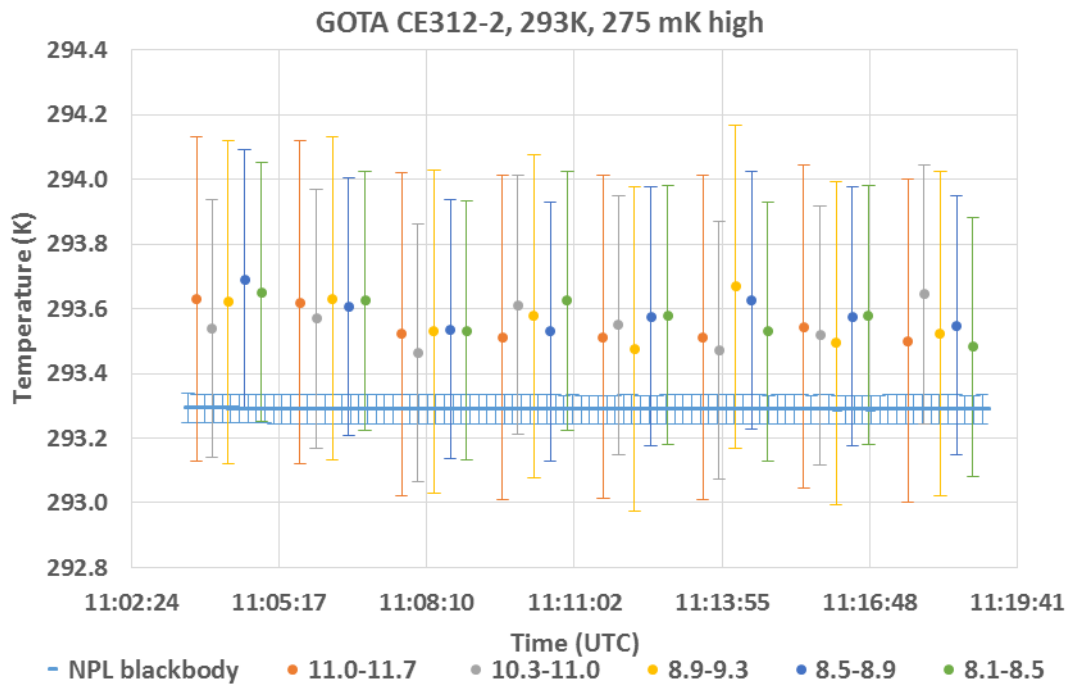


Figure 3.10.5: Measurements of the GOTA CIMEL CE312-2 radiometer viewing the NPL blackbody maintained at about 20°C.

Table 3.10.5, shown below, indicates the deviation of the different radiometer channels δT from the average blackbody temperature, over the measurement interval for a nominal blackbody temperature of 20 °C.

Table 3.10.5: The deviation of the different radiometer channels δT from the average blackbody temperature, over the measurement interval for a nominal blackbody temperature of 20 °C.

Channel (μm)	δT (mK)
11.0-11.7	255
10.3-11.0	257
8.9-9.3	276
8.5-8.9	297
8.1-8.5	287

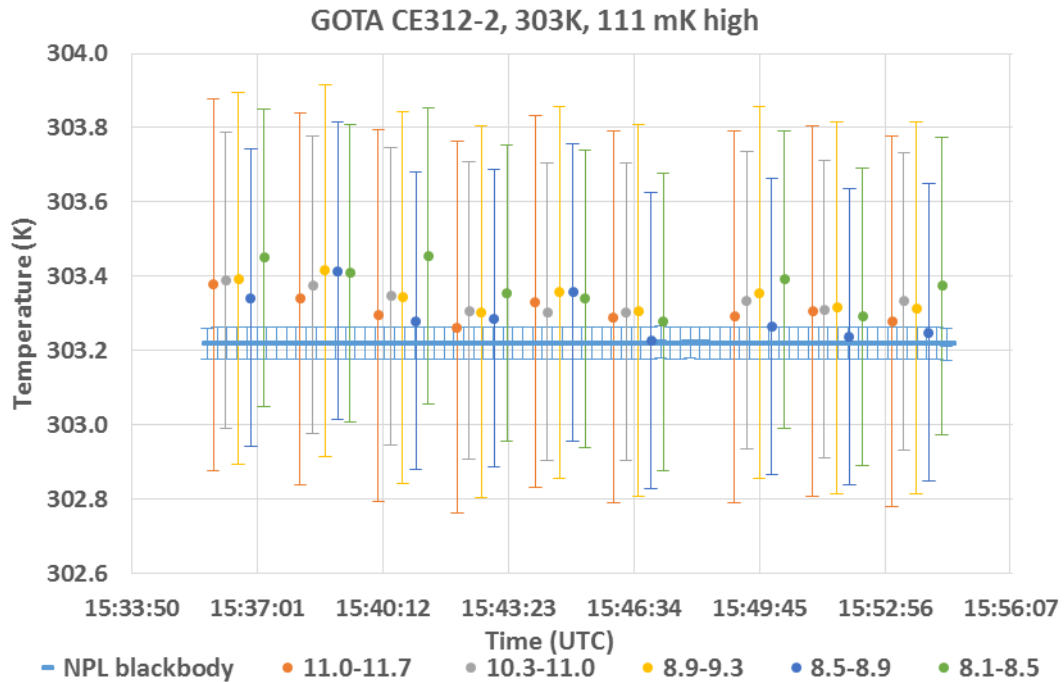


Figure 3.10.6: Measurements of the GOTA CIMEL CE312-2 radiometer viewing the NPL blackbody maintained at about 30 °C.

Table 3.10.6, shown below, indicates the deviation of the different radiometer channels δT from the average blackbody temperature, over the measurement interval for a nominal blackbody temperature of 30 °C.

Table 3.10.6: The deviation of the different radiometer channels δT from the average blackbody temperature, over the measurement interval for a nominal blackbody temperature of 30 °C.

Channel (μm)	δT (mK)
11.0-11.7	88
10.3-11.0	114
8.9-9.3	95
8.5-8.9	75
8.1-8.5	151

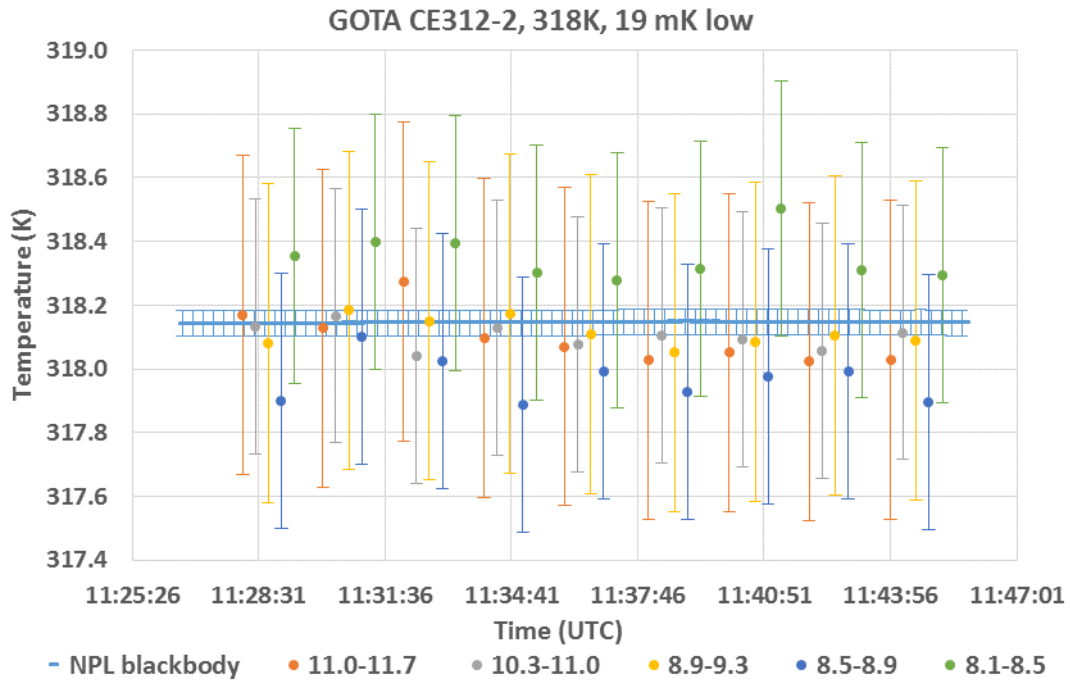


Figure 3.10.7: Measurements of the GOTA CIMEL CE312-2 radiometer viewing the NPL blackbody maintained at about 45 °C.

Table 3.10.7, shown below, indicates the deviation of the different radiometer channels δT from the average blackbody temperature, over the measurement interval for a nominal blackbody temperature of 45 °C.

Table 3.10.7: The deviation of the different radiometer channels δT from the average blackbody temperature, over the measurement interval for a nominal blackbody temperature of 45 °C.

Channel (μm)	δT (mK)
11.0-11.7	48
10.3-11.0	43
8.9-9.3	31
8.5-8.9	178
8.1-8.5	206

3.11 MEASUREMENTS MADE BY RSMAS, UNIVERSITY OF MIAMI

Institute/organisation: Rosenstiel School of Marine and Atmospheric Science
 University of Miami, 4600 Rickenbacker Causeway,
 Miami, FL 33149, USA
 Contact Name: Prof. Peter Minnett
 Email: pminnett@rsmas.miami.edu

3.11.1 Description of radiometer and route of traceability

Type:	M-AERI Mk2/3 (ASIST)
Field of view:	22.5 mrad half angle
Spectral band:	525 – 3300 cm^{-1}
Entrance aperture:	25 mm
Spectral resolution:	0.5 cm^{-1}
Digitizer resolution:	16-bit
Radiance resolution:	< 0.05 mW/ ($\text{m}^2 \text{sr cm}^{-1}$)
Temperature resolution:	0.005 K

The Marine-Atmospheric Emitted Radiance Interferometers (M-AERI) are a series of Fourier-Transform Infrared Spectroradiometers. The first generation instruments were developed in the mid-1990's and these were replaced by Mk-2 instruments beginning in 2010. A Mk-3 instrument was delivered in 2013, and it was this instrument that was used in the FRM4STS Workshop at the NPL in June 2016. All versions of the instrument use a Michelson-Morley interferometer design with the path differences being generated by an oscillating yoke with a corner-cube reflector on each arm. Wavenumber calibration is accomplished using a HeNe laser that sends monochromatic light through the interferometer. Radiometric calibration achieved by using two blackbody cavities at known temperatures, at each of which the field of view of the interferometer is directed sequentially before and after scene measurements. The M-AERIs use two detectors, one of InSb and the other of HgCdTe, to achieve the broad spectral range; the detectors are chilled to ~77 K (~boiling point of liquid N₂) by Stirling Cycle mechanical coolers. The M-AERIs operate under computer control.

The M-AERI Mk2s are much smaller than the first generation instruments, and the Mk3 is smaller again, this being achieved by smaller optics and more compact electronics and computer modules.

The errors and uncertainties in the internal radiometric calibration procedure are frequently checked, usually before and after each ship deployment, using a laboratory blackbody target that is a thin copper cone paint matt black immersed in a water-bath which can be stabilized and desired temperatures. Two precision thermistors with SI-traceable calibration are used to monitor the water bath temperatures.

Uncertainties in the measurement are wavelength dependent and the Tables below are for two selected wavenumbers that we use most frequently in our measurements.

3.11.2 Uncertainty contributions associated with RSMAS' measurements at NPL

Uncertainty Contribution Tables

Wavenumber = 1000 cm^{-1}

Parameter	Type A Uncertainty in Value [K]	Type B Uncertainty in K	Uncertainty in Brightness temp K
Repeatability of Measurement (1)	0.014		0.014
Reproducibility of Measurement (2)	0.0058 (0.0035)		0.0058 (0.0035)
Linearity of radiometer (3)		0.0003	0.0003
Primary calibration (4)		0.0097	0.0097
Drift since calibration (5)			0
RMS total	0.0152 (0.0144)	0.0102	0.0182 (0.0176)

Wavenumber = 1302.5 cm^{-1}

Parameter	Type A Uncertainty in Value [K]	Type B Uncertainty in K	Uncertainty in Brightness temp K
Repeatability of Measurement (1)	0.0349		0.0349
Reproducibility of Measurement (2)	0.0178 (0.0089)		0.0178
Linearity of radiometer (3)		0.0003	0.0003
Primary calibration (4)		0.0086	0.0086
Drift since calibration (5)			0
RMS total	0.0392 (0.0360)	0.0091	0.0402 (0.0372)

(1) **Repeatability of measurement:** Typical value of the standard deviation of measurements at fixed black body temperature without re-alignment of radiometer.

The standard deviation estimate is based on average of between 17 and 143 separate temperature measurements of three target temperatures (~288, 293 and 303 K below, near and

above ambient temperature). Each measurement is an average of 46 spectra and the instrument is internally calibrated before each measurement. One measurement cycle takes approximately 4 to 5 minutes.

(2) **Reproducibility of measurement:** Typical value of difference between two runs of radiometer measurements at the same black body temperature including re-alignment.

We did not have the chance to set up the experiment to measure the reproducibility as described above instead our reproducibility estimate is the typical value of difference between two radiometer measurements at the same blackbody temperature obtained during two different experiments both conducted in June 2016. The first experiment took place in RSMAS lab in Miami before the instrument was shipped to London and the second one took place at NPL. This estimate is likely too high as besides the alignment also the target temperature varied slightly between the two experiments as did the ambient conditions. For comparison we calculated for all runs in both experiments the differences between 1st and 2nd half of measurement and an average of these is given in brackets (i.e. Reproducibility without the change in alignment).

(3) **Linearity of radiometer:** uncertainty of a linear regression between the Miami Water-Bath Blackbody temperatures and radiometer brightness temperatures.

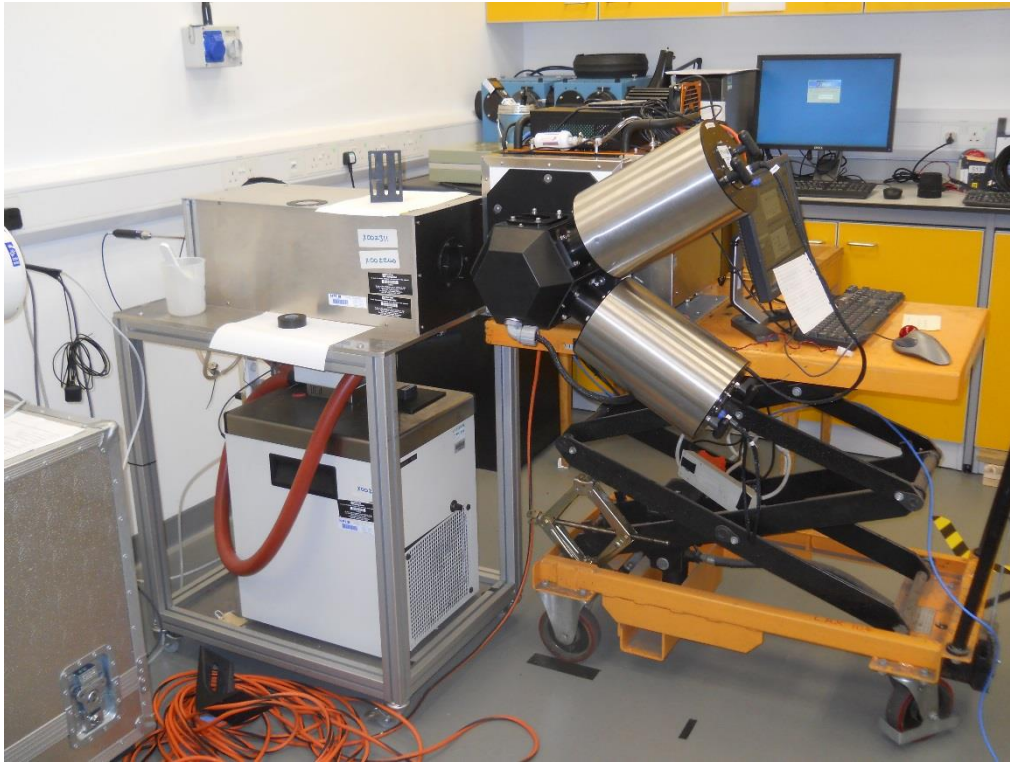
(4) **Primary calibration:** Typical value of difference between radiometer brightness temperatures and the Miami Water-Bath Blackbody temperatures. This depends of course on the temperature of the target. The values we give are the average of the difference at three target temperature ~288, 293 and 303 K.

(5) **Drift estimate:** We base our drift estimate on three consecutive calibration of the instrument. The ambient conditions change from one measurement to another and if they are not accounted for the ambient signal might obscure instrument drift. In the table below we show the date of the measurement and the value of the difference between the target temperature and the MAERI temperature corrected for the contribution of the ambient environment temperature to the MAERI measurement. These values were obtained for the 1302.5 cm⁻¹ wavenumber near ambient target temperatures (to further minimize error due to the ambient temperature contribution to the measurement). There is no systematic change in the Target – MAERI_{corr} difference from one calibration to another.

Date of calibration	Target – MAERI _{corr}
5th February 2016 (Miami)	-0.0021
3rd June 2016 (Miami)	-0.0025
23rs June 2016 (NPL)	-0.0017

3.11.3 Comparison of the RSMAS radiometer to NPL reference blackbody

The photo below shows the RSMAS radiometer viewing the NPL reference blackbody.



The RSMAS radiometer viewing the NPL reference blackbody.

Figures 3.11.1 to 3.11.7 show the measurements completed by the RSMAS radiometer when it was viewing the NPL blackbody maintained at different temperatures. The uncertainty bars shown in orange and grey in the figures represent the uncertainty values provided by RSMAS which correspond to the measurements shown in the Figures. Also shown in blue in these Figures are the values of the brightness temperature of the NPL reference blackbody along with their combined uncertainty values.

Due to alignment issues and a limited schedule, no data was submitted by RSMAS for measurements made at $-30\text{ }^{\circ}\text{C}$ or $20\text{ }^{\circ}\text{C}$ blackbody temperatures.

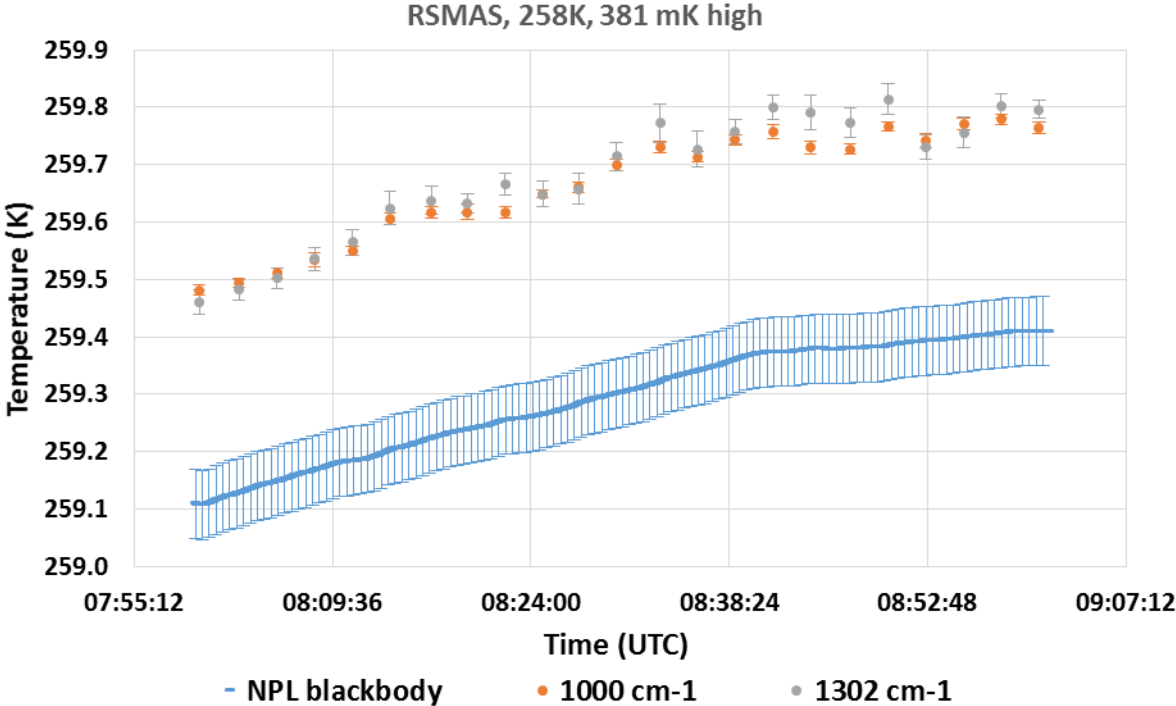


Figure 3.11.1: Measurements of the RSMAS radiometer viewing the NPL blackbody at about -15 °C.

Table 3.11.1, shown below, indicates the deviation of the different RSMAS radiometer channels δT from the average blackbody temperature, over the measurement interval for a nominal blackbody temperature of -15 °C.

Table 3.11.1: The deviation of the two radiometer channels δT from the average blackbody temperature, over the measurement interval for a nominal blackbody temperature of -15 °C.

Channel (cm ⁻¹)	δT (mK)
1000	373
1302	390

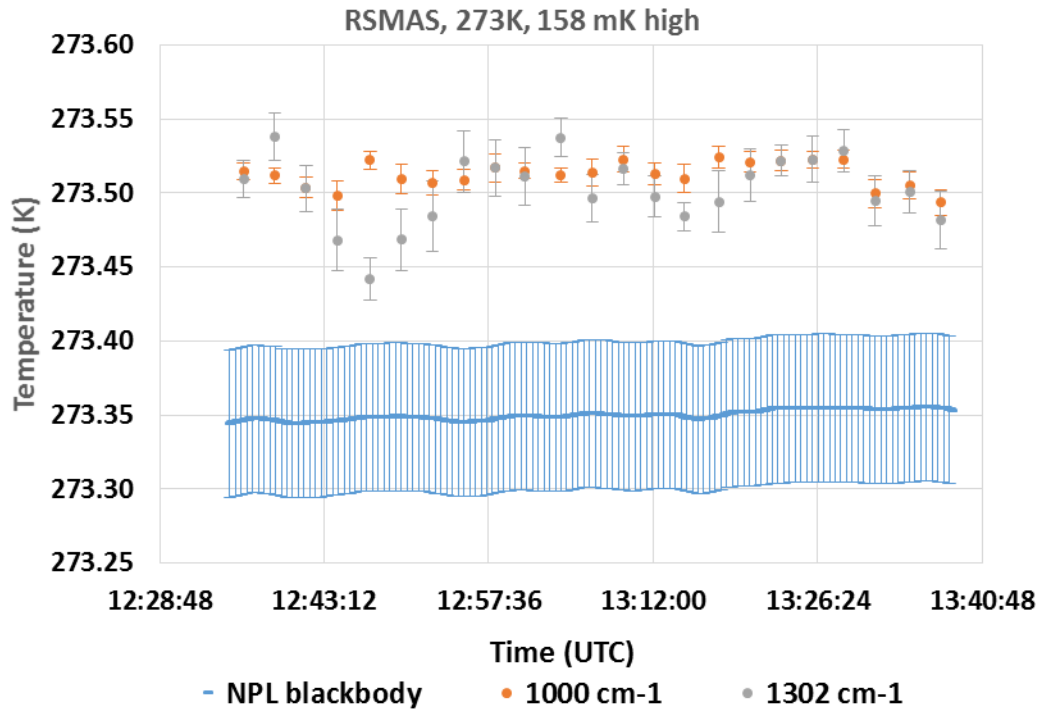


Figure 3.11.2: Measurements of the RSMAS radiometer viewing the NPL blackbody at about 0 °C.

Table 3.11.2, shown below, indicates the deviation δT of the different RSMAS radiometer channels from the average blackbody temperature, over the measurement interval for a nominal blackbody temperature of 0 °C.

Table 3.11.2: The deviation δT of the two radiometer channels from the average blackbody temperature, over the measurement interval, for a nominal blackbody temperature of 0 °C.

Channel (cm ⁻¹)	δT (mK)
1000	163
1302	153

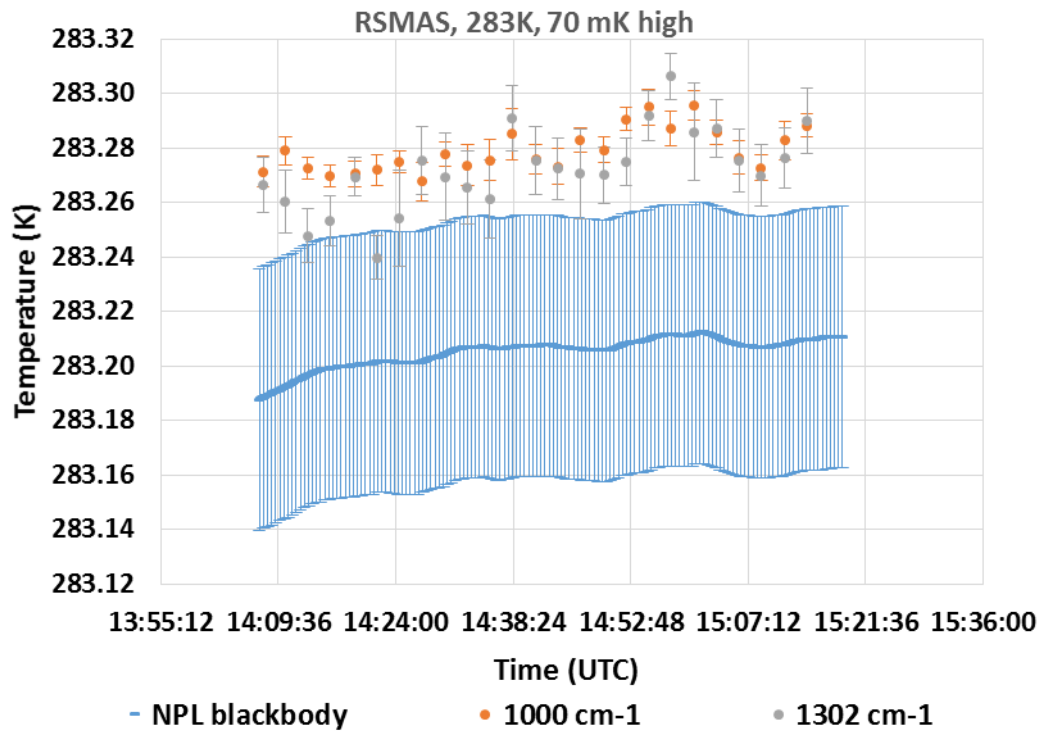


Figure 3.11.3: Measurements of the RSMAS radiometer viewing the NPL blackbody at about 10 °C.

Table 3.11.3, shown below, indicates the deviation δT of the different RSMAS radiometer channels from the average blackbody temperature, over the measurement interval for a nominal blackbody temperature of 10 °C.

Table 3.11.3: The deviation δT of the two radiometer channels from the average blackbody temperature, over the measurement interval for a nominal blackbody temperature of 10 °C.

Channel (cm ⁻¹)	δT (mK)
1000	74
1302	67

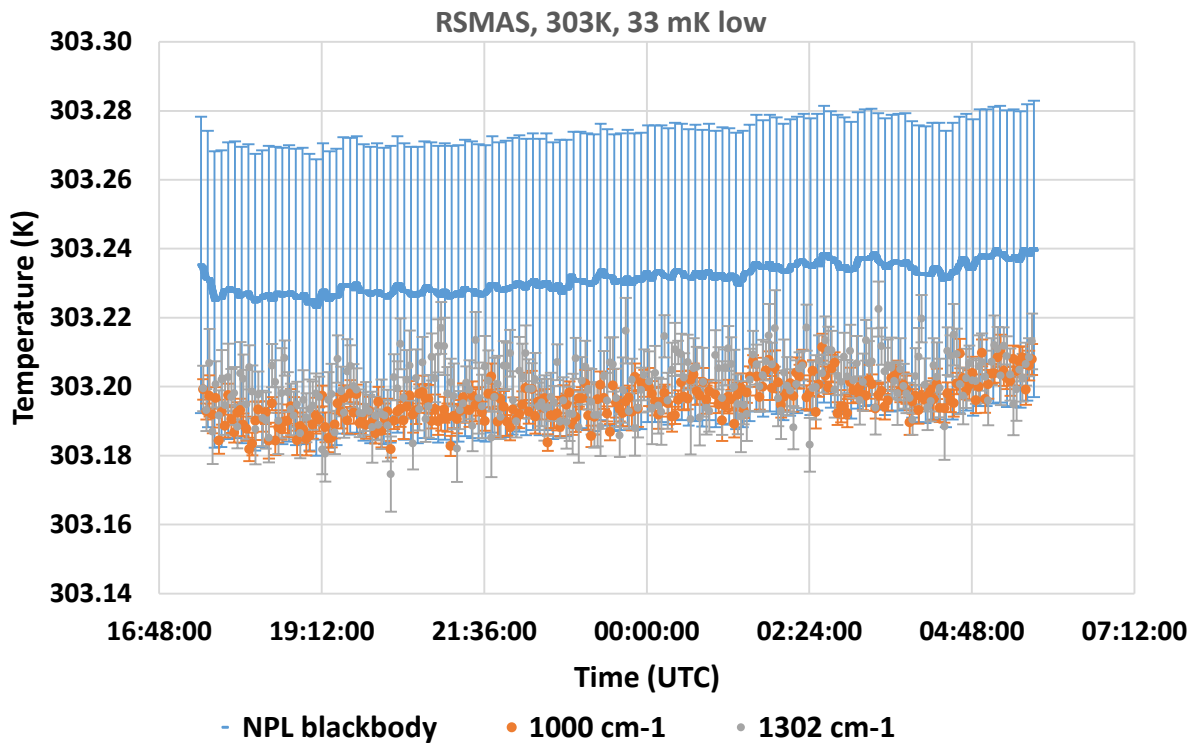


Figure 3.11.4: Measurements of the RSMAS radiometer viewing the NPL blackbody at about 30°C.

Table 3.11.4, shown below, indicates the deviation δT of the different RSMAS radiometer channels from the average blackbody temperature, over the measurement interval for a nominal blackbody temperature of 30 °C.

Table 3.11.4: The deviation δT of the two radiometer channels from the average blackbody temperature, over the measurement interval, for a nominal blackbody temperature of 30 °C.

Channel (cm ⁻¹)	δT (mK)
1000	36
1302	31

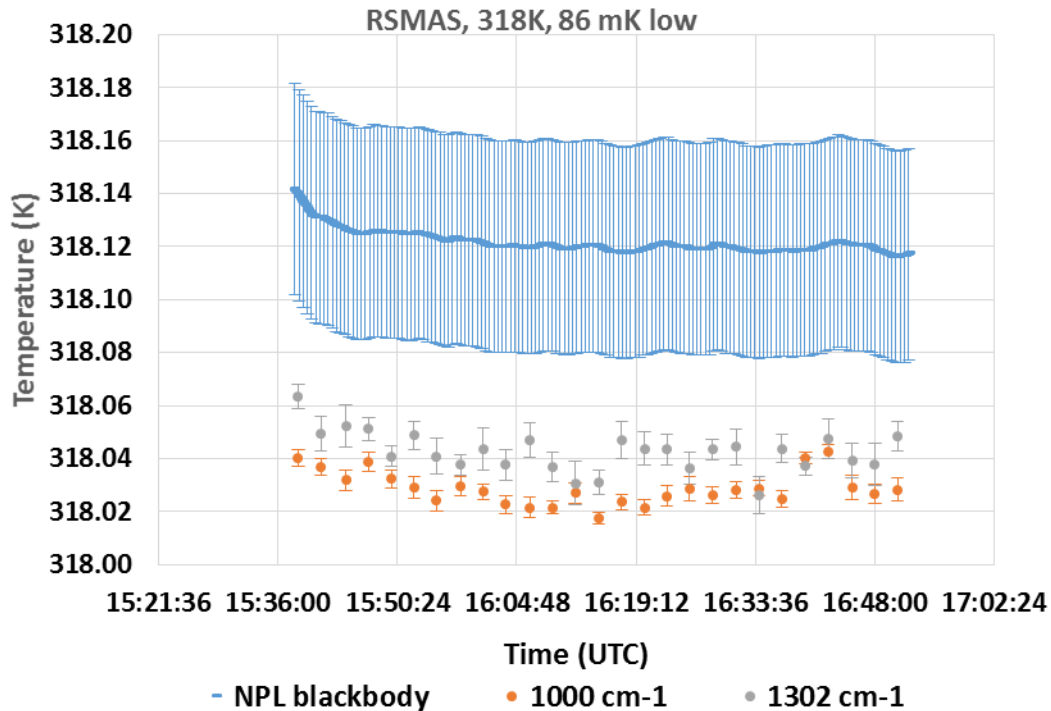


Figure 3.11.5: Measurements of the RSMAS radiometer viewing the NPL blackbody at about 45 °C.

Table 3.11.5, shown below, indicates the deviation δT of the different RSMAS radiometer channels from the average blackbody temperature, over the measurement interval, for a nominal blackbody temperature of 45 °C.

Table 3.11.5: The deviation δT of the two radiometer channels from the average blackbody temperature, over the measurement interval, for a nominal blackbody temperature of 45 °C.

Channel (cm ⁻¹)	δT (mK)
1000	93
1302	79

4 SUMMARY OF THE RESULTS

This section provides a summary of the results provided by the participants of the IR comparison of brightness temperature of the reference (SI traceable) variable temperature blackbody completed at NPL on the 20th June to the 24th June 2016. The following set of Tables and Figures represent the measurements completed during this measurement campaign. It is important to stress that the temperatures of the reference blackbody were nominal and not necessarily perfectly stable. The uncertainty bars represent the standard uncertainty ($k=1$) unless otherwise stated. Uncertainty bars are provided whenever these were available.

Table 4.1 shows the difference of the measurements completed by participants on the NPL variable temperature blackbody from the blackbody temperature.

Table 4.1: Summary of the difference of the measurements from the reference blackbody.

	Set temperature (°C)	Diff. from NPL BB (mK)		Set temperature (°C)	Diff. from NPL BB (mK)
University of Valencia	45	-133	University of Valencia	45	-147
CE312-2	30	-51	CE312-2	30	-49
Unit 1	20	-9	Unit 2	20	0
10.54 μm	10	29	10.54 μm	10	36
	0	80		0	79
	-15	65		-15	94
	-30	171		-30	441
University of Valencia	45	-81	University of Valencia	45	-97
CE312-2	30	-81	CE312-2	30	-59
Unit 1	20	-39	Unit 2	20	-20
11.30 μm	10	-31	11.30 μm	10	6
	0	0		0	39
	-15	68		-15	111
	-30	293		-30	552
University of Valencia	45	-120	University of Valencia	45	-125
CE312-2	30	-101	CE312-2	30	-79
Unit 1	20	-59	Unit 2	20	-30
10.57 μm	10	9	10.57 μm	10	26
	0	110		0	139
	-15	293		-15	326
	-30	819		-30	1004
University of Valencia	45	-203	University of Valencia	45	-165
CE312-2	30	-161	CE312-2	30	-119
Unit 1	20	-59	Unit 2	20	-50
9.14 μm	10	29	9.14 μm	10	46
	0	220		0	259
	-15	469		-15	581
	-30	1398		-30	1782
University of Valencia	45	-193	University of Valencia	45	-219
CE312-2	30	-81	CE312-2	30	-89
Unit 1	20	-9	Unit 2	20	10
8.68 μm	10	49	8.68 μm	10	76
	0	140		0	189
	-15	209		-15	299
	-30	583		-30	935
University of Valencia	45	-293	University of Valencia	45	-217
CE312-2	30	-211	CE312-2	30	-119
Unit 1	20	-79	Unit 2	20	-60
8.42 μm	10	59	8.42 μm	10	86
	0	280		0	349
	-15	611		-15	726
	-30	1798		-30	2126

	Set temperature (°C)	Diff. from NPL BB (mK)		Set temperature (°C)	Diff. from NPL BB (mK)
OUC	45	728	GOTA	45	48
ISAR	30	94	CE312-2	30	88
	20	71	11.0-11.7	20	255
	10	157		10	599
	0	229		0	589
	-15	515		-15	966
	-30	2413		-30	2632
OUC	45	-18	GOTA	45	43
FIRST	30	-22	CE312-2	30	114
	20	-27	10.3-11.0	20	257
	10	6		10	432
	0	-125		0	593
	-15	-102		-15	791
	-30	538		-30	2182
RSMAS	45	-93	GOTA	45	31
FTIR	30	-36	CE312-2	30	95
1000 nm	20	-	8.9-9.3	20	276
	10	74		10	572
	0	163		0	552
	-15	373		-15	1055
-	-30	-		-30	2645
RSMAS	45	-79	GOTA	45	178
FTIR	30	-31	CE312-2	30	75
1302 nm	20	-	8.5-8.9	20	297
	10	67		10	255
	0	153		0	207
	-15	390		-15	996
	-30	-		-30	2248
			GOTA	45	206
			CE312-2	30	151
			8.1-8.5	20	287
				10	184
				0	596
				-15	998
				-30	2670

Figures 4.1 to 4.7 show the plots of the mean of the differences of the radiometer readings from the corresponding temperature of the NPL reference blackbody, for all the blackbody temperatures at which the radiometers were compared. The uncertainty bars shown in these Figures represent the combined uncertainty ($k = 1$) of the measurements provided by the participants.

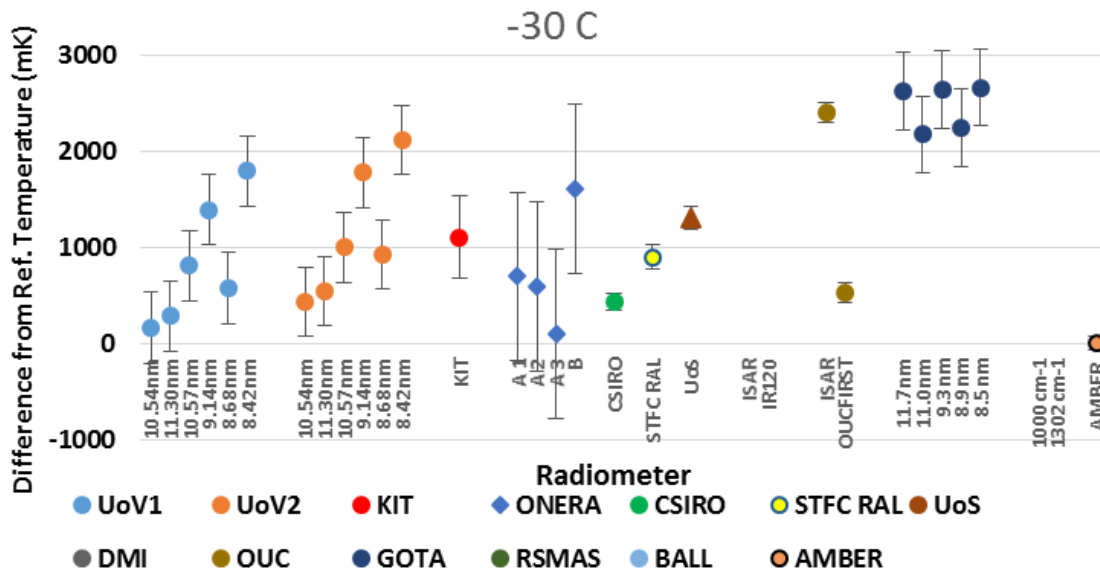


Figure 4.1: Plot of the mean of the differences of the radiometer readings from the temperature of the NPL reference blackbody, maintained at a nominal temperature of -30 °C.

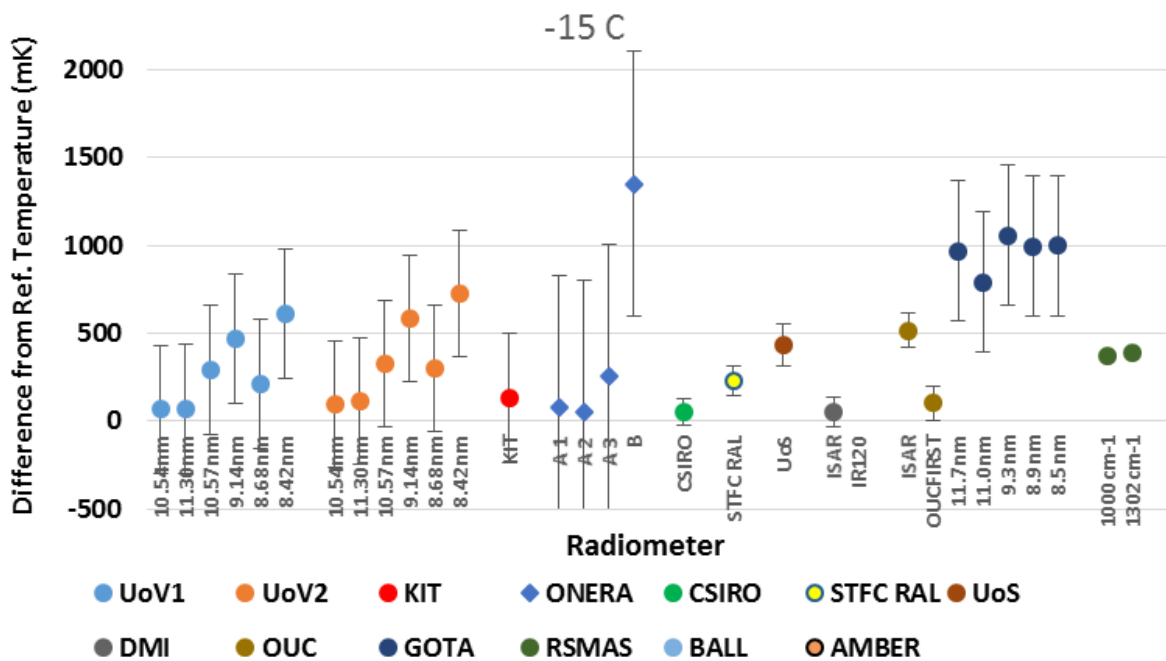


Figure 4.2: Plot of the mean of the differences of the radiometer readings from the temperature of the NPL reference blackbody, maintained at a nominal temperature of -15 °C.

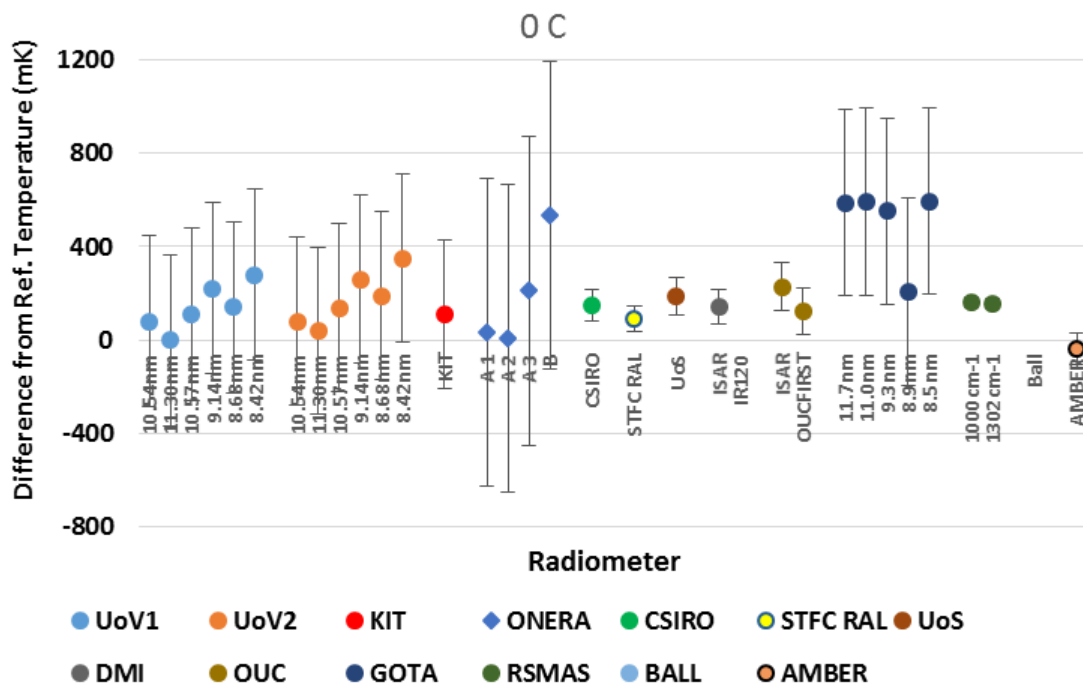


Figure 4.3: Plot of the mean of the differences of the radiometer readings from the temperature of the NPL reference blackbody, maintained at a nominal temperature of 0 °C.

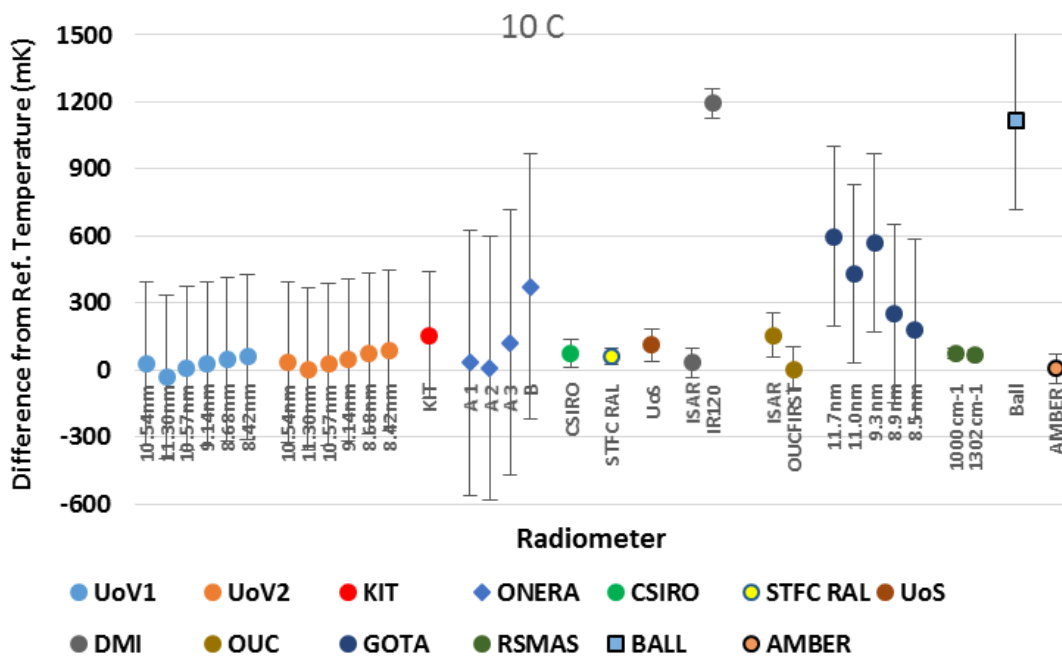


Figure 4.4: Plot of the mean of the differences of the radiometer readings from the temperature of the NPL reference blackbody, maintained at a nominal temperature of 10 °C.

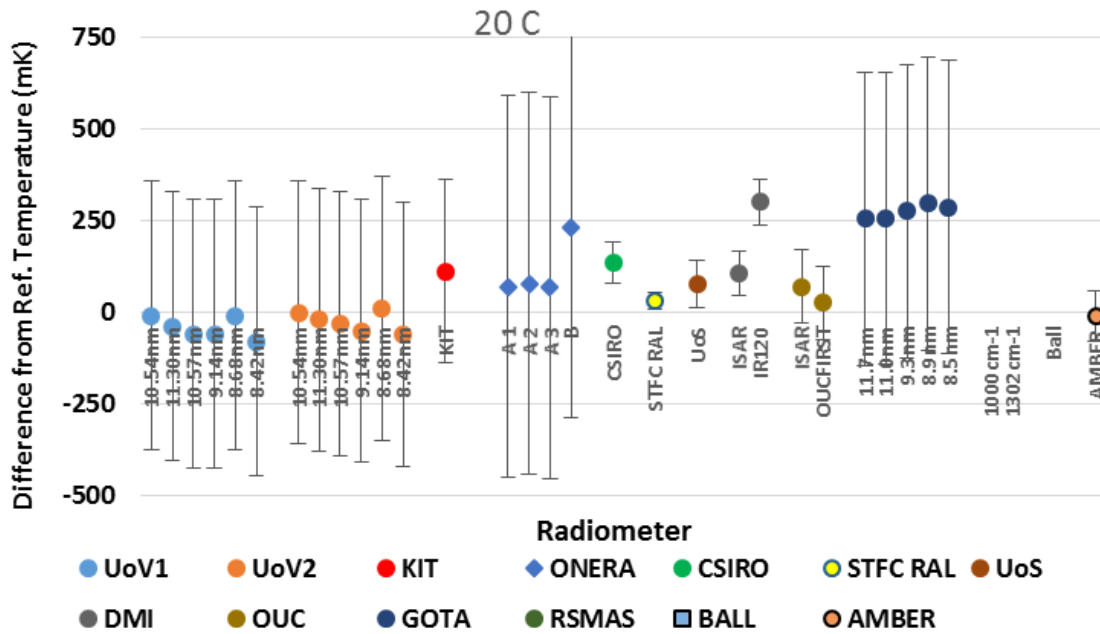


Figure 4.5: Plot of the mean of the differences of the radiometer readings from the temperature of the NPL reference blackbody, maintained at a nominal temperature of 20 °C.

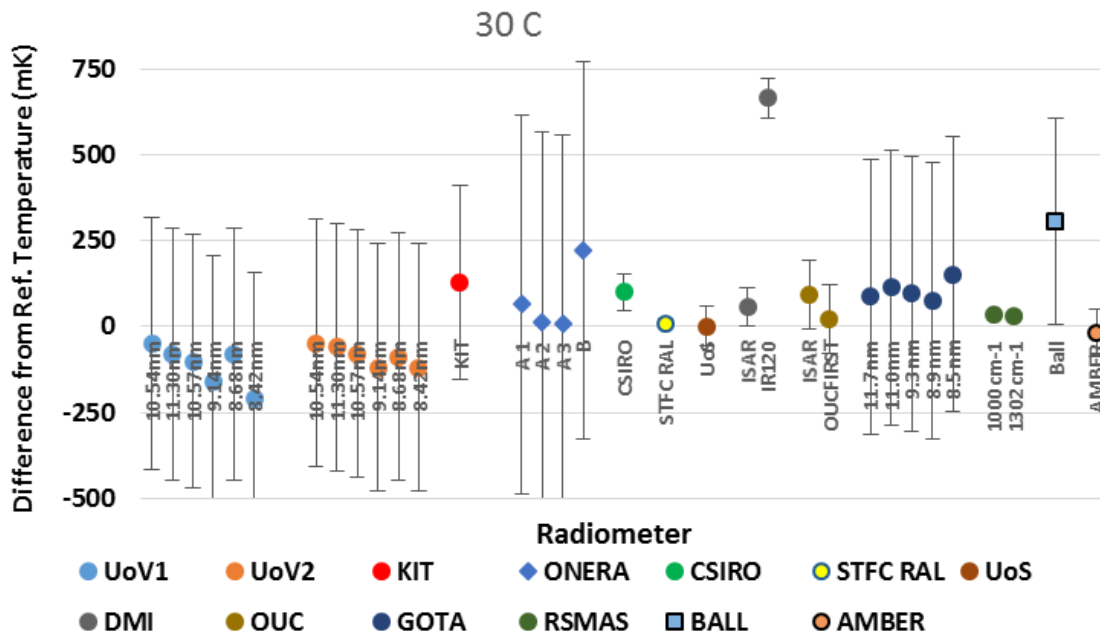


Figure 4.6: Plot of the mean of the differences of the radiometer readings from the temperature of the NPL reference blackbody, maintained at a nominal temperature of 30 °C.

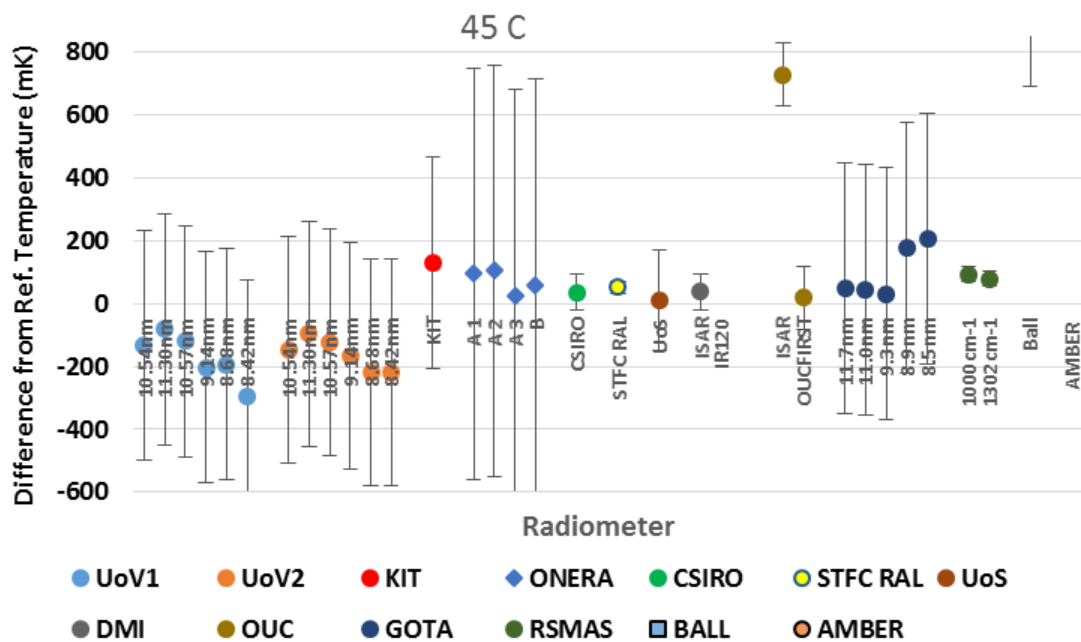


Figure 4.7: Plot of the mean of the differences of the radiometer readings from the temperature of the NPL reference blackbody, maintained at a nominal temperature of 45 °C.

5 DISCUSSION

Figures 4.1 to 4.7 show the differences of the radiometer readings from the corresponding temperature of the NPL reference blackbody, for all the blackbody temperatures at which the radiometers were compared. These Figures indicate that, for measurements corresponding to the reference blackbody operating at temperatures above 0 °C, the difference of the radiometer measurements from those of the ammonia heat-pipe blackbody cavity temperature is within the uncertainty of the measurements, with some exceptions. However, these differences become progressively larger as the reference blackbody temperature decreased to -15 °C and -30 °C. This observation is not altogether surprising because measurements were made in a lab, with the measuring radiometers operating at ambient temperatures. This meant that the internal blackbodies within the participating radiometers on which the radiometers were basing their calibrations were also operating at near ambient temperatures; hence for low temperatures of the ammonia heat-pipe blackbody, the difference between the temperature of the test blackbody and the internal reference blackbodies increased, resulting in the observed discrepancies. The discrepancies are likely to arise due to the large extrapolation ranges (typically 50 °C) in association with some invalid starting conditions of the original data. If, for example, the out-of-band response of the radiometer was measured incorrectly, then discrepancies are likely to arise. It is estimated that the output of a radiometer responding in the 10 μm to 11 μm region, which is calibrated at 30 °C and extrapolated to -30 °C, will be 0.26% different from the output obtained if the radiometer had an out-of-band response in the 5 μm to 6 μm region which was just 1% of the response in the 10 μm to 11 μm band.

It is important to point out that if the radiometers were used to measure low temperature targets such as the surface temperature of ice in the arctic, then the radiometers (as well as the internal blackbodies) will also be at low temperatures so the extrapolation will not be over a significant

temperature range. This means that the discrepancies between the radiometer measurement of the ice and the true surface temperature of ice are likely to be small.

Moreover, as the temperature of the reference blackbody decreases, the signal detected by the photodetectors within the radiometers also decreases, resulting in poorer signal-to-noise ratios and thus more unreliable measurements.

It is important to note that NPL AMBER was used in the past to measure the temperature of the same ammonia heat-pipe reference blackbody and the agreement between the NPL AMBER measurements and the blackbody measurements was good. In fact the difference between the NPL AMBER measurements and the reference blackbody measurements are included in the Figures for blackbody temperatures of $-30\text{ }^{\circ}\text{C}$, $0\text{ }^{\circ}\text{C}$, $10\text{ }^{\circ}\text{C}$, $20\text{ }^{\circ}\text{C}$ and $30\text{ }^{\circ}\text{C}$. The agreement between the AMBER and the reference blackbody measurements indicates that the discrepancies observed in the measurements of some radiometers (which can be as large as 2 K for blackbody temperatures around $-30\text{ }^{\circ}\text{C}$) do not arise due to issues with the blackbody but are likely to be associated with the participants' measurements. Furthermore, NPL AMBER was used to measure the temperature of the ammonia heat-pipe blackbody of PTB, the German national standards lab and that comparison also showed good agreement between the measurements provided by NPL AMBER and those provided by the PTB reference blackbody. Full information on that comparison can be found in the paper by Gutschwager (Gutschwager et al., 2013).

5.1 FIELD-OF-VIEW (FOV) ISSUES

Figure 5.1 shows a schematic of the ammonia heat-pipe blackbody. The blackbody cavity aperture has a 75 mm diameter and is enclosed in a metal casing. The blackbody cavity is seen through a 75 mm diameter aperture on the front of the casing, although this aperture can be made smaller by adding apertures smaller than 75 mm in diameter on the blackbody casing. Finally, the distance between the front of the blackbody cavity and the aperture on the casing was also 75 mm, meaning that the Field of View (FoV) of a radiometer placed against the casing would be overfilled by the blackbody cavity provided its half angle was less than 26.5° (53° full angle). Although the 75 mm diameter of the blackbody and its position were defined and open for review in the protocol before the measurements took place, this was a cause of issue for radiometers with a large angle field of view which could not be positioned close to the blackbody casing aperture. For these radiometers, the measurements taken would likely capture the edges of the cavity, as well as capturing reflected or emitted radiation for the external edges of the reference blackbody cavity, thus introducing biases to the measurements. To avoid this problem, some participants made their measurements with their radiometers as close to the blackbody front aperture as possible. Other than increasing potential of interactions between the blackbody and the radiometer this was in general considered to be a satisfactory compromise.

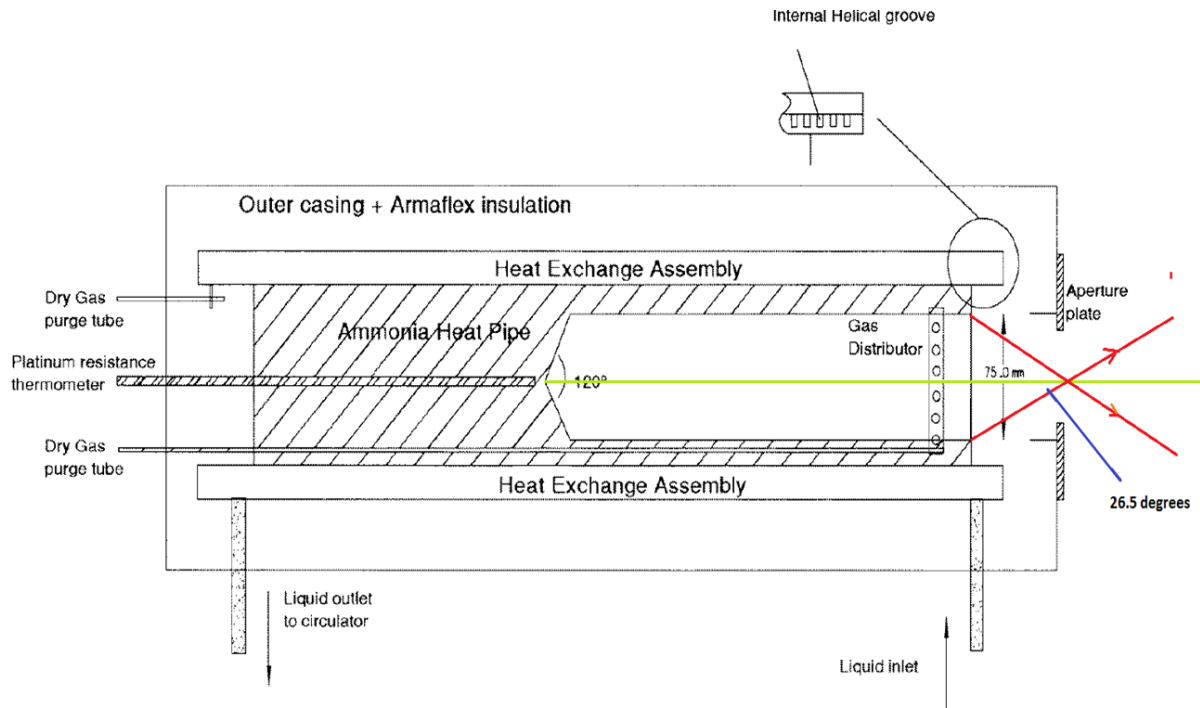


Figure 5.1: Schematic of the ammonia heat-pipe blackbody.

5.2 WATER CONDENSATION AND ICING OF CAVITY

For the temperatures below 0°C , ice began to form near the aperture of the reference blackbody cavity. While the ice only formed near the entrance to the cavity (the cavity was continuously purged with dry nitrogen gas), the presence of the ice may have affected the effective emissivity of the areas on which ice was deposited and thus alter the effective emissivity of the reference blackbody for radiometers with very large FoVs. This may also have impacted some of the results associated with the measurement of the temperature of blackbody cavity. However, the same measurements were made using the NPL AMBER radiometer and no discrepancies were observed for temperatures as low as -45°C , indicating that no ice was formed inside the reference blackbody cavity.

5.3 CALIBRATION RANGE OF RADIOMETERS

For the majority of instruments being compared, their intended use was for sea surface temperature measurements. This would mean their calibration range is for temperatures above 0°C . This, in turn, means that some measurements taken during this laboratory comparison were outside the range of calibrated temperatures for these instruments. Any consideration of irregularities with the values for measurements and their associated uncertainties made below 0°C should take this into account.

5.4 LESSONS LEARNT

The aim of this section is to highlight issues and lessons learnt during the 2016 radiometer laboratory comparison, so they can be avoided or their effects diminished in future comparisons.

- i. The aperture of the reference blackbody should be large enough to enable the FoV of the participating radiometers to be well overfilled by the reference blackbody aperture.
- ii. In cases where the radiometer cannot be placed close to the reference blackbody aperture, the extra distance between the reference blackbody and the radiometer should be included in the calculations to ensure that the reference blackbody aperture still overfills the FoV of the radiometer.
- iii. The temperature of the reference blackbody which is viewed by the radiometers should be as spatially uniform as possible.
- iv. The area of the reference blackbody observed by the different radiometers should be large enough to average out possible spatial non-uniformities in the temperature of the cavity of the blackbody.
- v. Because different radiometers have different FoVs, it is recommended that in future participating radiometers should be placed at different distances from the reference blackbody so that the FoVs of the radiometers “cover” the same (identical) area of the back wall of the reference blackbody. The aim of this is to ensure that the same temperature non-uniformities of the blackbody cavity are seen (and averaged out) by every participating radiometer.
- vi. The emissivity of the reference blackbody should be provided to all participants in order to enable them to calculate the corrections which will account for the reflections from the blackbody cavity.
- vii. During the 2016 radiometer comparison, a 30 minute period was allocated to each participant to allow for the alignment of the radiometer to the reference blackbody aperture and the making of the measurements at a particular blackbody temperature. Some participants reported that 30 minutes was not enough. However, because of the number of radiometers participating in the 2016 comparison and the number of temperatures which had to be completed over the week-long comparison, the 30 minute period could not be extended. It is recommended that in future comparisons, participants should be asked to state how long they would ideally like to align and complete a measurement (at a particular blackbody temperature). If the total duration of the comparison could not be extended, or the number of participating radiometers could not be reduced, then the number of reference blackbody temperatures at which measurements are done should be reduced to allow participants the extra time periods they require to complete their measurements.

6 REFERENCES

- Barker Snook, I., Theocharous, E. and Fox, N. P., 2017, “2016 comparison of IR brightness temperature measurements in support of satellite validation. Part 3: Water surface temperature comparison of radiation thermometers”, NPL Report ENV 15.
- Barton, I. J., Minnett, P. J., Maillet K. A., Donlon, C. J., Hook, S. J., Jessup, A. T. and Nightingale, T.J., 2004, “The Miami 2001 infrared radiometer calibration and intercomparison: Part II Shipboard results”, *Journal of Atmospheric and Oceanic Technology*, **21**, 268-283.

Berry, K., 1981, "Emissivity of a cylindrical black-body cavity with a re-entrant cone end face", *J. Phys. E: Scientific Instruments*, **4**, 629–632.

Betts D B *et al.*, 1985, "Infrared reflection properties of five types of black coating for radiometric detectors", *J. Phys. E:Sci. Instrum.*, **18**, 689–696.

Chu, B and Machin, G., 1999, "A low-temperature blackbody reference source to -40 °C", *Measurement Science and Technology*, **10**, 1–6

Gutschwager, B, Theocharous, E., Monte, C., Adibekyan, A., Reiniger, M., Fox, N.P. and Hollandt, J., "Comparison of the radiation temperature scales of the PTB and the NPL in the temperature range from -57 °C to 50 °C", *Measurement Science and Technology*, 24, Article No 095002, 2013

Rice, J. P., Butler, J. I., Johnson, B. C., Minnett, P. J., Maillet K. A., Nightingale, T. J, Hook, S. J., Abtahi, A., Donlon, and. Barton, I. J., 2004, "The Miami 2001 infrared radiometer calibration and intercomparison. Part I: Laboratory characterisation of blackbody targets", *Journal of Atmospheric and Oceanic Technology*, **21**, 258-267.

Theocharous, E., Fox, N. P., Sapritsky, V. I., Mekhontsev, S. N. and Morozova, S. P., 1998, "Absolute measurements of black-body emitted radiance", *Metrologia*, **35**, 549-554.

Theocharous, E., Usadi, E. and Fox, N. P., 2010, "CEOS comparison of IR brightness temperature measurements in support of satellite validation. Part I: Laboratory and ocean surface temperature comparison of radiation thermometers", NPL Report COM OP3.

Theocharous, E. and Fox, N. P., 2010, "CEOS comparison of IR brightness temperature measurements in support of satellite validation. Part II: Laboratory comparison of the brightness temperature of blackbodies", NPL Report COM OP4.

Theocharous, E., Barker Snook, I. and Fox, N. P., 2017, "2016 comparison of IR brightness temperature measurements in support of satellite validation. Part 1: Laboratory comparison of the brightness temperature of blackbodies", NPL Report ENV 12.

Theocharous, E., Barker Snook, I. and Fox, N. P., 2017a, "2016 comparison of IR brightness temperature measurements in support of satellite validation. Part 4: Land surface temperature comparison of radiation thermometers", NPL Report ENV 13.

Acknowledgements

The authors wish to thank Miss Helen McEvoy and Mr Jamie McMillan for their assistance in operating the ammonia heat-pipe blackbody and with the testing surrounding the radiometer laboratory comparison. The authors also wish to thank Miss Perdi Williams for her assistance during the laboratory measurement campaign. The University of Valencia participation in the 2016 FRM4STS comparison was funded by the Spanish Ministerio de Economía y Competitividad and the European Regional Development Fund (FEDER) through the project CGL2015-64268-R (MINECO/FEDER, UE) and by the Ministerio de Economía y Competitividad through the project CGL2013-46862-C2-1-P (MINECO).